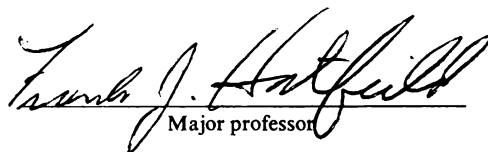




3 1293 00882 6343

This is to certify that the
dissertation entitled
Static Analysis of Structural Thin
Flat Membranes
presented by
Abdelilah Elguennouni

has been accepted towards fulfillment
of the requirements for
Doctor of Philosophy degree in Civil Engineering


Major professor

Date August 5, 1992

**LIBRARY
Michigan State
University**

PLACE IN RETURN BOX to remove this checkout from your record.
TO AVOID FINES return on or before date due.

DATE DUE	DATE DUE	DATE DUE
_____	_____	_____
_____	_____	_____
_____	_____	_____
_____	_____	_____
_____	_____	_____
_____	_____	_____
_____	_____	_____

MSU Is An Affirmative Action/Equal Opportunity Institution

c:\crl\datedue.pm3-p.1

**STATIC ANALYSIS OF STRUCTURAL THIN
FLAT MEMBRANES**

By

ABDELILAH ELGUENNOUNI

A DISSERTATION

**Submitted to
Michigan State University
in partial fulfillment of the requirements
for the degree of**

DOCTOR OF PHILOSOPHY

Department of Civil and Environmental Engineering

1992

698-0430

ABSTRACT

STATIC ANALYSIS OF STRUCTURAL THIN FLAT MEMBRANES

By

ABDELILAH ELGUENNOUNI

The static nonlinear behavior of structural thin flat membranes which are subjected to transverse loading was investigated. Using a nondimensional formulation, two geometrically nonlinear finite element models were considered. First, a simplified model based on the von Kármán strain-displacement relationships was developed and validated by comparison to previously developed models. Then, a general model based on the exact strain-displacement relationships was developed.

A comparison between the two models was made to determine the limitations of the simplified model. An extension to deformation-dependent loading was also studied. Several parametric studies were conducted to investigate the effect of Poisson's ratio, initial prestressing, and membrane boundary conditions on deflections and stresses. An incremental-iterative procedure was used to solve the nonlinear finite element equations. To overcome the difficulty associated with the ill-conditioning encountered for the first several increments, a new technique referred to as "initial virtual prestressing" was developed. This was found to be effective

and convenient compared to the usual strategy of guessing the initial deflected shape.

It was shown that a nondimensional coefficient k which is a function of five parameters (load intensity, characteristic length of the membrane, Young's modulus, Poisson's ratio and membrane thickness) determines the state of straining in the membrane. For values of k smaller than 0.01, the maximum strain is less than 1.75%. The simplified model leads to results that are sufficiently accurate for design purposes. For values of k greater than 0.05, the maximum strain exceeds 5%, and the accuracy of the simplified model diminishes.

The use by previous investigators of second Piola-Kirchhoff stresses is inappropriate because Cauchy stresses are the more accurate representation of real stresses. However, for values of k smaller than 0.01, the numerical difference between the two stress measures was found to be negligible. Also, it was shown that for values of k smaller than 0.05, external pressure loading may be assumed to be deformation-independent. Variation of Poisson's ratio, initial real prestressing and membrane boundary conditions were shown to have significant effects on deflections and stresses.

To the memory of my father

MOHAMED ELGUENNOUNI

and to my mother

DAOURA AICHA

FOR THEIR LOVE AND SACRIFICE

Acknowledgments

I am gratefully indebted to Dr. Frank Hatfield, my major professor, for his invaluable advice and continuous support throughout the course of this study.

Sincere appreciation is extended to the guidance committee members: Dr. Fred Bakker-Arkema, Dr. John Masterson, Dr. Parviz Soroushian, and the late Dr. William Bradley.

The Hassan II Agronomic and Veterinary Institute, Rabat, Morocco, facilitated and encouraged my research; the United States Agency for International Development provided financial support; and the International Agricultural Programs of the University of Minnesota handled administrative functions. This research would not have been possible without the existence of those three institutions, and I am deeply grateful to them.

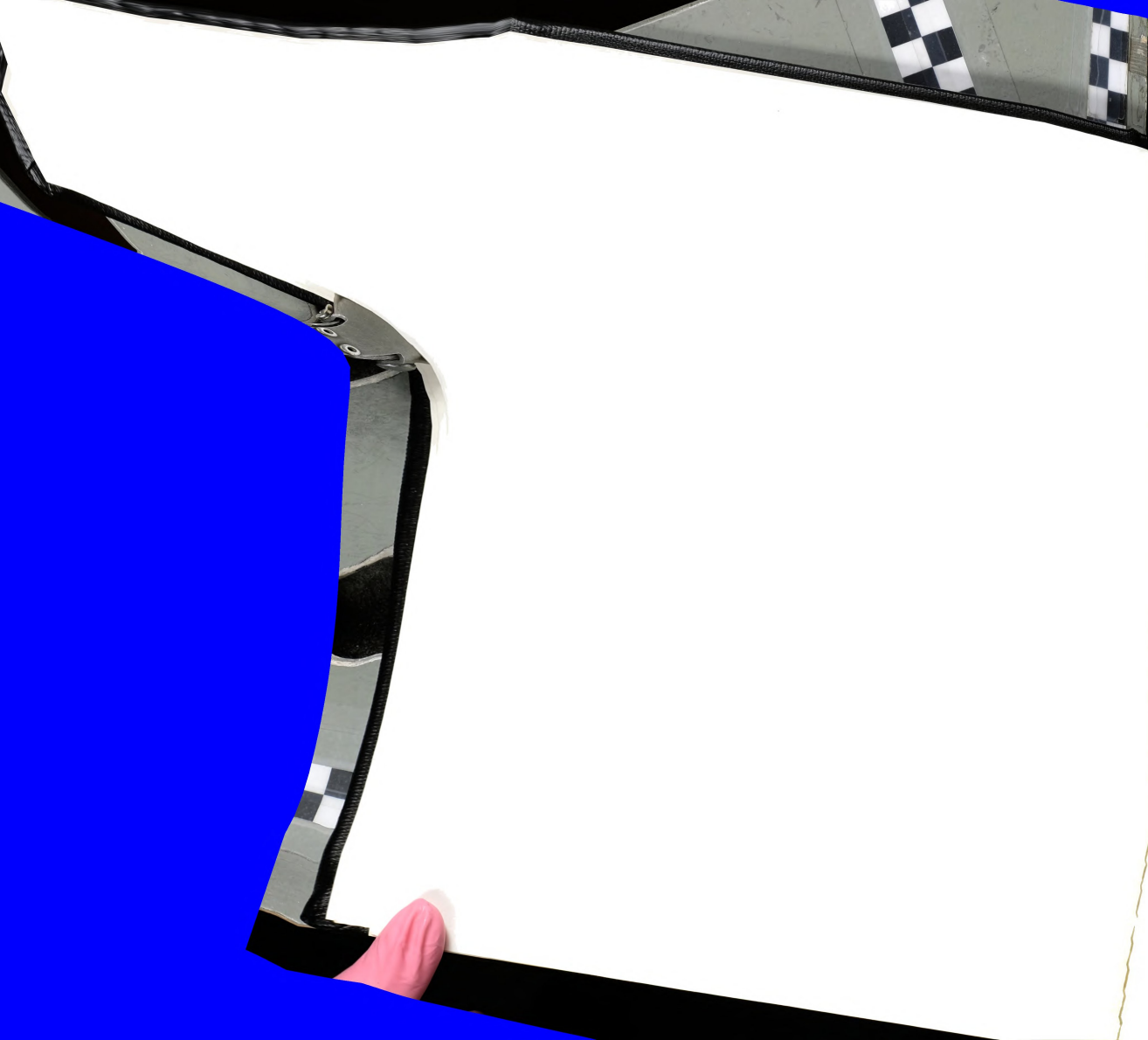
TABLE OF CONTENTS

LIST OF TABLES

LIST OF FIGURES

LIST OF SYMBOLS

1. Introduction and Background	1
1.1 Introduction.....	1
1.2 Review of Technical Literature.....	3
1.3 Scope of the Research.....	11
2. Theory and Implementation	13
2.1 Introduction.....	13
2.2 Basic Assumptions.....	15
2.3 Fundamental Equations Using a Nonlinear Finite Element Formulation.....	16
2.3.1 Basic Problem.....	16
2.3.2 Formulation of the Continuum Mechanics Equations of Equilibrium.....	17
2.3.3 Description of the Curved Isoparametric Finite Element Used and the Corresponding Shape Functions.....	18
2.3.4 Reformulation of the Equilibrium Equations.....	21
2.3.5 Incremental Equilibrium Equations.....	22
3. Fundamental Equations for the von Kármán Model	25
3.1 Derivation of Element Matrices.....	25
3.1.1 Derivation of the Basic Element Matrices..	25
3.1.2 Derivation of Element Stiffness Matrices..	29
3.2 Rearrangement of Element Stiffness Matrices for Computer Implementation.....	33
3.2.1 Numerical Integration.....	33
3.2.2 Rearrangement of Element Matrices.....	35
3.3 Nondimensional Formulation of the Incremental Equilibrium Equations.....	37



4. Extension to the General Nonlinear Model	46
4.1 Derivation of Element Matrices.....	46
4.1.1 Derivation of the Basic Element Matrices..	46
4.1.2 Derivation of Element Stiffness Matrices..	48
4.2 Nondimensional Formulation of the Incremental Equilibrium Equations.....	50
4.3 Extension to the Case of External Pressure.....	56
5. Solution Technique	66
5.1 Assemblage of Structure Matrices.....	66
5.2 Solution of Equilibrium Equations.....	66
5.2.1 The Incremental Iterative Solution Strategy	66
5.2.2 Convergence Criteria.....	68
5.2.3 The Initial Virtual Prestressing Technique.....	68
5.3 Evaluation of Strains and Stresses.....	72
5.3.1 Evaluation of Strains.....	72
5.3.2 Evaluation of Second Piola-Kirchhoff Stresses.....	72
5.3.3 Evaluation of Cauchy Stresses.....	72
6. Model Validation and Parametric Studies	74
6.1 Model Validation.....	75
6.1.1 Convergence of the von Kármán Model.....	75
6.1.2 Comparison of the von Kármán Model with Previous Models.....	80
6.1.3 Discussion.....	82
6.1.4 Comparison of the von Kármán Model with the General Model.....	87
6.2 Parametric Studies.....	110
6.2.1 Effect of Poisson's Ratio.....	110
6.2.2 Effect of Initial Prestressing.....	112
6.2.3 Effect of the Boundary Conditions.....	114
6.2.4 Effect of Nonconservative Loading: Case of External Pressure.....	119
6.2.5 Comments About the Initial Virtual Prestressing Technique.....	119
7. Summary and Conclusions	120
7.1 Summary.....	120
7.2 Conclusions.....	121
7.2.1 Comparison of the von Kármán Model to Previously Developed Models.....	121
7.2.2 Second Piola-Kirchhoff Stresses and Cauchy Stresses.....	122
7.2.3 Limitation of the von Kármán Model.....	122
7.2.4 Effect of Poisson's Ratio.....	123
7.2.5 Effect of Initial Prestressing.....	123
7.2.6 Effect of Boundary Conditions.....	124



7.2.7 Effect of Nonconservative Loading.....	124
7.2.8 Use of the Initial Virtual Prestressing Technique.....	124
Bibliography	126

LIST OF TABLES

Table 1	: Square Membrane Under Uniform Transverse Loading Comparing Different Models.....	81
Table 2	: Rectangular Membrane Under Uniform Transverse Loading ($\nu=5/7$) Comparing Different Models.....	81
Table 3	: Rectangular Membrane Under Uniform Transverse Loading ($\nu=2/5$) Comparing Different Models.....	82
Table 4	: Stress Coefficients for a Square Membrane.....	83
Table 5	: Stress Coefficients for a Rectangular Membrane ($\nu=5/7$)	84
Table 6	: Stress Coefficients for a Rectangular Membrane ($\nu=2/5$)	84
Table 7	: Relative error in Stress Coefficients.....	85
Table 8	: Strains in a Square Membrane.....	86
Table 9	: Strains in a Rectangular Membrane ($\nu=5/7$)	87
Table 10	: Strains in a Rectangular Membrane ($\nu=2/5$)	87
Table 11	: Central Deflection Coefficients.....	92
Table 12	: Cauchy Stress Coefficients in a Square Membrane.....	93
Table 13	: Cauchy Stress Coefficients in a Rectangular Membrane ($\nu=5/7$)	93
Table 14	: Cauchy Stress Coefficients in a Rectangular Membrane ($\nu=2/5$)	94
Table 15	: Relative Error for a Square Membrane.....	95
Table 16	: Relative Error for a Rectangular Membrane ($\nu=5/7$)	95
Table 17	: Relative Error for a Rectangular Membrane ($\nu=2/5$)	96
Table 18	: Comparison of Strains for a Square Membrane.....	97
Table 19	: Comparison of Strains for a Rectangular Membrane ($\nu=5/7$)	97

Table 20 : Comparison of Strains for a Rectangular	
Membrane ($\nu=2/5$)	98

LIST OF FIGURES

Figure 1	: Representation of the Eight-Node Master Element.....	19
Figure 2	: Region for Rectangular Membrane.....	75
Figure 3	: Convergence of Deflection and Stresses for a Square Membrane.....	77
Figure 4	: Convergence of Deflection and Stresses for a Rectangular Membrane ($\nu=5/7$)	78
Figure 5	: Convergence of Deflection and Stresses for a Rectangular Membrane ($\nu=2/5$)	79
Figure 6	: General Model Convergence of Deflection and Stresses for a Square Membrane.....	89
Figure 7	: General Model Convergence of Deflection and Stresses for a Rectangular Membrane ($\nu=5/7$)	90
Figure 8	: General Model Convergence of Deflection and Stresses for a Rectangular Membrane ($\nu=2/5$)	91
Figure 9	: Typical Quarter of a Membrane.....	99
Figure 10	: Deflection Coefficient Distribution for a Square Membrane.....	100
Figure 11	: Deflection Coefficient Distribution Along The Shorter Side of a Rectangular Membrane ($\nu=5/7$)	101
Figure 12	: Deflection Coefficient Distribution Along The Longer Side of a Rectangular Membrane ($\nu=5/7$)	102
Figure 13	: Deflection Coefficient Distribution Along The Shorter Side of a Rectangular Membrane ($\nu=2/5$)	103
Figure 14	: Deflection Coefficient Distribution Along The Longer Side of a Rectangular Membrane ($\nu=2/5$)	104

Figure 15 :	Stress Coefficient Distribution for a Square Membrane.....	105
Figure 16 :	Stress Coefficient Distribution Along The Shorter Side of a Rectangular Membrane ($\nu=5/7$)	106
Figure 17 :	Stress Coefficient Distribution Along The Longer Side of a Rectangular Membrane ($\nu=5/7$)	107
Figure 18 :	Stress Coefficient Distribution Along The Shorter Side of a Rectangular Membrane ($\nu=2/5$)	108
Figure 19 :	Stress Coefficient Distribution Along The Longer Side of a Rectangular Membrane ($\nu=2/5$)	109
Figure 20 :	Effect of Poisson's Ratio.....	111
Figure 21 :	Effect of Initial Prestraining.....	113
Figure 22 :	Comparison of Normal Deflections Along the Center Line a-a.....	115
Figure 23 :	Comparison of Normal Deflections Along the Center Line d-d.....	116
Figure 24 :	Comparison of Cauchy Stresses Along the Center Line a-a.....	117
Figure 25 :	Comparison of Cauchy Stresses Along the Center Line d-d.....	118

LIST OF SYMBOLS

a	= half-length of the longer side of a rectangular membrane
\mathbf{a}	= nodal displacement vector
b	= half-length of the shorter side of a rectangular membrane
\mathbf{B}	= strain-displacement matrix
\mathbf{D}	= elasticity matrix
E	= Young's modulus
\mathbf{f}	= external load vector per unit area
\mathbf{f}^B	= vector of body forces per unit volume
\mathbf{f}^S	= vector of surface tractions per unit area
F	= stress function
\mathbf{F}	= vector of external loads
h	= membrane thickness
\mathbf{J}	= Jacobian matrix
k	= nondimensional coefficient characterizing The membrane problem
\mathbf{K}_L	= linear stiffness matrix
\mathbf{K}_{NL}	= nonlinear stiffness matrix
\mathbf{K}_q	= load stiffness matrix
\mathbf{K}_T	= tangent stiffness matrix
\mathbf{K}_σ	= stress stiffness matrix
L	= a characteristic length of the membrane
N_x, N_y, N_{xy}	= in-plane stress resultant components
N_i	= nodal shape functions
\mathbf{N}	= Matrix of shape functions

P = vector of equivalent internal forces
 q = normal load intensity
 r, s = natural coordinates
 u, v = displacement components respectively
 in the x- and y- directions
 w = displacement component in the z-direction
 also called normal deflection
 V_0^e = volume of membrane element in the
 initial configuration
 S_0^e = surface area of the membrane element
 in the initial configuration
 U = displacement vector
 ϵ = Green-Lagrange strain vector
 $\epsilon_x, \epsilon_y, \epsilon_{xy}$ = Green-Lagrange strain components

 ν = Poisson's ratio
 $\sigma_x, \sigma_y, \sigma_{xy}$ = second Piola-Kirchhoff stress
 components

 σ = second Piola-Kirchhoff stress vector
 $\tau_x, \tau_y, \tau_{xy}$ = Cauchy Stress components

1. INTRODUCTION AND BACKGROUND

1.1 Introduction

The high capital cost of glass greenhouses has stimulated interest in film plastic clad alternatives which require only 20 to 45% of the capital required for glass¹.

In Morocco, there is a trend toward the construction of plastic film greenhouses. More than 1000 hectares for banana production have been covered by this type of structure during the period 1981-1988².

Because of the favorable horticultural qualities of polyethylene film (particularly for the Mediterranean climate) and its low price compared to other covering materials, it has been used extensively for greenhouses. Due to the fact that the structural behavior of this covering material is not well known, particularly under the random action of wind, the reliability of these greenhouse structures remains uncertain. Existing designs span a large range of reliability; some are prone to structural failure while others appear to be overdesigned to an uneconomic degree.

Greenhouse structures are hybrid systems in which plastic membrane panels span between primary load carrying members such as prestressed cables and rigid elements. Some of the advantages of membrane structures are:

- they are lightweight and collapsible and therefore easy to transport and erect;
- the environmental loads are efficiently carried by direct stress without bending;
- they are load-adaptive in that the members change geometry to better accommodate changes in load patterns and magnitudes.

The structural mechanics of tension structures such as greenhouses is well described in references^{3 4 5 6 7}. Large deformations due to wind pressure, the resulting tearing of the plastic due to the high membrane tension, and the collapse of other structural elements are critical problems.

Since the typical cost of greenhouse structures designed for Morocco is between 250,000 and 300,000 Dirhams^a per hectare, failure of a greenhouse represents a significant loss. Therefore, an efficient and safe structural design of these buildings must be achieved. To do this, several factors that influence the design must be considered. The main factors that are specific for these structures are the design wind load and the structural behavior of film plastic membranes. The first factor has received considerable attention; only a few investigations have been concerned with the latter.

1.2 Review of Technical Literature

A membrane can only sustain tensile stresses. Therefore, in order to be stable , i.e. have an equilibrium position, it

^a. In June 1989, 1 Dirham = \$ 0.125.

must be prestretched. This can be effected by tensile forces acting on the membrane edges, by selfweight, or, when a space is completely enclosed, by pressurizing. Prestretching forces stabilize the structure and provide stiffness against further deflections. Membrane structures respond in a nonlinear fashion to both prestretching and service loads, regardless of linearity of materials, even if the loading is deformation-independent.

The static analysis of prestretched structures comprises two main problems:

- 1- Determination of the prestretching forces at equilibrium;
- 2- Establishment of the maximum tensile forces arising in the system at the given load application. These, together with the strength of the membrane, determine the maximum size of the panel.

In order to determine the required prestretching forces as well as the maximum stresses, it is necessary first to determine the internal forces. The ordinary membrane theory of shells may be used, provided the material is only slightly deformable so that the loads can be considered to act on the undeformed system. It is far more difficult to determine the state of stress for highly deformed membranes. In this case the initial shape is incapable of supporting any load, and the membrane undergoes finite deformations until an equilibrium shape is reached. The state of stress depends markedly on the final shape of the membrane. However, this shape is unknown,

as are the internal forces. When the equilibrium state of a system must be determined for the deformed position, it is necessary to apply the theory of finite deformations, using nonlinear strain-displacement relationships. This leads to nonlinear displacement equations.

According to Shaw and Perrone⁸, the governing nonlinear equations of membranes were first derived by Föppl and Teubner⁹. These equations follow directly from the von Kármán large deflection flat-plate equations by setting the plate stiffness identically zero. The von Kármán equations for the large deflection of a thin flat plate of uniform thickness are¹⁰:

$$\frac{\partial^4 F}{\partial x^4} + 2 \frac{\partial^4 F}{\partial x^2 \partial y^2} + \frac{\partial^4 F}{\partial y^4} = E \left[\left(\frac{\partial^2 w}{\partial x \partial y} \right)^2 - \frac{\partial^2 w}{\partial x^2} \frac{\partial^2 w}{\partial y^2} \right] \quad (1.1)$$

$$\frac{\partial^4 w}{\partial x^4} + 2 \frac{\partial^4 w}{\partial x^2 \partial y^2} + \frac{\partial^4 w}{\partial y^4} = \frac{h}{D} \left(\frac{q}{h} + \frac{\partial^2 F}{\partial y^2} \frac{\partial^2 w}{\partial x^2} + \frac{\partial^2 F}{\partial x^2} \frac{\partial^2 w}{\partial y^2} - 2 \frac{\partial^2 F}{\partial x \partial y} \frac{\partial^2 w}{\partial x \partial y} \right) \quad (1.2)$$

where w is the normal deflection, $q=q(x,y)$ is the applied normal load intensity, h is the plate thickness, E is Young's modulus for the plate material, D its bending stiffness defined as $Eh^3/12(1-\nu^2)$ where ν is Poisson's ratio, and F is a stress function related to the forces per unit length in the plane of the plate by the formulas:

$$N_x = h \frac{\partial^2 F}{\partial y^2} \quad N_y = h \frac{\partial^2 F}{\partial x^2} \quad N_{xy} = -h \frac{\partial^2 F}{\partial x \partial y} \quad (1.3)$$

Making the bending stiffness zero results in two simultaneous nonlinear equations relating the membrane deflection and the stress function

$$\frac{\partial^4 F}{\partial x^4} + 2 \frac{\partial^4 F}{\partial x^2 \partial y^2} + \frac{\partial^4 F}{\partial y^4} = E \left[\left(\frac{\partial^2 w}{\partial x \partial y} \right)^2 - \frac{\partial^2 w}{\partial x^2} \frac{\partial^2 w}{\partial y^2} \right] \quad (1.4)$$

$$\frac{q}{h} + \frac{\partial^2 F}{\partial y^2} \frac{\partial^2 w}{\partial x^2} + \frac{\partial^2 F}{\partial x^2} \frac{\partial^2 w}{\partial y^2} - 2 \frac{\partial^2 F}{\partial x \partial y} \frac{\partial^2 w}{\partial x \partial y} = 0 \quad (1.5)$$

The exact solution for the uniformly loaded rectangular membrane has not been obtained.

In 1920, Föppl and Föppl¹¹ used the energy approach to obtain an approximate solution for stress and deflection at the center of a square membrane. They assumed a trigonometric function for the membrane deformations. This function, which contains a certain number of unknown coefficients, was chosen so as to satisfy the boundary and symmetry conditions. The unknown coefficients were evaluated by minimizing the total energy of the membrane. A year later, Hencky¹² achieved a rather lengthy numerical finite difference solution for a square membrane. His results differ slightly from Föppl and Föppl's.

According to Borg¹³, in 1940 Neubert and Sommer¹⁴ carried through the Föppl's computations for the rectangular case and drew curves for stresses and deflections. Additionally, Neubert and Sommer obtained satisfactory experimental

verification for the Föppl's and Hencky solution for the square membrane, but did not test a rectangular membrane. Head and Sechler¹⁵ got similar results from their experimental work, but, for rectangular membranes with high aspect ratios, they noted a discrepancy from the Föppl and Föppl solution for stresses. Borg¹³ obtained an exact solution for the semi-infinite membrane by taking the limit of the semi-infinite tied-plate¹⁶ as the plate bending stiffness approaches zero. He estimated the deflections and stresses of rectangular membranes by interpolating results for square and semi-infinite rectangular membranes. He drew curves for central deflection and central stress between the two limits in such a way as to satisfy known experimental requirements. Differences of the order of 19 per cent appeared between the Borg and Föppl's results in semi-infinite membrane solutions. Borg attributed this discrepancy to the fact that as the aspect ratio decreases, the trigonometric function assumed by Föppl and Föppl becomes less accurate.

In 1954 Shaw and Perrone⁸ employed a finite difference approximation in conjunction with a nonlinear relaxation technique to obtain a solution for an aspect ratio of 5/7. Rather than using the Föppl's formulation, the membrane problem was dealt with numerically in terms of displacement components. Their results compared fairly well with Borg's. In 1972 Kao and Perrone¹⁷ extended the solution to other aspect ratios.

In 1987, Allen and Al-Qarra¹⁸ used an incremental finite element method in a total Lagrangian coordinate system. An advantage of the method is that the problem of the large deflection of thin flat membranes subjected to normal forces is formulated in terms of simple physical concepts, and a numerical solution is achieved without dealing directly with the complex nonlinear differential equations.

All the investigations described above used Hooke's law to express the stress-strain relationships, which for an elastic and isotropic material are

$$\sigma = D \epsilon \quad (1.6)$$

where the stress vector σ , the strain vector ϵ , and the elasticity matrix D are given by:

$$\sigma = \{\sigma_x, \sigma_y, \sigma_{xy}\}^T \quad (1.7)$$

$$\epsilon = \{\epsilon_x, \epsilon_y, \epsilon_{xy}\}^T \quad (1.8)$$

$$D = \frac{E}{1-\nu^2} \begin{bmatrix} 1 & \nu & 0 \\ \nu & 1 & 0 \\ 0 & 0 & \frac{1-\nu}{2} \end{bmatrix} \quad (1.9)$$

When large displacements are considered, Hooke's law may still be valid provided that second Piola-Kirchhoff stresses are used in conjunction with Green-Lagrange strains and the material straining is small¹⁹. Consequently, the previous research mentioned above used implicitly second Piola-Kirckhoff stress as a measure of stresses. There has been much

discussion about the physical nature of the second Piola-Kirchhoff stress tensor^{19,20}. However, It should be recognized that the second Piola -Kirchhoff stresses have little physical meaning, and in practice, Cauchy stresses should be the stress quantities to be compared to available experimental work.

The general definition of strains which, is valid whether displacements or strains are small or large, was introduced by Green and St.Venant, and is known as the Green's strain tensor or the Green-Lagrange strain tensor. In a fixed xyz-Cartesian coordinate system, the strain components in terms of the displacement components are:

$$\epsilon_x = \frac{\partial u}{\partial x} + \frac{1}{2} \left[\left(\frac{\partial u}{\partial x} \right)^2 + \left(\frac{\partial v}{\partial x} \right)^2 + \left(\frac{\partial w}{\partial x} \right)^2 \right] \quad (1.10)$$

$$\epsilon_y = \frac{\partial v}{\partial y} + \frac{1}{2} \left[\left(\frac{\partial u}{\partial y} \right)^2 + \left(\frac{\partial v}{\partial y} \right)^2 + \left(\frac{\partial w}{\partial y} \right)^2 \right] \quad (1.11)$$

$$\epsilon_{xy} = \frac{\partial u}{\partial y} + \frac{\partial v}{\partial x} + \frac{\partial u}{\partial x} \frac{\partial u}{\partial y} + \frac{\partial v}{\partial x} \frac{\partial v}{\partial y} + \frac{\partial w}{\partial x} \frac{\partial w}{\partial y} \quad (1.12)$$

The investigators mentioned above, except Allen and Al-Qarra¹⁶, utilized a simplified geometric nonlinear model in which it is assumed that the squares and products of derivatives of the in-plane displacement components u and v are small compared with those of w and therefore may be neglected. Thus, the following strain-displacement relationships were used

$$\epsilon_x = \frac{\partial u}{\partial x} + \frac{1}{2} \left(\frac{\partial w}{\partial x} \right)^2 \quad (1.13)$$

$$\epsilon_y = \frac{\partial v}{\partial y} + \frac{1}{2} \left(\frac{\partial w}{\partial y} \right)^2 \quad (1.14)$$

$$\epsilon_{xy} = \frac{\partial u}{\partial y} + \frac{\partial v}{\partial x} + \frac{\partial w}{\partial y} \frac{\partial w}{\partial y} \quad (1.15)$$

From now on, the term "von Kármán model" will refer to a model using equations (1.13-14-15) as the strain-displacement relationships, while the term "general model" will refer to a model using equations (1.10-11-12).

Allen and Al-Qarra mentioned in their paper¹⁸ the use of a general model and that their results compared well with the previous von Kármán models cited above, but did not draw any conclusions regarding this point. This does not seem to be coherent, since an obvious and important conclusion that should be drawn from their work is that analysis of membranes with large displacements does not require the use of a general model. Also, it is clear from Equations 13 of their paper¹⁸ that the values of the load intensity, length of the membrane, membrane thickness and Young's modulus might have a significant effect on the results for deflections and stresses. Therefore, the use of the general model by Allen and Al-Qarra is questioned.

Thin flat structural membranes with negligible bending stiffness rely on catenary action to support transverse loading. Therefore, in the initial flat position, the problem has no linear solution. An iterative procedure is then necessary. The procedure employed by Allen and Al-Qarra¹⁸ is

based on the generalized Newton-Raphson method; a deflected shape for the loaded membrane was assumed as an initial guess to start the numerical procedure. In some applications of this technique, ill-conditioned stiffness matrices may arise from an improper choice of the deflected shape. This situation can be circumvented by arbitrarily prescribing a new set of initial displacements. The convergence rate is sensitive to the accuracy of the assumed deflected shape, which depends on the problem at hand, and on the analyst's intuition and experience. To improve significantly the rate of convergence, Oden and Sato²¹ proposed to start the analysis with a coarse finite element representation of the membrane, then use the results obtained as starting values for a more refined representation, the displacements of the added node points being obtained through linear interpolation. Dealing with the complete set of undetermined displacements when guessing the initial deflected shape, is a cumbersome task, particularly when there are few restraints on the membrane edges.

1.3 Scope of the Research

The present research will investigate the static behavior of thin flat membranes which are subjected to transverse loads. It will include the following parts:

1. Theoretical development and computer implementation of a nondimensional incremental nonlinear finite element model using von Kármán's strain-displacement relationships to

analyze thin flat membranes subjected to transverse loading. A total Lagrangian formulation will be used.

2. Implementation of a new numerical technique which will reduce the number of variables in the initial guess of the deflected shape to at most three. These variables will be referred to as "the initial virtual prestressing variables" and the numerical technique as "the initial virtual prestressing technique".

3. Investigation of several numerical examples in order to test the validity of the model by comparison to the results of previous research.

4. Evaluation of Cauchy stresses in the membrane to allow meaningful comparisons with experimental results.

5. Theoretical development of a general incremental nonlinear finite element model where the general strain-displacement relationships will be used instead of those of von Kármán.

6. Comparison of the von Kármán model and the general model and determination of the range of applicability of the von Kármán model.

7. Investigation of the effect of membrane aspect ratio on deflections and stresses.

8. Investigation of the effect of Poisson's ratio on stresses and deflections.

9. Investigation of the effect of membrane initial prestressing.

10. Investigation of the effect of varying the boundary conditions.

11. Investigation of the effect of considering a nonconservative loading ,that is, one that changes due to deformation. This permits a more accurate representation of differential air pressure.

2.Theory and Implementation

2.1 Introduction

Because of the lack of bending stiffness, membrane structures show large displacements. Prestressing forces stabilize the structure and provide stiffness against further displacements. The response to prestressing forces is always nonlinear because the equilibrium configuration as well as the state of stress are dependent on those forces. But the response to in-service loads may be either nonlinear or quasi-linear depending on the directions and magnitudes of the in-service forces compared to stresses and deformations of the prestressed structure. Three phases may be distinguished in the physical behavior of a membrane structure⁷:

Deployment phase

During this phase, the membrane unfolds from its compact configuration into a state of incipient straining and is stress-free. The membrane behavior is lightly nonlinear, but the equations of statics and constitutive equations are not of interest until the state of incipient straining is reached and the prestressing phase begins.

Prestressing phase

During this phase the structure undergoes large displacements until a static equilibrium configuration is reached. Therefore, nonlinear strain-displacement



relationships are needed. Strains are small but relative rotations may be large and thus second-order terms of displacement gradients may be significant. During the prestressing phase displacements predominate over strain effects.

In-service phase

The additional displacements due to in-service loads are generally much smaller than the prestressing displacements. This is due to the fact that the prestressing stiffens the membrane structure. The membrane behavior during this phase is either nonlinear or quasi-linear depending on the relative magnitudes of the prestressing forces and the in-service loads.

The state of stress in a membrane subjected to loads normal to its plane depends markedly on the final shape of the membrane. However, this shape is unknown, as are the in-plane membrane sectional loads. Accordingly, the theory of finite deformations has to be applied, and therefore nonlinear strain-displacement relationships are needed. These strain-displacement relationships are given by Equations 1.6, 1.7, and 1.8. Also, the equilibrium conditions of the membrane should be considered in the deformed configuration.

2.2 Basic Assumptions

The present work is concerned with the static behavior of thin flat membranes which are subjected to transverse loading. The following are the basic assumptions:

- the initial state of the membrane is either a state of incipient straining or is initially prestressed by in-plane forces so that the initial configuration can be assumed to be in a state of equilibrium prior to load application,
- The membrane is assumed to be flat in its initial configuration, i.e. lying in the x-y plane of a fixed Cartesian coordinate system xyz.
- the membrane material is homogeneous and isotropic and has a linear elastic constitutive behavior.
- the membrane bending stiffness is generally negligible and therefore may be discounted. Consequently, the membrane may be considered as a two-dimensional material body in a biaxial state of stress where only in-plane stresses occur.
- Due to the fact that generally the membrane thickness is very small compared to the other dimensions of the membrane, a uniform stress distribution across the membrane thickness may be assumed. Therefore, the membrane stresses may be replaced by membrane sectional loads defined as the statically equivalent loads per unit length of section.



2.3 Fundamental Equations Using a Nonlinear Finite Element Formulation

2.3.1 Basic problem

In the development to follow, a thin flat structural membrane in a Cartesian coordinate system is considered. When subjected to transverse loading, the membrane can experience large displacements and large strains, but exhibits a linearly elastic constitutive response. However, there is a strong geometric nonlinearity in the deformation process of the membrane. The aim is to determine the configuration of the membrane in its final state of equilibrium and the corresponding state of stress.

In order to include the effect of large deformation for this geometrically nonlinear problem, special treatment is required. The underlying theories and their solutions can be formulated by means of nonlinear equations or through equivalent variational principles. The latter approach will be used in conjunction with the finite element method. This has the advantage of solving the problem without dealing directly with the complex nonlinear equations, and allows an easier computer implementation.

To develop a finite element strategy, the membrane continuum will be approximated by a finite number of small components called elements. These elements are assumed to be connected on their boundaries at selected node points on the

membrane. Thus, the continuum is represented by a discrete model at the onset. This way, the problem reduces to one of evaluating a finite number of discrete variables which are the displacement components of the node points.

2.3.2 Formulation of the Continuum Mechanics Equations of Equilibrium

Using a total Lagrangian approach, the equilibrium of a membrane finite element in the final configuration is expressed by applying the principle of virtual displacements:

$$\int_{V_0^e} \delta \epsilon^T \sigma \, dV_0^e = \int_{V_0^e} \delta U^T f^B \, dV_0^e + \int_{S^e} \delta U^{sT} f^s \, dS^e + \sum_i \delta U_i^T F_i \quad (2.1)$$

where:

V_0^e is the volume of the membrane element in the initial configuration,

S^e is the surface area of the membrane element in the initial configuration,

f^B is the vector of body forces,

f^s is the vector of surface tractions,

F_i are concentrated forces,

U is the displacement vector,

U^s is the surface displacement vector,

U_i is the displacement vector corresponding to points of application of concentrated forces F_i ,

σ is the second Piola-Kirchhoff stress vector,

ϵ is the Green-Lagrange strain vector, and

δ means "variation in".

In the development to follow, it will be assumed that no point forces are applied to the membrane element and that body forces are either negligible compared to transverse loading or will be embedded in the vertical component of the transverse loading. Equation 2.1 may be written as:

$$\int_{V_0^e} \delta \boldsymbol{\varepsilon}^T \boldsymbol{\sigma} dV_0^e = \int_{S^e} \delta \boldsymbol{U}^{sT} \boldsymbol{f}^s dS^e \quad (2.2)$$

For clarity, the superscripts "e" and "S" will be dropped, and Equation 2.2 may be written as:

$$\int_{V_0} \delta \boldsymbol{\varepsilon}^T \boldsymbol{\sigma} dV_0 = \int_S \delta \boldsymbol{U}^T \boldsymbol{f} dS \quad (2.3)$$

2.3.3 Description of the Curved Isoparametric Finite Element and the Corresponding Shape Functions

2.3.3.1 Isoparametric Finite Element

There are many possible choices for the master finite element. As mentioned earlier, the membrane problem may be considered as a plane stress problem. In a Cartesian coordinate system, the simplest element form is a rectangle. An eight-node isoparametric element called "serendipity element" was chosen because it allows more accurate modelling than a four-node element (see Figure 1 below). To ensure that a small number of elements can represent a relatively complex form, the two-dimensional rectangular element will be mapped into a distorted rectangular element²².

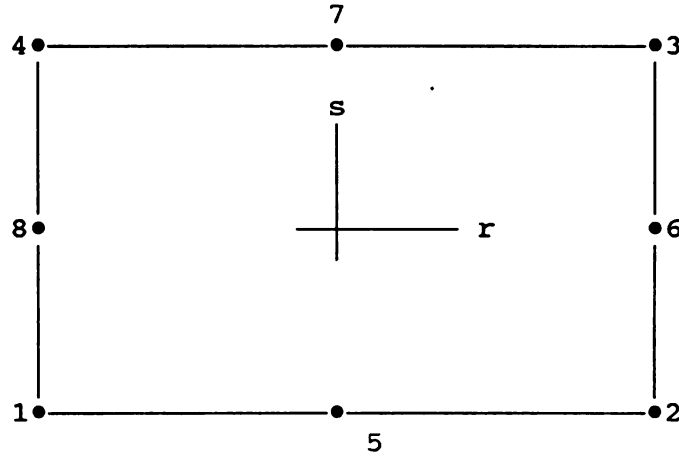


Figure 1: Representation of the Eight-Node Master Element

2.3.3.2 Shape Functions

The basic procedure in the isoparametric finite element formulation is to express the element coordinates and element displacements in the form of interpolations using the natural coordinate system of the element. The coordinate interpolations are:

$$x = \sum_{i=1}^8 N_i x_i \quad y = \sum_{i=1}^8 N_i y_i \quad (2.4)$$

where x and y are the coordinates at any point of the element. It should be mentioned that in a total Lagrangian formulation, all computations are referred to the initial configuration of the membrane. Therefore, the element nodal displacements will be chosen aligned with the global assemblage nodal displacements, and the element local coordinate systems coincide with the global coordinate system.



The interpolation functions also called shape functions are defined in the natural coordinate system of the element, which has variables r and s that each vary from -1 to $+1$. They are defined as follows (see Fig.1 above):

- for corner nodes ($i=1,2,3,4$)

$$N_i = \frac{1}{4} (1+r_0) (1+s_0) (r_0+s_0-1) \quad (2.5a)$$

where:

$$r_0 = r_i r \quad s_0 = s_i s \quad (2.5b)$$

r_i and s_i are the natural coordinates of node i , respectively, in the r and s directions.

- for midside nodes ($i=5,6,7,8$)

$$N_i = \frac{r_i^2}{2} (1+r_0) (1-s^2) + \frac{s_i^2}{2} (1+s_0) (1-r^2) \quad (2.5c)$$

2.3.3.3 Degrees of Freedom

In what follows, only the translational degrees of freedom u , v , and w will be considered. Therefore, there will be 3 degrees of freedom per node.

In the isoparametric formulation, the element displacements are interpolated in the same way as the geometry:

$$u = \sum_{i=1}^8 N_i u_i \quad v = \sum_{i=1}^8 N_i v_i \quad w = \sum_{i=1}^8 N_i w_i \quad (2.6)$$

where u , v and w are the local element displacements at any point of the element and u_i , v_i , and w_i , $i=1, \dots, 8$, are the corresponding element displacement at its nodes.

2.3.4 Reformulation of the Equilibrium Equations

Let:

$$\mathbf{U} = \{u, v, w\}^T \quad \mathbf{a} = \{u_1, v_1, w_1, \dots, u_8, v_8, w_8\}^T \quad (2.7)$$

The displacement vector \mathbf{U} may be written as:

$$\mathbf{U} = \mathbf{N} \mathbf{a} \quad (2.8)$$

where \mathbf{N} is a 3×24 matrix defined as

$$\mathbf{N} = [N_1 \mathbf{I}_3 | \dots | N_i \mathbf{I}_3 | \dots | N_8 \mathbf{I}_3] \quad (2.9)$$

and \mathbf{I}_3 is the 3×3 identity matrix. Also, if \mathbf{B} is the strain-displacement matrix (to be defined later), then

$$\delta \boldsymbol{\varepsilon} = \mathbf{B} \delta \mathbf{a} \quad d\boldsymbol{\varepsilon} = \mathbf{B} d\mathbf{a} \quad (2.10)$$

Consequently, Equation 2.3 becomes

$$\delta \mathbf{a}^T \left(\int_{V_0} \mathbf{B}^T \boldsymbol{\sigma} dV_0 - \int_S \mathbf{N}^T \mathbf{f} dS \right) = 0 \quad (2.11)$$

$\delta \mathbf{a}$ being an arbitrary variation of \mathbf{a} , Equation 2.11 may be rewritten as

$$\int_{V_0} \mathbf{B}^T \boldsymbol{\sigma} dV_0 - \mathbf{F} = 0 \quad (2.12)$$

where

$$\mathbf{F} = \int_S \mathbf{N}^T \mathbf{f} dS \quad (2.13)$$

Equation 2.12 constitutes the nonlinear equilibrium equations of the finite element model of the membrane problem. In the

solution procedure, a direct method does not guarantee convergence to the solution, and consequently Equation 2.12 will not be used directly. Instead, an incremental version of this equation will be derived.

2.3.5 Incremental Equilibrium Equations

The basic approach for deriving the incremental equilibrium equations is to assume that the solution for load q is known, and that the solution for load $q+\Delta q$ is required, where Δq is a suitably chosen load increment.

The equilibrium equations corresponding to $q+\Delta q$ is:

$$\psi(q+\Delta q) = 0 \quad (2.14a)$$

or

$$P(q+\Delta q) - F(q+\Delta q) = 0 \quad (2.14b)$$

where

$$P = \int_{V_0} B^T \sigma dV_0 \quad (2.15)$$

and F is defined by Equation 2.13.

Since the solution corresponding to load q is known,

$$P(q+\Delta q) = P(q) + \Delta P \quad (2.16)$$

where ΔP is the increment in nodal point forces corresponding to the increment in element displacements and stresses from load q to load $q+\Delta q$. ΔP can be approximated using a tangent stiffness matrix $K_T(q)$ which corresponds to the geometric conditions at load q as

$$\Delta P = K_T(q) \Delta a \quad (2.17)$$

where Δa is a vector of incremental nodal displacements.

Substituting Equations 2.17 and 2.16 into Equation 2.14b gives

$$K_T(q) \Delta a = F(q+\Delta q) - P(q) \quad (2.18)$$

and solving for Δa approximates the displacements for the load $q+\Delta q$ as

$$a(q+\Delta q) = a(q) + \Delta a \quad (2.19)$$

The exact displacements at load $q+\Delta q$ are those that correspond to the applied load $F(q+\Delta q)$. Because Equation 2.17 was used, the displacements computed in Equation 2.19 are only an approximation to the exact displacements. Having an approximation for $a(q+\Delta q)$, the strains, stresses and corresponding nodal forces at load $q+\Delta q$ may be evaluated. Then the next increment is started. Due to the approximation made in Equation 2.17, and in order to avoid instability, an iteration process is required in order to obtain a sufficiently accurate solution of Equation 2.14b. By combining the Newton-Raphson iterative method with the incremental method described above, Equations 2.18 and 2.19 become, respectively,

$$K_T^{(i-1)}(q+\Delta q) \Delta a^{(i)}(q+\Delta q) = F^{(i)}(q+\Delta q) - P^{(i-1)}(q+\Delta q) \quad (2.20)$$

$$a^{(i)}(q+\Delta q) = a^{(i-1)}(q+\Delta q) + \Delta a^{(i)} \quad (2.21)$$

where i is the iteration number.

The initial conditions are:

$$\left. \begin{aligned} \kappa_T^{(0)}(q+\Delta q) &= \kappa_T(q) \\ a^{(0)}(q+\Delta q) &= a(q) \\ p^{(0)}(q+\Delta q) &= p(q) \end{aligned} \right\} \quad (2.22)$$

If an index m describing the m th increment is introduced, the above equations may be written as

$$\kappa_{T_m}^{(i-1)} \Delta a_m^{(i)} = F_m^{(i)} - p_m^{(i-1)} \quad (2.23)$$

$$a_m^{(i)} = a_m^{(i-1)} + \Delta a_m^{(i)} \quad (2.24)$$

$$\left. \begin{aligned} \kappa_{T_m}^{(0)} &= \kappa_{T_{m-1}} \\ a_m^{(0)} &= a_{m-1} \\ p_m^{(0)} &= p_{m-1} \end{aligned} \right\} \quad (2.25)$$

3. Fundamental Equations for the von Kármán Model

3.1 Derivation of Element Matrices

3.1.1 Derivation of the Basic Element Matrices

The von Kármán strain-displacement relationships are defined by Equations 1.13, 1.14, and 1.15. Rewriting these three equations in a vectorial form gives

$$\boldsymbol{\varepsilon}^1 = \begin{Bmatrix} \varepsilon_x \\ \varepsilon_y \\ \varepsilon_{xy} \end{Bmatrix} = \begin{Bmatrix} \frac{\partial u}{\partial x} \\ \frac{\partial v}{\partial y} \\ \frac{\partial u}{\partial y} + \frac{\partial v}{\partial x} \end{Bmatrix} + \begin{Bmatrix} \frac{1}{2} \left(\frac{\partial w}{\partial x} \right)^2 \\ \frac{1}{2} \left(\frac{\partial w}{\partial y} \right)^2 \\ \frac{\partial w}{\partial x} \frac{\partial w}{\partial y} \end{Bmatrix} \quad (3.1)$$

$$\boldsymbol{\varepsilon}^1 = \boldsymbol{\varepsilon}_L + \boldsymbol{\varepsilon}_{NL}^1 \quad (3.2)$$

$$\boldsymbol{\varepsilon}_L = \begin{Bmatrix} \frac{\partial u}{\partial x} \\ \frac{\partial v}{\partial y} \\ \frac{\partial u}{\partial y} + \frac{\partial v}{\partial x} \end{Bmatrix} = \begin{bmatrix} \frac{\partial}{\partial x} & 0 & 0 \\ 0 & \frac{\partial}{\partial y} & 0 \\ \frac{\partial}{\partial y} & \frac{\partial}{\partial x} & 0 \end{bmatrix} \begin{Bmatrix} u \\ v \\ w \end{Bmatrix} = \mathbf{L} \mathbf{U} \quad (3.3)$$

where the subscript 1 refers to the von Kármán model, and

$$\mathbf{L} = \begin{bmatrix} \frac{\partial}{\partial x} & 0 & 0 \\ 0 & \frac{\partial}{\partial y} & 0 \\ \frac{\partial}{\partial y} & \frac{\partial}{\partial x} & 0 \end{bmatrix} \quad (3.4)$$

From Equation 2.8,

$$\epsilon_L = B_L a \quad (3.5)$$

where

$$B_L = L N \quad (3.6)$$

With the help of Equation 2.9,

$$B_L = [B_L^1 | \dots | B_L^i | \dots | B_L^s] \quad (3.7)$$

where

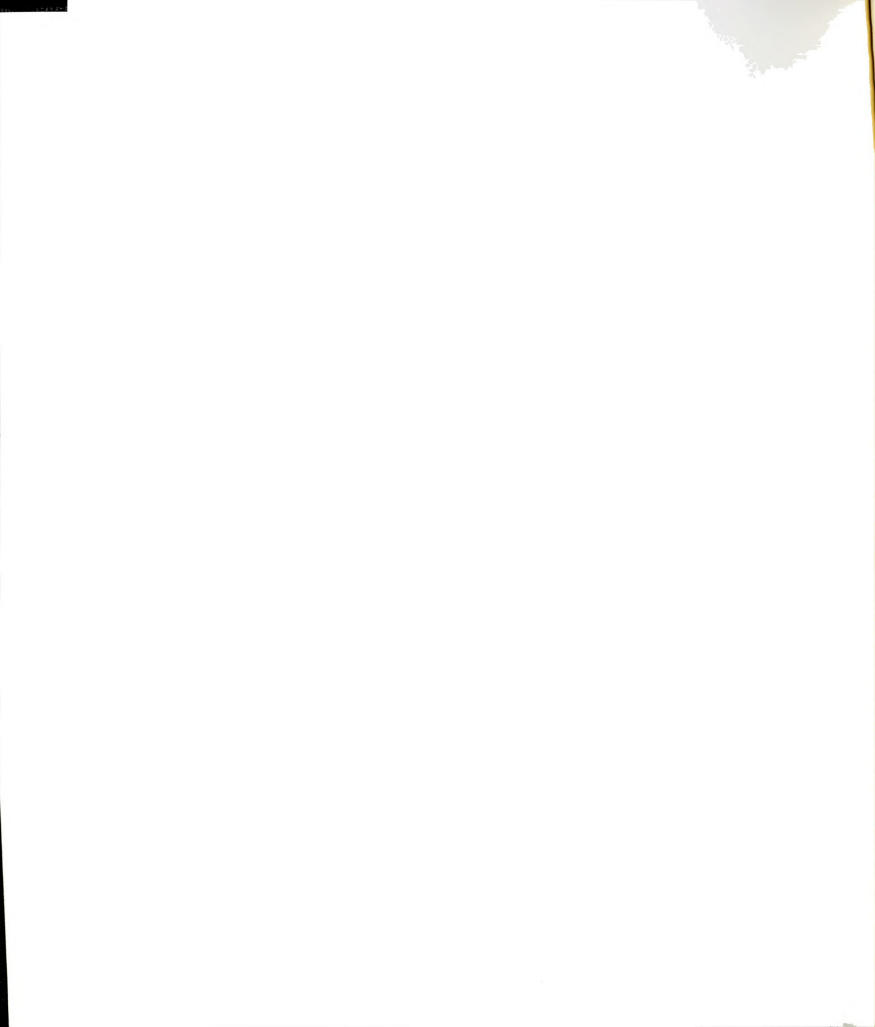
$$B_L^i = L [N_i I_3] = \begin{bmatrix} \frac{\partial N_i}{\partial x} & 0 & 0 \\ 0 & \frac{\partial N_i}{\partial y} & 0 \\ \frac{\partial N_i}{\partial y} & \frac{\partial N_i}{\partial x} & 0 \end{bmatrix} \quad (3.8)$$

also,

$$\epsilon_{NL}^i = \begin{Bmatrix} \frac{1}{2} \left(\frac{\partial w}{\partial x} \right)^2 \\ \frac{1}{2} \left(\frac{\partial w}{\partial y} \right)^2 \\ \frac{\partial w}{\partial x} \frac{\partial w}{\partial y} \end{Bmatrix} = \frac{1}{2} \begin{bmatrix} \frac{\partial w}{\partial x} & 0 \\ 0 & \frac{\partial w}{\partial y} \\ \frac{\partial w}{\partial y} & \frac{\partial w}{\partial x} \end{bmatrix} \begin{Bmatrix} \frac{\partial w}{\partial x} \\ \frac{\partial w}{\partial y} \end{Bmatrix} = \frac{1}{2} A_1 \theta_i \quad (3.9)$$

where

$$A_1 = \begin{bmatrix} \frac{\partial w}{\partial x} & 0 \\ 0 & \frac{\partial w}{\partial y} \\ \frac{\partial w}{\partial y} & \frac{\partial w}{\partial x} \end{bmatrix} \quad (3.10)$$



$$\theta = \begin{Bmatrix} \frac{\partial w}{\partial x} \\ \frac{\partial w}{\partial y} \end{Bmatrix} = \begin{bmatrix} 0 & 0 & \frac{\partial}{\partial x} \\ 0 & 0 & \frac{\partial}{\partial y} \end{bmatrix} \begin{Bmatrix} u \\ v \\ w \end{Bmatrix} = L' U \quad (3.11)$$

With the help of Equations 2.8 and 2.9,

$$\theta_1 = G_1 a \quad (3.12)$$

where

$$G_1 = [G_1^1 | \dots | G_1^i | \dots | G_1^8] \quad (3.13)$$

$$G_1^i = L' [N_i I_3] = \begin{bmatrix} 0 & 0 & \frac{\partial N_i}{\partial x} \\ 0 & 0 & \frac{\partial N_i}{\partial y} \end{bmatrix} \quad (3.14)$$

By taking the variation of Equation 3.2, and using Equations 3.5 and 3.9,

$$\delta \varepsilon^1 = \delta \varepsilon_L + \delta \varepsilon_{NL}^1 \quad (3.15)$$

$$\delta \varepsilon_L = B_L \delta a \quad (3.16)$$

$$\delta \varepsilon_{NL}^1 = \frac{1}{2} \delta A_1 \theta_1 + \frac{1}{2} A_1 \delta \theta_1 \quad (3.17)$$

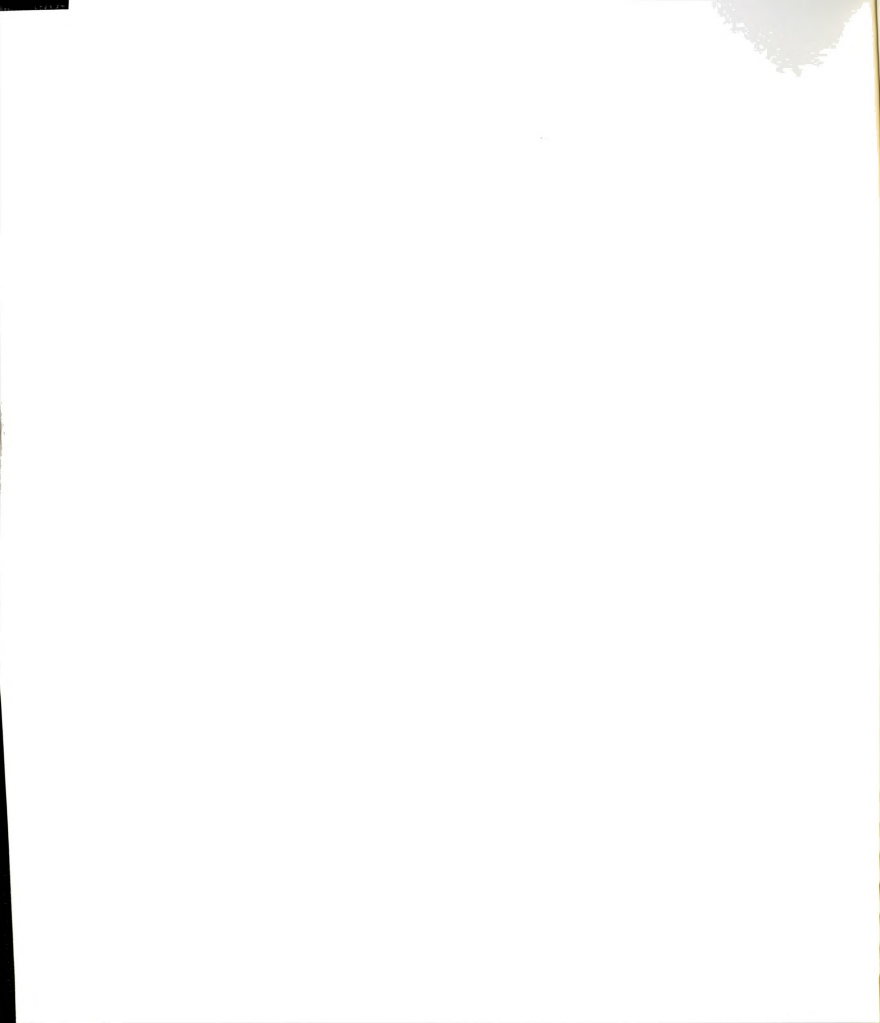
but

$$\delta A_1 \theta = A_1 \delta \theta \quad (3.18)$$

therefore

$$\delta \varepsilon_{NL}^1 = B_{NL1} \delta a \quad (3.19)$$

$$B_{NL1} = A_1 G_1 \quad (3.20)$$



With the help of Equation 3.13,

$$B_{NL1} = [B_{NL1}^1 | \dots | B_{NL1}^i | \dots | B_{NL1}^8] \quad (3.21)$$

$$B_{NL1}^i = \begin{bmatrix} 0 & 0 & \frac{\partial w}{\partial x} \frac{\partial N_i}{\partial x} \\ 0 & 0 & \frac{\partial w}{\partial y} \frac{\partial N_i}{\partial y} \\ 0 & 0 & \frac{\partial w}{\partial y} \frac{\partial N_i}{\partial x} + \frac{\partial w}{\partial x} \frac{\partial N_i}{\partial y} \end{bmatrix} \quad (3.22)$$

Using Equations 3.16 and 3.19,

$$\delta \epsilon_1 = B_1 \delta a \quad (3.23a)$$

$$B_1 = B_L + B_{NL1} \quad (3.23b)$$

Equation 3.2 becomes

$$\epsilon_1 = B_1' a \quad (3.24a)$$

$$B_1' = B_L + \frac{1}{2} B_{NL1} \quad (3.24b)$$

or, in a partitioned form

$$B_1' = [B_1'^1 | \dots | B_1'^i | \dots | B_1'^8] \quad (3.25a)$$

where

$$B_1'^i = B_L^i + \frac{1}{2} B_{NL1}^i \quad (3.25b)$$

$$B_1^H = \begin{bmatrix} \frac{\partial N_i}{\partial x} & 0 & \frac{1}{2} \frac{\partial N_i}{\partial x} \frac{\partial w}{\partial x} \\ 0 & \frac{\partial N_i}{\partial y} & \frac{1}{2} \frac{\partial N_i}{\partial y} \frac{\partial w}{\partial y} \\ \frac{\partial N_i}{\partial y} & \frac{\partial N_i}{\partial x} & \frac{1}{2} \left(\frac{\partial N_i}{\partial x} \frac{\partial w}{\partial y} + \frac{\partial N_i}{\partial y} \frac{\partial w}{\partial x} \right) \end{bmatrix} \quad (3.25c)$$

3.1.2 Derivation of Element Stiffness Matrices

In the following paragraphs, it is assumed that the loading is deformation-independent and the dimensions of each finite element are sufficiently small that the load intensity q is uniform over each element. Thus,

$$\mathbf{F} = q \int_{S_0} \mathbf{N}^T \mathbf{e}_z dS_0 \quad (3.26)$$

where \mathbf{e}_z is the unit vector normal to the membrane in its initial configuration.

The nonlinear equilibrium equations of the finite element model of the membrane problem are given by (see Equations 2.12 and 2.13):

$$\boldsymbol{\psi}(\mathbf{a}) = \int_{V_0} \mathbf{B}_1^T \boldsymbol{\sigma}_1 dV_0 - \mathbf{F} = 0 \quad (3.27)$$

By letting

$$\boldsymbol{\sigma}_1 = \frac{E}{1-\nu^2} \boldsymbol{\sigma}'_1 \quad \boldsymbol{\sigma}'_1 = \{\sigma'_x, \sigma'_y, \sigma'_{xy}\}^T \quad (3.28)$$

and using

$$dV_0 = h dS_0 \quad (3.29)$$

Equation 3.27 becomes

$$\Psi(\mathbf{a}) = \frac{Eh}{1-\nu^2} \int_{S_0} \mathbf{B}_1^T \boldsymbol{\sigma}'_1 dS_0 - \mathbf{F} = 0 \quad (3.30)$$

The tangent stiffness matrix is defined by

$$d\Psi = \mathbf{K}_{T1} d\mathbf{a} \quad (3.31)$$

Differentiating Equation 3.30 with respect to \mathbf{a} , and using the assumption that \mathbf{F} is independent of \mathbf{a} , gives

$$d\Psi = \frac{Eh}{1-\nu^2} \left(\int_{S_0} d\mathbf{B}_1^T \boldsymbol{\sigma}'_1 dS_0 + \int_{S_0} \mathbf{B}_1^T d\boldsymbol{\sigma}'_1 dS_0 \right) \quad (3.32)$$

The stress-strain relationship is

$$\boldsymbol{\sigma}_1 = \mathbf{D} \boldsymbol{\epsilon}_1 + \boldsymbol{\sigma}_0 \quad (3.33)$$

or equivalently

$$\boldsymbol{\sigma}'_1 = \mathbf{D}' \boldsymbol{\epsilon}_1 + \boldsymbol{\sigma}'_0 \quad (3.34)$$

where

$$\mathbf{D} = \frac{E}{1-\nu^2} \mathbf{D}' \quad \boldsymbol{\sigma}_0 = \frac{E}{1-\nu^2} \boldsymbol{\sigma}'_0 \quad (3.35)$$

$$\mathbf{D}' = \begin{bmatrix} 1 & \nu & 0 \\ \nu & 1 & 0 \\ 0 & 0 & \frac{1-\nu}{2} \end{bmatrix} \quad (3.36)$$

Using Equations 3.23a and 3.34,

$$d\boldsymbol{\sigma}'_1 = \mathbf{D}' d\boldsymbol{\epsilon}_1 = \mathbf{D}' \mathbf{B}_1 d\mathbf{a} \quad (3.37)$$

then

$$\int_{S_0} \mathbf{B}_1^T d\boldsymbol{\sigma}'_1 dS_0 = \int_{S_0} \mathbf{B}_1^T \mathbf{D}' \mathbf{B}_1 dS_0 d\mathbf{a} = (\mathbf{K}'_L + \mathbf{K}'_{NL1}) d\mathbf{a} \quad (3.38)$$

where

$$\mathbf{K}'_L = \int_{S_0} \mathbf{B}_L^T \mathbf{D}' \mathbf{B}_L dS_0 \quad (3.39)$$

$$\mathbf{K}'_{NL1} = \int_{S_0} (\mathbf{B}_L^T \mathbf{D}' \mathbf{B}_{NL1} + \mathbf{B}_{NL1}^T \mathbf{D}' \mathbf{B}_L + \mathbf{B}_{NL1}^T \mathbf{D}' \mathbf{B}_{NL1}) dS_0 \quad (3.40)$$

Also, using Equation 3.20,

$$\int_{S_0} d\mathbf{B}_1^T \boldsymbol{\sigma}'_1 dS_0 = \int_{S_0} \mathbf{G}_1^T d\mathbf{A}_1^T \boldsymbol{\sigma}'_1 dS_0 \quad (3.41)$$

$$d\mathbf{A}_1^T \boldsymbol{\sigma}'_1 = \begin{bmatrix} d\left(\frac{\partial w}{\partial x}\right) & 0 & d\left(\frac{\partial w}{\partial y}\right) \\ 0 & d\left(\frac{\partial w}{\partial y}\right) & d\left(\frac{\partial w}{\partial x}\right) \end{bmatrix} \begin{Bmatrix} \sigma'_x \\ \sigma'_y \\ \sigma'_{xy} \end{Bmatrix} = \begin{bmatrix} \sigma'_x & \sigma'_{xy} \\ \sigma'_{xy} & \sigma'_y \end{bmatrix} \begin{Bmatrix} d\left(\frac{\partial w}{\partial x}\right) \\ d\left(\frac{\partial w}{\partial y}\right) \end{Bmatrix} \quad (3.42)$$

$$d\mathbf{A}_1^T \boldsymbol{\sigma}'_1 = \mathbf{S}'_1 d\boldsymbol{\theta}_1 \quad (3.43)$$

where

$$\mathbf{S}'_1 = \begin{bmatrix} \sigma'_x & \sigma'_{xy} \\ \sigma'_{xy} & \sigma'_y \end{bmatrix} \quad (3.44)$$

using Equation 3.12,

$$d\boldsymbol{\theta}_1 = \mathbf{G}_1 d\mathbf{a} \quad (3.45)$$

$$\int_{S_0} d\mathbf{B}_1^T \boldsymbol{\sigma}'_1 dS_0 = \int_{S_0} \mathbf{G}_1^T \mathbf{S}'_1 \mathbf{G}_1 dS_0 d\mathbf{a} = \mathbf{K}'_{\sigma 1} d\mathbf{a} \quad (3.46)$$

and

$$\mathbf{K}'_{\sigma 1} = \int_{S_0} \mathbf{G}_1^T \mathbf{S}'_1 \mathbf{G}_1 dS_0 \quad (3.47)$$

$$\mathbf{K}_{T1} = \frac{Eh}{1-\nu^2} \mathbf{K}'_{T1} \quad (3.48)$$

where

$$\mathbf{K}'_{T1} = \mathbf{K}'_L + \mathbf{K}'_{NL1} + \mathbf{K}'_{\sigma 1} \quad (3.49)$$

or, alternatively

$$\mathbf{K}_{T1} = \mathbf{K}_L + \mathbf{K}_{NL1} + \mathbf{K}_{\sigma 1} \quad (3.50)$$

\mathbf{K}_{T1} is the element tangential stiffness matrix

$$\mathbf{K}_L = \frac{Eh}{1-\nu^2} \mathbf{K}'_L \quad (3.51a)$$

\mathbf{K}_L is the linear element stiffness matrix

$$\mathbf{K}_{NL1} = \frac{Eh}{1-\nu^2} \mathbf{K}'_{NL1} \quad (3.51b)$$

\mathbf{K}_{NL1} is the nonlinear element stiffness matrix, also termed the geometric stiffness matrix

$$\mathbf{K}_{\sigma 1} = \frac{Eh}{1-\nu^2} \mathbf{K}'_{\sigma 1} \quad (3.51c)$$

and $\mathbf{K}_{\sigma 1}$ is the element stress matrix.

The components of \mathbf{s}'_1 are given by

$$\left. \begin{aligned} \sigma'_x &= \varepsilon_x + \nu \varepsilon_y + \sigma'_{0x} \\ \sigma'_y &= \nu \varepsilon_x + \varepsilon_y + \sigma'_{0y} \\ \sigma'_{xy} &= \frac{1-\nu}{2} \varepsilon_{xy} + \sigma'_{0xy} \end{aligned} \right\} \quad (3.52)$$

3.2 Rearrangement of Element Stiffness Matrices for Computer Implementation

3.2.1 Numerical Integration

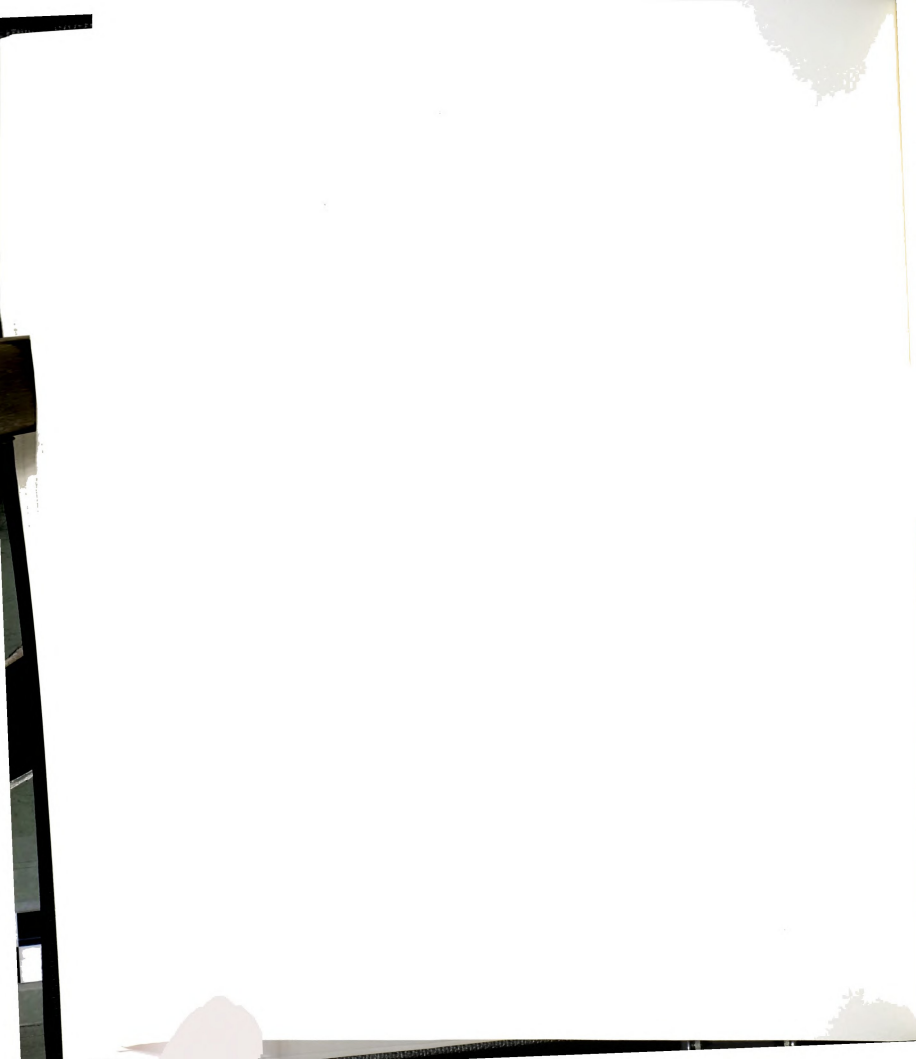
To be able to evaluate the element stiffness matrices, it is necessary to compute the basic element matrices B_L , B_{NLI} , and G_1 . These matrices are obtained in terms of derivatives of element displacements or element shape functions with respect to the local coordinates. The derivatives should be expressed in terms of derivatives with respect to the natural coordinates r and s as follows

$$\begin{Bmatrix} \frac{\partial}{\partial x} \\ \frac{\partial}{\partial y} \end{Bmatrix} = J^{-1} \begin{Bmatrix} \frac{\partial}{\partial r} \\ \frac{\partial}{\partial s} \end{Bmatrix} \quad (3.53)$$

where J is the Jacobian matrix defined as

$$J = \begin{bmatrix} \frac{\partial x}{\partial r} & \frac{\partial y}{\partial r} \\ \frac{\partial x}{\partial s} & \frac{\partial y}{\partial s} \end{bmatrix} \quad (3.54)$$

Also the element surface is expressed as



$$dS_0 = J dr ds \quad (3.55)$$

where J is the determinant of the Jacobian matrix.

The general expression of element stiffness matrices can then be written as

$$\mathbf{K}' = \int_{S_0} \mathbf{K}'_0 dS_0 = \int_{-1}^1 \int_{-1}^1 \mathbf{K}'_0(r, s) J(r, s) dr ds \quad (3.56)$$

To evaluate explicitly the surface integrals in the expressions of element matrices is not effective. Therefore, numerical integration is employed. In fact, numerical integration is an integral part of the isoparametric element matrix evaluations. Practically, when using this numerical integration procedure a choice should be made concerning the kind of integration scheme and the order of integration. Gauss quadrature was chosen because it requires fewer function evaluations to get accurate results. However, it should be mentioned that the Newton-Cotes formulas also may be efficient¹⁹. According to Bathe¹⁹, a third order Gaussian-quadrature is a reliable integration order for an eight-node isoparametric element.

Using numerical integration, Equation 3.56 may be written as:

$$\mathbf{K}' = \sum_{i=1}^3 \sum_{j=1}^3 \mathbf{K}'_0(r_i, s_j) J(r_i, s_j) w_i w_j \quad (3.57)$$

where r_i , and s_j are the natural coordinates of Gauss points, and w_i , and w_j are the corresponding Gauss weights.

The expression of the load vector F can be written as

$$F = q \int_{S_0} F_0 dS_0 = q \int_{-1}^{-1} \int_{-1}^{-1} F_0(r, s) J(r, s) dr ds \quad (3.58)$$

where

$$F_0 = N^T e_s \quad (3.59)$$

or, by using numerical integration

$$F = q \sum_{i=1}^3 \sum_{j=1}^3 F_0(r_i, s_j) J(r_i, s_j) w_i w_j \quad (3.60)$$

The element internal force vector P appearing in the right-hand side of Equation 2.23 may be written as

$$P_1 = \frac{Eh}{1-\nu^2} \int_{S_0} B_1^T \sigma'_1 dS_0 \quad (3.61)$$

$$P_1 = \frac{Eh}{1-\nu^2} \int_{S_0} P_{0,1} dS_0 = \frac{Eh}{1-\nu^2} \int_{-1}^{-1} \int_{-1}^{-1} P_{0,1}(r, s) J(r, s) dr ds \quad (3.62)$$

where

$$P_{0,1} = B_1^T \sigma'_1 \quad (3.63)$$

or, using numerical integration

$$P_1 = \frac{Eh}{1-\nu^2} \sum_{i=1}^3 \sum_{j=1}^3 P_{0,1}(r_i, s_j) J(r_i, s_j) w_i w_j \quad (3.64)$$

For clarity, the arguments r and s will be dropped in the following paragraphs.

3.2.2 Rearrangement of Element Matrices

The derived expressions of element matrices are very general. To allow easy implementation of these matrices in a

computer program, the partitioning properties of matrices will be used.

Because an element has eight nodes with three degrees of freedom each, the element stiffness matrices will be of order 24. By taking advantage of the general form of the elementary matrices B_L , G_L , and B_{NL1} (Equations 3.7, 3.13, and 3.21), and using partitioning, all the element stiffness matrices K'_0 may be put in the following form:

$$K'_0 = \begin{bmatrix} \cdot & \cdot & \cdot \\ \cdot & [K'^{ij}_{0L}]_{3 \times 3} & \cdot \\ \cdot & \cdot & \cdot \end{bmatrix} \quad (3.65)$$

where i is a row index, and j is a column index, both taking values from 1 to 8. K is thus partitioned into 64 submatrices K'^{ij}_{0L} of order three. The expressions of the typical submatrix for each element stiffness matrix are given by

$$K'^{ij}_{0L} = B_L^{iT} D' B_L^j \quad (3.66)$$

$$K'_{0NL1} = K'_{0NL1,1} + K'_{0NL1,2} + K'_{0NL1,3} \quad (3.67)$$

where

$$K_{0NL1,1}^{ij} = B_L^{iT} D' B_{NL1}^j \quad (3.68a)$$

$$K_{0NL1,2}^{ij} = B_{NL1}^{iT} D' B_L^j \quad (3.68b)$$

$$K_{0NL1,3}^{ij} = B_{NL1}^{iT} D' B_{NL1}^j \quad (3.68c)$$

$$K_{0\sigma 1}^{ij} = G_1^{iT} S_1' G_1^j \quad (3.69)$$

The load vector integrand F_0 may also be written in a partitioned form as

$$F_0 = [F_0^{1^T} | \dots | F_0^{i^T} | \dots | F_0^{8^T}]^T \quad (3.70)$$

where

$$F_0^i = N_i I_3 e_x = N_i e_x = \begin{Bmatrix} 0 \\ 0 \\ N_i \end{Bmatrix} \quad (3.71)$$

3.3 Nondimensional Formulation of the Incremental Equilibrium Equations

Instead of dealing with all the parameters involved in membrane analysis in its original form, it is more interesting to recast the above formulation in a nondimensional form. This has the advantage of reducing the number of parameters involved by grouping them into a smaller number. In addition, solving one problem gives the solution of a whole class of problems.



The variables L_1 , L_2 , h , E , ν , q and W defining the membrane problem may be related by a function:

$$f_1(L_1, L_2, h, E, \nu, W) = 0 \quad (3.72)$$

where

L_1 , L_2 are two orthogonal representative dimensions of the membrane in its plane, and W is a representative displacement of an arbitrary membrane point e.g. one of the displacement components u , v , w .

Using the Pi Theorem²³, a relation equivalent to Equation 3.72, but expressed in terms of nondimensional parameters, can be found:

$$f_2(\pi_1, \pi_2, \pi_3, \pi_4, \pi_5) = 0 \quad (3.73)$$

where

$$\pi_1 = \nu; \quad \pi_2 = \frac{L_2}{L_1}; \quad \pi_3 = \frac{L_1}{h}; \quad \pi_4 = \frac{q}{E}; \quad \pi_5 = \frac{W}{L_1} \quad (3.74)$$

or, alternatively, by combining dimensionless parameters

$$W = L_1 f_2\left(\nu, \frac{L_2}{L_1}, \frac{h}{L_1}, \frac{qL_1}{Eh}\right) \quad (3.75)$$

It is clear that the nondimensionless parameter qL_1/Eh is the most important among the four dimensionless parameters included in Equation 3.75.

To permit comparison with previous work, the following relationships are used⁸:

$$k = 2(1-\nu^2) \frac{qL}{Eh} \quad (3.76)$$

$$x = L\tilde{x}; \quad y = L\tilde{y} \quad (3.77a)$$

$$u = Lk^{\frac{2}{3}}\tilde{u} \quad v = Lk^{\frac{2}{3}}\tilde{v} \quad w = Lk^{\frac{1}{3}}\tilde{w} \quad (3.77b)$$

$$\tilde{\mathbf{a}} = \{\tilde{u}_1, \tilde{v}_1, \tilde{w}_1, \dots, \tilde{u}_8, \tilde{v}_8, \tilde{w}_8\}^T \quad (3.77c)$$

where L replaces L_1 and the factor $2(1-\nu^2)$ is introduced.

Then, it may be shown that

$$\mathbf{a} = Lk^{\frac{1}{3}}\mathbf{M}\tilde{\mathbf{a}} \quad (3.78a)$$

where \mathbf{M} is a 24 by 24 diagonal matrix written in a partitioned form as

$$\mathbf{M} = \begin{bmatrix} \mathbf{M}_0 & 0 & 0 & 0 & 0 & 0 & 0 & 0 \\ 0 & \mathbf{M}_0 & 0 & 0 & 0 & 0 & 0 & 0 \\ 0 & 0 & \mathbf{M}_0 & 0 & 0 & 0 & 0 & 0 \\ 0 & 0 & 0 & \mathbf{M}_0 & 0 & 0 & 0 & 0 \\ 0 & 0 & 0 & 0 & \mathbf{M}_0 & 0 & 0 & 0 \\ 0 & 0 & 0 & 0 & 0 & \mathbf{M}_0 & 0 & 0 \\ 0 & 0 & 0 & 0 & 0 & 0 & \mathbf{M}_0 & 0 \\ 0 & 0 & 0 & 0 & 0 & 0 & 0 & \mathbf{M}_0 \end{bmatrix} \quad (3.78b)$$

$$\mathbf{M}_0 = \begin{bmatrix} k^{\frac{1}{3}} & 0 & 0 \\ 0 & k^{\frac{1}{3}} & 0 \\ 0 & 0 & 1 \end{bmatrix} \quad (3.78c)$$

and $\mathbf{0}$ is a 3 by 3 null matrix.



If the variables with the tilde symbol are the "nondimensional variables", then

$$dS_0 = L^2 d\tilde{S}_0 \quad J = L^2 \tilde{J} \quad (3.79a)$$

$$\frac{\partial u}{\partial x} = k^{\frac{2}{3}} \frac{\partial \tilde{u}}{\partial \tilde{x}}; \quad \frac{\partial v}{\partial x} = k^{\frac{2}{3}} \frac{\partial \tilde{v}}{\partial \tilde{x}}; \quad \frac{\partial w}{\partial x} = k^{\frac{1}{3}} \frac{\partial \tilde{w}}{\partial \tilde{x}} \quad (3.79b)$$

$$\frac{\partial u}{\partial y} = k^{\frac{2}{3}} \frac{\partial \tilde{u}}{\partial \tilde{y}}; \quad \frac{\partial v}{\partial y} = k^{\frac{2}{3}} \frac{\partial \tilde{v}}{\partial \tilde{y}}; \quad \frac{\partial w}{\partial y} = k^{\frac{1}{3}} \frac{\partial \tilde{w}}{\partial \tilde{y}} \quad (3.79c)$$

$$\mathbf{e}_1 = k^{\frac{2}{3}} \tilde{\mathbf{e}}_1 \quad (3.80)$$

Equating Equations 3.24a, and 3.80, and using the two following relationships:

$$\tilde{\mathbf{B}}_L \mathbf{M} = k^{\frac{1}{3}} \tilde{\mathbf{B}}_L \quad \tilde{\mathbf{B}}_{NL1} \mathbf{M} = \tilde{\mathbf{B}}_{NL1} \quad (3.81)$$

$$\tilde{\mathbf{e}}_1 = \tilde{\mathbf{B}}_1' \tilde{\mathbf{a}} \quad (3.82a)$$

where

$$\tilde{\mathbf{B}}_1' = \tilde{\mathbf{B}}_L + \frac{1}{2} \tilde{\mathbf{B}}_{NL1} \quad (3.82b)$$

Then

$$\sigma_1' = k^{\frac{2}{3}} \tilde{\sigma}_1' \quad (3.83a)$$

$$s_1' = k^{\frac{2}{3}} \tilde{s}_1' \quad (3.83b)$$

The nondimensional stress-strain relationships are

$$\tilde{\sigma}'_1 = D' \tilde{\epsilon}_1 + \tilde{\sigma}'_0 \quad \sigma'_0 = k^{\frac{2}{3}} \tilde{\sigma}'_0 \quad (3.84)$$

Also

$$\left. \begin{aligned} \mathbf{A}_1 &= k^{\frac{1}{3}} \tilde{\mathbf{A}}_1; & \mathbf{G}_1 &= \frac{1}{L} \tilde{\mathbf{G}}_1 \\ \mathbf{B}_L &= \frac{1}{L} \tilde{\mathbf{B}}_L; & \mathbf{B}_{NL1} &= \frac{k^{\frac{1}{3}}}{L} \tilde{\mathbf{B}}_{NL1} \end{aligned} \right\} \quad (3.85)$$

$$\mathbf{B}_1 = \frac{1}{L} \tilde{\mathbf{B}}_1 \quad (3.86a)$$

$$\tilde{\mathbf{B}}_1 = \tilde{\mathbf{B}}_L + k^{\frac{1}{3}} \tilde{\mathbf{B}}_{NL1} \quad (3.86b)$$

Therefore

$$\mathbf{K}_{0L}^{(1j)} = \frac{1}{L^2} \tilde{\mathbf{K}}_{0L}^{(1j)} \quad (3.87)$$

$$\mathbf{K}_{0NL1,1}^{(1j)} = \frac{k^{\frac{1}{3}}}{L^2} \tilde{\mathbf{K}}_{0NL1,1}^{(1j)} \quad (3.88a)$$

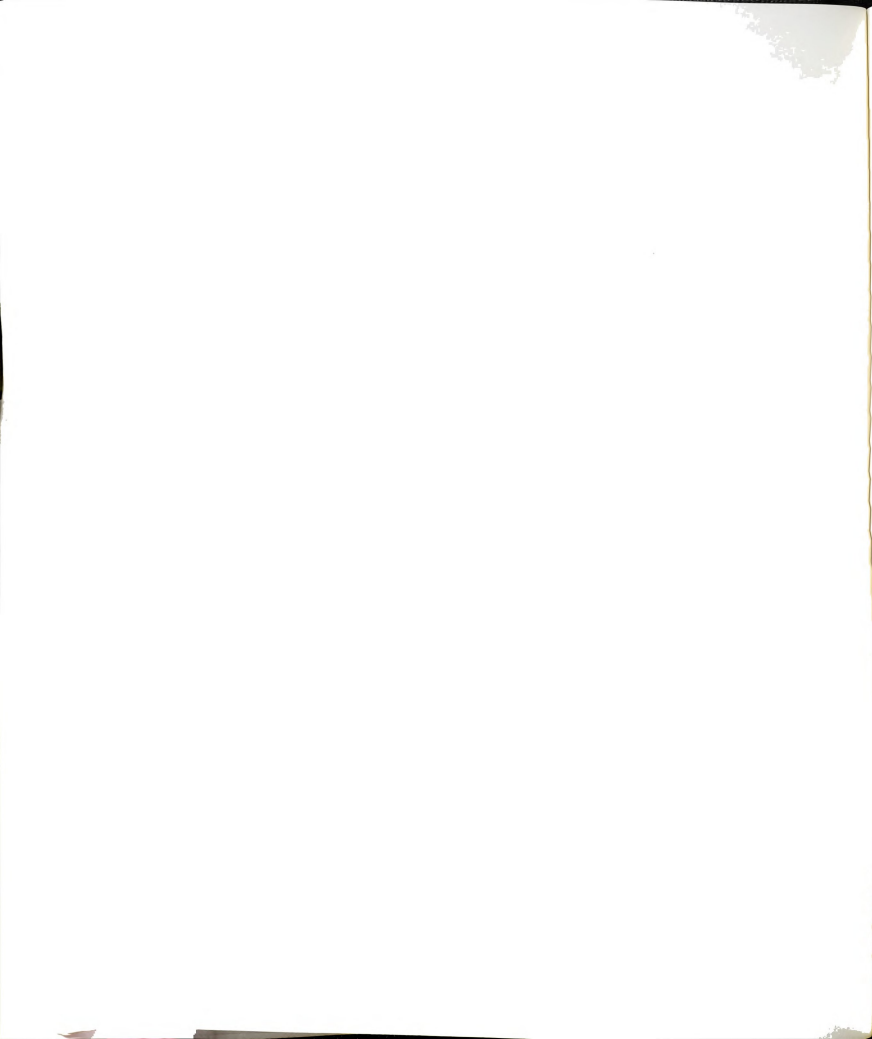
$$\mathbf{K}_{0NL1,2}^{(1j)} = \frac{k^{\frac{1}{3}}}{L^2} \tilde{\mathbf{K}}_{0NL1,2}^{(1j)} \quad (3.88b)$$

$$\mathbf{K}_{0NL1,3}^{(1j)} = \frac{k^{\frac{2}{3}}}{L^2} \tilde{\mathbf{K}}_{0NL1,3}^{(1j)} \quad (3.88c)$$

Then

$$\mathbf{K}_{0NL1}^{(1j)} = \frac{k^{\frac{1}{3}}}{L^2} \tilde{\mathbf{K}}_{0NL1}^{(1j)} \quad (3.89a)$$

where



$$\tilde{K}_{0NL1}^{ij} = \tilde{K}_{0NL1,1}^{ij} + \tilde{K}_{0NL1,2}^{ij} + k^{\frac{1}{3}} \tilde{K}_{0NL1,3}^{ij} \quad (3.89b)$$

Also

$$K_{0\sigma 1}^{ij} = \frac{k^{\frac{2}{3}}}{L^2} \tilde{K}_{0\sigma 1}^{ij} \quad (3.90)$$

Then, with

$$K_{0T1}^{ij} = K_{0L}^{ij} + K_{0NL1}^{ij} + K_{0\sigma 1}^{ij} \quad (3.91)$$

$$K_{0T1}^{ij} = \frac{1}{L^2} \tilde{K}_{0T1}^{ij} \quad (3.92)$$

where

$$\tilde{K}_{0T1}^{ij} = \tilde{K}_{0L}^{ij} + k^{\frac{1}{3}} \tilde{K}_{0NL1}^{ij} + k^{\frac{2}{3}} \tilde{K}_{0\sigma 1}^{ij} \quad (3.93)$$

Also

$$K_{0T1}^{ij} M_0 = \frac{k^{\frac{1}{3}}}{L^2} \tilde{K}_{0T1}^{ij*} \quad (3.94)$$

where

$$\tilde{K}_{0T1}^{ij*} = \tilde{K}_{0L}^{ij} + \tilde{K}_{0NL1,1}^{ij} + k^{\frac{1}{3}} (\tilde{K}_{0NL1,2}^{ij} + \tilde{K}_{0NL1,3}^{ij} + \tilde{K}_{0\sigma 1}^{ij}) \quad (3.95)$$

and

$$\tilde{K}_{0T1}^{ij*}(1,1) = \frac{\partial N_i}{\partial \tilde{x}} \frac{\partial N_j}{\partial \tilde{x}} + \frac{1-\nu}{2} \frac{\partial N_i}{\partial \tilde{y}} \frac{\partial N_j}{\partial \tilde{y}} \quad (3.96a)$$

$$\tilde{K}_{0T1}^{ij*}(1,2) = \nu \frac{\partial N_i}{\partial \tilde{x}} \frac{\partial N_j}{\partial \tilde{y}} + \frac{1-\nu}{2} \frac{\partial N_i}{\partial \tilde{y}} \frac{\partial N_j}{\partial \tilde{x}} \quad (3.96b)$$

$$\tilde{K}_{0T1}^{ij*}(1,3) = \frac{\partial N_i}{\partial \bar{x}} \left(\frac{\partial N_j}{\partial \bar{x}} \frac{\partial \tilde{w}}{\partial \bar{x}} + \nu \frac{\partial N_j}{\partial \bar{y}} \frac{\partial \tilde{w}}{\partial \bar{y}} \right) + \frac{1-\nu}{2} \frac{\partial N_i}{\partial \bar{y}} \left(\frac{\partial N_j}{\partial \bar{x}} \frac{\partial \tilde{w}}{\partial \bar{y}} + \frac{\partial N_j}{\partial \bar{y}} \frac{\partial \tilde{w}}{\partial \bar{x}} \right) \quad (3.96c)$$

$$\tilde{K}_{0T1}^{ij*}(2,1) = \nu \frac{\partial N_i}{\partial \bar{y}} \frac{\partial N_j}{\partial \bar{x}} + \frac{1-\nu}{2} \frac{\partial N_i}{\partial \bar{x}} \frac{\partial N_j}{\partial \bar{y}} \quad (3.96d)$$

$$\tilde{K}_{0T1}^{ij*}(2,2) = \frac{\partial N_i}{\partial \bar{y}} \frac{\partial N_j}{\partial \bar{y}} + \frac{1-\nu}{2} \frac{\partial N_i}{\partial \bar{x}} \frac{\partial N_j}{\partial \bar{x}} \quad (3.96e)$$

$$\tilde{K}_{0T1}^{ij*}(2,3) = \frac{\partial N_i}{\partial \bar{y}} \left(\nu \frac{\partial N_j}{\partial \bar{x}} \frac{\partial \tilde{w}}{\partial \bar{x}} + \frac{\partial N_j}{\partial \bar{y}} \frac{\partial \tilde{w}}{\partial \bar{y}} \right) + \frac{1-\nu}{2} \frac{\partial N_i}{\partial \bar{x}} \left(\frac{\partial N_j}{\partial \bar{x}} \frac{\partial \tilde{w}}{\partial \bar{y}} + \frac{\partial N_j}{\partial \bar{y}} \frac{\partial \tilde{w}}{\partial \bar{x}} \right) \quad (3.96f)$$

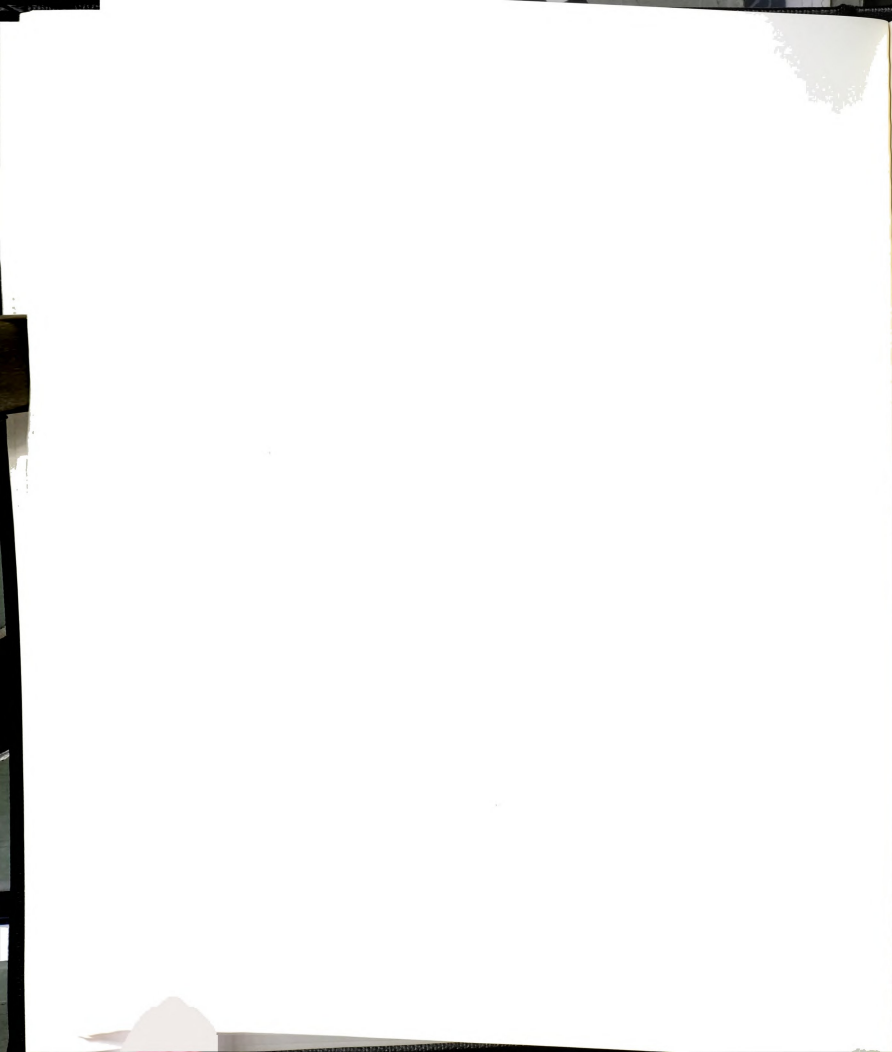
$$\tilde{K}_{0T1}^{ij*}(3,1) = k^{\frac{1}{3}} \left[\frac{\partial N_j}{\partial \bar{x}} \left(\frac{\partial N_i}{\partial \bar{x}} \frac{\partial \tilde{w}}{\partial \bar{x}} + \nu \frac{\partial N_i}{\partial \bar{y}} \frac{\partial \tilde{w}}{\partial \bar{y}} \right) + \frac{1-\nu}{2} \frac{\partial N_j}{\partial \bar{y}} \left(\frac{\partial N_i}{\partial \bar{x}} \frac{\partial \tilde{w}}{\partial \bar{y}} + \frac{\partial N_i}{\partial \bar{y}} \frac{\partial \tilde{w}}{\partial \bar{x}} \right) \right] \quad (3.96g)$$

$$\tilde{K}_{0T1}^{ij*}(3,2) = k^{\frac{1}{3}} \left[\frac{\partial N_j}{\partial \bar{y}} \left(\nu \frac{\partial N_i}{\partial \bar{x}} \frac{\partial \tilde{w}}{\partial \bar{x}} + \frac{\partial N_i}{\partial \bar{y}} \frac{\partial \tilde{w}}{\partial \bar{y}} \right) + \frac{1-\nu}{2} \frac{\partial N_j}{\partial \bar{x}} \left(\frac{\partial N_i}{\partial \bar{x}} \frac{\partial \tilde{w}}{\partial \bar{y}} + \frac{\partial N_i}{\partial \bar{y}} \frac{\partial \tilde{w}}{\partial \bar{x}} \right) \right] \quad (3.96h)$$

$$\begin{aligned} \tilde{K}_{0T1}^{ij*}(3,3) = k^{\frac{1}{3}} & \left[\frac{\partial N_i}{\partial \bar{x}} \frac{\partial \tilde{w}}{\partial \bar{x}} \left(\frac{\partial N_j}{\partial \bar{x}} \frac{\partial \tilde{w}}{\partial \bar{x}} + \nu \frac{\partial N_j}{\partial \bar{y}} \frac{\partial \tilde{w}}{\partial \bar{y}} \right) \right. \\ & + \frac{\partial N_i}{\partial \bar{y}} \frac{\partial \tilde{w}}{\partial \bar{y}} \left(\frac{\partial N_j}{\partial \bar{y}} \frac{\partial \tilde{w}}{\partial \bar{y}} + \nu \frac{\partial N_j}{\partial \bar{x}} \frac{\partial \tilde{w}}{\partial \bar{x}} \right) \\ & + \frac{1-\nu}{2} \left(\frac{\partial N_i}{\partial \bar{x}} \frac{\partial \tilde{w}}{\partial \bar{y}} + \frac{\partial N_i}{\partial \bar{y}} \frac{\partial \tilde{w}}{\partial \bar{x}} \right) \left(\frac{\partial N_j}{\partial \bar{x}} \frac{\partial \tilde{w}}{\partial \bar{y}} + \frac{\partial N_j}{\partial \bar{y}} \frac{\partial \tilde{w}}{\partial \bar{x}} \right) \\ & \left. + \frac{\partial N_i}{\partial \bar{x}} \left(\sigma'_{xy} \frac{\partial N_j}{\partial \bar{x}} + \sigma'_{xy} \frac{\partial N_j}{\partial \bar{y}} \right) + \frac{\partial N_i}{\partial \bar{y}} \left(\sigma'_{xy} \frac{\partial N_j}{\partial \bar{x}} + \sigma'_{xy} \frac{\partial N_j}{\partial \bar{y}} \right) \right] \quad (3.96i) \end{aligned}$$

Using Equations 3.57, 3.65, 3.78, 3.79a, 3.92 and 3.94,

$$\mathbf{K}'_{T1} = \tilde{\mathbf{K}}'_{T1} \quad (3.97a)$$



$$\tilde{\mathbf{K}}'_{T1} \mathbf{M} = k^{\frac{1}{3}} \tilde{\mathbf{K}}'^*_{T1} \quad (3.97b)$$

Also, with the help of Equations 3.58 and 3.59,

$$\mathbf{F}_0 = \tilde{\mathbf{F}}_0 \quad \mathbf{F} = L^2 \tilde{\mathbf{F}} \quad (3.98)$$

where

$$\left. \begin{aligned} \tilde{\mathbf{F}} &= q \tilde{\mathbf{F}}' \\ \tilde{\mathbf{F}}' &= \sum_{i=1}^3 \sum_{j=1}^3 \tilde{\mathbf{F}}_0(r_i, s_j) \tilde{J}(r_i, s_j) w_i w_j \end{aligned} \right\} \quad (3.99)$$

Also, using Equations 3.63 and 3.64,

$$P_{0,1} = \frac{k^{\frac{2}{3}}}{L} \tilde{P}_{0,1} \quad P_1 = L k^{\frac{2}{3}} \tilde{P}_1 \quad (3.100)$$

$$\left. \begin{aligned} \tilde{P}_1 &= \frac{Eh}{1-\nu^2} \tilde{P}'_1 \\ \tilde{P}'_1 &= \sum_{i=1}^3 \sum_{j=1}^3 \tilde{P}_{0,1}(r_i, s_j) \tilde{J}(r_i, s_j) w_i w_j \end{aligned} \right\} \quad (3.101)$$

Using Equation 3.76,

$$P_1 = \frac{2qL^2}{k^{\frac{1}{3}}} \tilde{P}'_1 \quad (3.102)$$

The incremental equilibrium equations are given by Equation 2.23. If the indices m and i are dropped, this equation may be written as

$$\mathbf{K}_{T1} \Delta \mathbf{a} = \mathbf{F} - \mathbf{P}_1 \quad (3.103)$$

Using Equations 3.48, 3.76, 3.78, 3.97, 3.98, 3.99, and 3.102, Equation 3.103 becomes

If Δq_j is the incremental load at the j th increment where $j \leq m$, the load intensity at the m th increment is

$$q_m = \sum_{j=1}^m \Delta q_j \quad (3.105)$$

Letting

$$\beta_j = \frac{\Delta q_j}{q} \quad \alpha_m = \sum_{j=1}^m \beta_j \quad k_m = \frac{2q_m L}{Eh} (1 - \nu^2) \quad (3.106)$$

gives

$$q_m = \alpha_m q \quad k_m = \alpha_m k \quad (3.107)$$

If k is replaced by k_m , the incremental equilibrium equation becomes

$$[\tilde{\mathbf{K}}_{\mathbf{II}}]_m^{(i-1)} \{\Delta \tilde{\mathbf{a}}\}_m^{(i)} = \frac{\alpha_m^{\frac{1}{3}}}{2} k^{\frac{1}{3}} \tilde{\mathbf{F}}_m^{(i)} - \tilde{\mathbf{F}}_{1m}^{(i-1)} \quad (3.108)$$

Equation 3.108 has been derived for an arbitrary element. However, it still represents the structure's fundamental equation, provided each term contained in this equation be regarded as the equivalent term corresponding to the assembled structure. The assemblage procedure will be discussed in Chapter 5.



4. Extension to the General Nonlinear Model

4.1 Derivation of Element Matrices

4.1.1 Derivation of the Basic Element Matrices

The general strain-displacement relationships are defined by Equations 1.10-11-12. Rewriting these three equations in matrix form gives

$$\epsilon_2 = \epsilon_1 + \Delta \epsilon \quad (4.1)$$

where the subscripts 1 and 2 refer to the von Kármán model and to the general model, respectively, and

$$\Delta \epsilon = \begin{Bmatrix} \Delta \epsilon_x \\ \Delta \epsilon_y \\ \Delta \epsilon_{xy} \end{Bmatrix} = \frac{1}{2} \begin{Bmatrix} \left(\frac{\partial u}{\partial x} \right)^2 + \left(\frac{\partial v}{\partial x} \right)^2 \\ \left(\frac{\partial u}{\partial y} \right)^2 + \left(\frac{\partial v}{\partial y} \right)^2 \\ 2 \left(\frac{\partial u}{\partial x} \frac{\partial u}{\partial y} + \frac{\partial v}{\partial x} \frac{\partial v}{\partial y} \right) \end{Bmatrix} \quad (4.2)$$

or

$$\Delta \epsilon = \frac{1}{2} \mathbf{A}_2 \theta_2 \quad (4.3)$$

where

$$\theta = \left\{ \frac{\partial u}{\partial x}, \frac{\partial v}{\partial x}, \frac{\partial u}{\partial y}, \frac{\partial v}{\partial y} \right\}^T \quad (4.4a)$$



$$\mathbf{A}_2 = \begin{bmatrix} \frac{\partial u}{\partial x} & \frac{\partial v}{\partial x} & 0 & 0 \\ 0 & 0 & \frac{\partial u}{\partial y} & \frac{\partial v}{\partial y} \\ \frac{\partial u}{\partial y} & \frac{\partial v}{\partial y} & \frac{\partial u}{\partial x} & \frac{\partial v}{\partial x} \end{bmatrix} \quad (4.4b)$$

also

$$\theta_2 = \mathbf{G}_2 \mathbf{a} \quad (4.5)$$

where

$$\mathbf{G}_2 = [\mathbf{G}_2^1 | \dots | \mathbf{G}_2^i | \dots | \mathbf{G}_2^8] \quad (4.6a)$$

$$\mathbf{G}_2^i = \begin{bmatrix} \frac{\partial N_i}{\partial x} & 0 & 0 \\ 0 & \frac{\partial N_i}{\partial x} & 0 \\ \frac{\partial N_i}{\partial y} & 0 & 0 \\ 0 & \frac{\partial N_i}{\partial y} & 0 \end{bmatrix} \quad (4.6b)$$

Differentiating Equation 4.1, there results

$$d\epsilon_2 = d\epsilon_1 + d\Delta\epsilon \quad (4.7)$$

$$d\Delta\epsilon = \frac{1}{2} d\mathbf{A}_2 \theta_2 + \frac{1}{2} \mathbf{A}_2 d\theta_2 \quad (4.8)$$

Using

$$d\mathbf{A}_2 \theta_2 = \mathbf{A}_2 d\theta_2 \quad (4.9)$$

$$d\Delta\epsilon = \mathbf{A}_2 d\theta_2 = \mathbf{A}_2 \mathbf{G}_2 d\mathbf{a} \quad (4.10)$$

then

$$d\Delta \epsilon = \Delta B da \quad (4.11)$$

where

$$\Delta B = \Lambda_2 G_2 \quad (4.12)$$

Therefore

$$d\epsilon_2 = B_2 da \quad (4.13)$$

$$B_2 = B_1 + \Delta B \quad (4.14)$$

Also using Equations 3.25a, 4.1 and 4.13, gives

$$\epsilon_2 = \dot{B}_2 a \quad (4.15)$$

where \dot{B}_2 is the strain-displacement matrix corresponding to the general model and is given by

$$\dot{B}_2 = \dot{B}_1 + \frac{1}{2} \Delta B \quad (4.16)$$

4.1.2 Derivation of Element Stiffness Matrices

Similarly to the the von Kármán model, the tangential stiffness for the general model may be written as

$$K_{T2} = \frac{Eh}{1-\nu^2} K'_{T2} \quad (4.17)$$

where

$$K'_{T2} = K'_L + K'_{NL2} + K'_{\sigma 2} \quad (4.18)$$

With the help of the equations derived in the previous paragraph together with those derived in Chapter 3, and using



the same matrix techniques, the following equations may be written

$$\mathbf{K}'_{NL2} = \mathbf{K}'_{NL1} + \Delta \mathbf{K}'_{NL} \quad (4.19)$$

$$\mathbf{K}'_{\sigma 2} = \mathbf{K}'_{\sigma 1} + \Delta \mathbf{K}'_{\sigma} \quad (4.20)$$

where

$$\Delta \mathbf{K}'_{NL} = \Delta \mathbf{K}'_{NL1} + \Delta \mathbf{K}'_{NL2} \quad (4.21)$$

$$\Delta \mathbf{K}'_{NL1} = \int_{S_0} \mathbf{B}_1^T \mathbf{D}' \Delta \mathbf{B} dS_0 \quad (4.22)$$

$$\Delta \mathbf{K}'_{NL2} = \int_{S_0} \Delta \mathbf{B}^T \mathbf{D}' \mathbf{B}_2 dS_0 \quad (4.23)$$

Letting

$$\boldsymbol{\sigma}_2 = \frac{E}{1-\nu^2} \boldsymbol{\sigma}'_2 \quad \boldsymbol{\sigma}'_2 = \{\sigma'_x, \sigma'_y, \sigma'_{xy}\}^T \quad (4.24)$$

$$\Delta \mathbf{K}'_{\sigma} = \int_{S_0} \mathbf{G}_2^T \mathbf{S}'_2 \mathbf{G}_2 dS_0 \quad (4.25a)$$

$$\mathbf{S}'_2 = \begin{bmatrix} \sigma'_x \mathbf{I}_2 & \sigma'_{xy} \mathbf{I}_2 \\ \sigma'_{xy} \mathbf{I}_2 & \sigma'_y \mathbf{I}_2 \end{bmatrix}_2 \quad (4.25b)$$

where \mathbf{I}_2 is the 2×2 identity matrix.

Then

$$\mathbf{K}'_{T2} = \mathbf{K}'_{T1} + \Delta \mathbf{K}'_T \quad (4.26)$$



where

$$\Delta K'_T = \Delta K'_{NL_1} + \Delta K'_{NL_2} + \Delta K'_o \quad (4.27)$$

4.2 Nondimensional Formulation of the Incremental Equilibrium Equations

Using Equations 3.67-68-69 defined in Chapter 3,

$$\left. \begin{aligned} A_2 &= k^{\frac{2}{3}} \tilde{A}_2 & G_2 &= \frac{1}{L} \tilde{G}_2 & \Delta B &= \frac{k^{\frac{2}{3}}}{L} \Delta \tilde{B} \\ B_2 &= \frac{1}{L} \tilde{B}_2 & \tilde{B}_2 &= \tilde{B}_1 + k^{\frac{2}{3}} \Delta \tilde{B} \end{aligned} \right\} \quad (4.28)$$

$$\Delta \epsilon = \frac{1}{2} \Delta \tilde{B} \mathbf{a} = \frac{k}{2} \Delta \tilde{B} \mathbf{M} \tilde{\mathbf{a}} \quad (4.29)$$

But employing

$$\Delta \tilde{B} \mathbf{M} = k^{\frac{1}{3}} \Delta \tilde{B} \quad (4.30)$$

$$\Delta \epsilon = \frac{k^{\frac{4}{3}}}{2} \Delta \tilde{B} \tilde{\mathbf{a}} \quad (4.31)$$

Then, with the help of Equation 3.73, Equation 4.1 becomes

$$\epsilon_2 = k^{\frac{2}{3}} \tilde{\epsilon}_2 \quad (4.32)$$

where

$$\tilde{\epsilon}_2 = \tilde{B}'_2 \tilde{\mathbf{a}} \quad (4.33)$$

and

$$\tilde{\mathbf{B}}_2' = \tilde{\mathbf{B}}_1' + \frac{k^{\frac{2}{3}}}{2} \Delta \tilde{\mathbf{B}} \quad (4.34)$$

The stress-strain relationships are given by

$$\sigma_2' = D' \epsilon_2 + \sigma_0' \quad (4.35)$$

Then

$$\sigma_2' = k^{\frac{2}{3}} \tilde{\sigma}_2' \quad s_2' = k^{\frac{2}{3}} \tilde{s}_2' \quad (4.36)$$

where

$$\tilde{\sigma}_2' = D' \tilde{\epsilon}_2 + \tilde{\sigma}_0' \quad \sigma_0' = k^{\frac{2}{3}} \tilde{\sigma}_0' \quad (4.37)$$

Using Equations 4.22, 4.23, 4.25a, and 4.27,

$$\Delta K_{NL_1}' = k^{\frac{2}{3}} \Delta \tilde{K}_{NL_1}' \quad (4.38)$$

$$\Delta K_{NL_2}' = k^{\frac{2}{3}} \Delta \tilde{K}_{NL_2}' \quad (4.39)$$

$$\Delta K_{\sigma}' = k^{\frac{2}{3}} \Delta \tilde{K}_{\sigma}' \quad (4.40)$$

$$\Delta K_T' = k^{\frac{2}{3}} \Delta \tilde{K}_T' \quad \Delta \tilde{K}_T' = \Delta \tilde{K}_{NL_1}' + \Delta \tilde{K}_{NL_2}' + \Delta \tilde{K}_{\sigma}' \quad (4.41)$$

The incremental equilibrium equations are given by Equation 2.23. If the indices m and i are dropped, this equation may be written as



$$\mathbf{K}_{T2} \Delta \mathbf{a} = \mathbf{F} - \mathbf{P}_2 \quad (4.42)$$

Using Equations 4.17, 4.26, 4.41 and 3.96, it is easy to show that

$$\mathbf{K}_{T2} = \frac{Eh}{1-\nu^2} \left(\tilde{\mathbf{K}}'_{T1} + k^{\frac{2}{3}} \Delta \tilde{\mathbf{K}}'_T \right) \quad (4.43)$$

Using Equations 3.76, 3.78, and 3.97, the left hand-side of Equation 4.42 becomes

$$\mathbf{K}_{T2} \Delta \mathbf{a} = \frac{2qL^2}{k^{\frac{1}{3}}} \tilde{\mathbf{K}}'^*_{T2} \Delta \tilde{\mathbf{a}} \quad (4.44)$$

where

$$\tilde{\mathbf{K}}'^*_{T2} = \tilde{\mathbf{K}}'^*_{T1} + \Delta \tilde{\mathbf{K}}'_T \quad (4.45a)$$

and

$$\Delta \tilde{\mathbf{K}}'_T = k^{\frac{1}{3}} \Delta \tilde{\mathbf{K}}'_T \mathbf{M} \quad (4.45b)$$

Let the following quantities be defined

$$\left. \begin{aligned} A_1 &= \frac{\partial N_i}{\partial \bar{x}} \frac{\partial N_j}{\partial \bar{x}} & A_2 &= \frac{\partial N_i}{\partial \bar{y}} \frac{\partial N_j}{\partial \bar{y}} \\ A_3 &= \frac{\partial N_i}{\partial \bar{x}} \frac{\partial N_j}{\partial \bar{y}} & A_4 &= \frac{\partial N_i}{\partial \bar{y}} \frac{\partial N_j}{\partial \bar{x}} \end{aligned} \right\} \quad (4.46a)$$

$$\left. \begin{aligned} B_1 &= \frac{\partial N_j}{\partial \bar{x}} \frac{\partial \tilde{w}}{\partial \bar{x}} & B_2 &= \frac{\partial N_j}{\partial \bar{y}} \frac{\partial \tilde{w}}{\partial \bar{y}} \\ B_3 &= \frac{\partial N_j}{\partial \bar{x}} \frac{\partial \tilde{w}}{\partial \bar{y}} & B_4 &= \frac{\partial N_j}{\partial \bar{y}} \frac{\partial \tilde{w}}{\partial \bar{x}} \end{aligned} \right\} \quad (4.46b)$$

$$C_1 = A_1 \bar{\sigma}_x' + A_2 \bar{\sigma}_y' + (A_3 + A_4) \bar{\sigma}_{xy}' \quad (4.46c)$$

$$\left. \begin{aligned} E_1 &= \frac{\partial N_j}{\partial \bar{x}} \frac{\partial \bar{u}}{\partial \bar{x}} & E_2 &= \frac{\partial N_j}{\partial \bar{y}} \frac{\partial \bar{u}}{\partial \bar{y}} \\ E_3 &= \frac{\partial N_j}{\partial \bar{x}} \frac{\partial \bar{u}}{\partial \bar{y}} & E_4 &= \frac{\partial N_j}{\partial \bar{y}} \frac{\partial \bar{u}}{\partial \bar{x}} \end{aligned} \right\} \quad (4.46d)$$

$$\left. \begin{aligned} F_1 &= \frac{\partial N_j}{\partial \bar{x}} \frac{\partial \bar{v}}{\partial \bar{x}} & F_2 &= \frac{\partial N_j}{\partial \bar{y}} \frac{\partial \bar{v}}{\partial \bar{y}} \\ F_3 &= \frac{\partial N_j}{\partial \bar{x}} \frac{\partial \bar{v}}{\partial \bar{y}} & F_4 &= \frac{\partial N_j}{\partial \bar{y}} \frac{\partial \bar{v}}{\partial \bar{x}} \end{aligned} \right\} \quad (4.46e)$$

$$\left. \begin{aligned} G_1 &= \frac{\partial N_i}{\partial \bar{x}} \frac{\partial \bar{u}}{\partial \bar{x}} & G_2 &= \frac{\partial N_i}{\partial \bar{y}} \frac{\partial \bar{u}}{\partial \bar{y}} \\ G_3 &= \frac{\partial N_i}{\partial \bar{x}} \frac{\partial \bar{u}}{\partial \bar{y}} & G_4 &= \frac{\partial N_i}{\partial \bar{y}} \frac{\partial \bar{u}}{\partial \bar{x}} \end{aligned} \right\} \quad (4.46f)$$

$$\left. \begin{aligned} H_1 &= \frac{\partial N_i}{\partial \bar{x}} \frac{\partial \bar{v}}{\partial \bar{x}} & H_2 &= \frac{\partial N_i}{\partial \bar{y}} \frac{\partial \bar{v}}{\partial \bar{y}} \\ H_3 &= \frac{\partial N_i}{\partial \bar{x}} \frac{\partial \bar{v}}{\partial \bar{y}} & H_4 &= \frac{\partial N_i}{\partial \bar{y}} \frac{\partial \bar{v}}{\partial \bar{x}} \end{aligned} \right\} \quad (4.46g)$$

$$\left. \begin{aligned} T_1 &= \frac{\partial N_i}{\partial \bar{x}} \frac{\partial \bar{w}}{\partial \bar{x}} & T_2 &= \frac{\partial N_i}{\partial \bar{y}} \frac{\partial \bar{w}}{\partial \bar{y}} \\ T_3 &= \frac{\partial N_i}{\partial \bar{x}} \frac{\partial \bar{w}}{\partial \bar{y}} & T_4 &= \frac{\partial N_i}{\partial \bar{y}} \frac{\partial \bar{w}}{\partial \bar{x}} \end{aligned} \right\} \quad (4.46h)$$

$$\left. \begin{aligned} Z_1 &= A_1 + \frac{1-\nu}{2} A_2 & Z_2 &= \nu A_3 + \frac{1-\nu}{2} A_4 \\ Z_3 &= \nu A_4 + \frac{1-\nu}{2} A_3 & Z_4 &= A_2 + \frac{1-\nu}{2} A_1 \end{aligned} \right\} \quad (4.46i)$$



$$\left. \begin{aligned} Z_5 &= E_1 + v E_2 & Z_6 &= E_2 + v E_1 \\ Z_7 &= F_1 + v F_2 & Z_8 &= F_2 + v F_1 \\ Z_9 &= B_1 + v B_2 & Z_{10} &= B_2 + v B_1 \end{aligned} \right\} \quad (4.46j)$$

$$\left. \begin{aligned} Z_{11} &= G_3 + G_4 & Z_{12} &= H_3 + H_4 & Z_{13} &= T_3 + T_4 \\ Z_{14} &= E_3 + E_4 & Z_{15} &= F_3 + F_4 & Z_{16} &= B_3 + B_4 \end{aligned} \right\} \quad (4.46k)$$

$$\left. \begin{aligned} Z_{17} &= Z_1 \frac{\partial \tilde{u}}{\partial \tilde{x}} & Z_{18} &= Z_2 \frac{\partial \tilde{u}}{\partial \tilde{y}} & Z_{19} &= Z_1 \frac{\partial \tilde{v}}{\partial \tilde{x}} \\ Z_{20} &= Z_2 \frac{\partial \tilde{v}}{\partial \tilde{y}} & Z_{21} &= Z_3 \frac{\partial \tilde{u}}{\partial \tilde{x}} & Z_{22} &= Z_4 \frac{\partial \tilde{u}}{\partial \tilde{y}} \\ Z_{23} &= Z_3 \frac{\partial \tilde{v}}{\partial \tilde{x}} & Z_{24} &= Z_4 \frac{\partial \tilde{v}}{\partial \tilde{y}} & Z_{25} &= Z_3 \frac{\partial \tilde{u}}{\partial \tilde{y}} \\ Z_{26} &= Z_2 \frac{\partial \tilde{u}}{\partial \tilde{x}} & Z_{27} &= Z_3 \frac{\partial \tilde{v}}{\partial \tilde{y}} & Z_{28} &= Z_2 \frac{\partial \tilde{v}}{\partial \tilde{x}} \\ Z_{29} &= \frac{1-v}{2} Z_{11} & Z_{30} &= \frac{1-v}{2} Z_{12} & Z_{31} &= \frac{1-v}{2} Z_{13} \end{aligned} \right\} \quad (4.46l)$$

$$\left. \begin{aligned} Z_{32} &= (Z_5 G_1 + Z_6 G_2 + Z_{14} Z_{29}) k^{\frac{2}{3}} \\ Z_{33} &= (Z_7 G_1 + Z_8 G_2 + Z_{15} Z_{29}) k^{\frac{2}{3}} \\ Z_{34} &= (Z_5 H_1 + Z_6 H_2 + Z_{14} Z_{30}) k^{\frac{2}{3}} \\ Z_{35} &= (Z_7 H_1 + Z_8 H_2 + Z_{15} Z_{30}) k^{\frac{2}{3}} \end{aligned} \right\} \quad (4.46m)$$

The coefficients of the 3×3 submatrix corresponding to $\Delta \tilde{K}_{0T}^*$ are given by

$$\left. \begin{aligned}
\Delta \tilde{K}_{0T}^*(1,1) &= (2Z_{17} + Z_{18} + Z_{25} + Z_{32} + C_1) k^{\frac{2}{3}} \\
\Delta \tilde{K}_{0T}^*(1,2) &= (Z_{19} + Z_{20} + Z_{22} + Z_{26} + Z_{33}) k^{\frac{2}{3}} \\
\Delta \tilde{K}_{0T}^*(1,3) &= (Z_9 G_1 + Z_{10} G_2 + Z_{16} Z_{29}) k^{\frac{2}{3}} \\
\Delta \tilde{K}_{0T}^*(2,1) &= (Z_{19} + Z_{21} + Z_{22} + Z_{27} + Z_{34}) k^{\frac{2}{3}} \\
\Delta \tilde{K}_{0T}^*(2,2) &= (Z_{23} + 2Z_{24} + Z_{28} + Z_{35} + C_1) k^{\frac{2}{3}} \\
\Delta \tilde{K}_{0T}^*(2,3) &= (Z_9 H_1 + Z_{10} H_2 + Z_{16} Z_{30}) k^{\frac{2}{3}} \\
\Delta \tilde{K}_{0T}^*(3,1) &= (Z_5 T_1 + Z_6 T_2 + Z_{14} Z_{31}) k^{\frac{1}{3}} \\
\Delta \tilde{K}_{0T}^*(2,3) &= (Z_7 T_1 + Z_8 T_2 + Z_{15} Z_{31}) k^{\frac{1}{3}} \\
\Delta \tilde{K}_{0T}^*(3,3) &= 0
\end{aligned} \right\} \quad (4.46n)$$

Equation 4.42 then becomes

$$\tilde{K}_{T2}^* \Delta \tilde{a} = \frac{k^{\frac{1}{3}}}{2} \tilde{F}' - \tilde{P}_2' \quad (4.47)$$

where

$$\left. \begin{aligned}
\tilde{P}_2' &= \sum_{i=1}^3 \sum_{j=1}^3 \tilde{P}_{0,2}(r_i, s_j) \tilde{J}(r_i, s_j) w_i w_j \\
\tilde{P}_{0,2} &= \tilde{B}_2^T \tilde{\sigma}_2'
\end{aligned} \right\} \quad (4.48)$$

By using Equation 3.107, and substituting k_m for k in the expressions of element matrices, the incremental equilibrium equation becomes

$$[\tilde{K}_{T2}^*]_m^{(i-1)} \{\Delta \tilde{a}\}_m^{(i)} = \frac{\alpha_m^{\frac{1}{3}}}{2} k^{\frac{1}{3}} \tilde{F}_m^{/(i)} - \tilde{P}_2_m^{/(i-1)} \quad (4.49)$$

4.3 Extension to the Case of External Pressure

The tangential stiffness matrix developed in the previous paragraphs is valid only for membranes subjected to loads which do not change in direction as the membrane deforms. This might be a severe restriction, particularly when the structural membrane exhibits large displacements and large deformations, since the loading applied to membrane structures is, in general, external pressure, which exerts force normal to the deformed surface. In this section, element stiffness matrices will be developed to account for changes in the external loading due to deformation.

The element load vector is given by Equation 2.13. The term $f dS$ in Equation 2.13 is the load vector acting on the deformed membrane element dS .

As the membrane deforms, there are changes in both the direction of the external pressure force and the area on which it acts. It is reasonable to assume that the intensity of the external pressure does not change with deformation and that the dimensions of the finite elements are sufficiently small that the external pressure is essentially uniform over the surfaces of each of them. Therefore,

$$\mathbf{f} = q \mathbf{E}_z \quad (4.50)$$

where \mathbf{E}_z is the outward unit vector normal to S at an arbitrary point of the deformed membrane.



Expressing the product $\mathbf{E}_z dS$ as a function of the unit vectors in the global fixed Cartesian system of coordinates and of the area dS_0 of the undeformed membrane element gives

$$\mathbf{E}_z dS = \left(\mathbf{e}_x + \frac{\partial \mathbf{U}}{\partial x} \right) \otimes \left(\mathbf{e}_y + \frac{\partial \mathbf{U}}{\partial y} \right) dS_0 \quad (4.51)$$

where the symbol \otimes stands for the cross product operation, and the displacement vector \mathbf{U} is given by

$$\mathbf{U} = u\mathbf{e}_x + v\mathbf{e}_y + w\mathbf{e}_z \quad (4.52)$$

Writing Equation 4.51 in vector form,

$$\mathbf{E}_z dS = \left\{ \begin{array}{c} \frac{\partial v}{\partial x} \frac{\partial w}{\partial y} - \frac{\partial w}{\partial x} \left(1 + \frac{\partial v}{\partial y} \right) \\ \frac{\partial u}{\partial y} \frac{\partial w}{\partial x} - \frac{\partial w}{\partial y} \left(1 + \frac{\partial u}{\partial x} \right) \\ \left(1 + \frac{\partial u}{\partial x} \right) \left(1 + \frac{\partial v}{\partial y} \right) - \frac{\partial u}{\partial y} \frac{\partial v}{\partial x} \end{array} \right\} dS_0 \quad (4.53)$$

Decomposing \mathbf{E}_z into a difference of a constant vector and a vector depending on the displacement components gives

$$\mathbf{E}_z dS = \left\{ \begin{array}{c} 0 \\ 0 \\ 1 \end{array} \right\} dS_0 - \left\{ \begin{array}{c} -\frac{\partial v}{\partial x} \frac{\partial w}{\partial y} + \frac{\partial w}{\partial x} \left(1 + \frac{\partial v}{\partial y} \right) \\ -\frac{\partial u}{\partial y} \frac{\partial w}{\partial x} + \frac{\partial w}{\partial y} \left(1 + \frac{\partial u}{\partial x} \right) \\ -\frac{\partial u}{\partial x} - \frac{\partial v}{\partial y} - \frac{\partial u}{\partial x} \frac{\partial v}{\partial y} + \frac{\partial u}{\partial y} \frac{\partial v}{\partial x} \end{array} \right\} dS_0 \quad (4.54)$$

The first vector on the right-hand-side of Equation 4.54 is $\mathbf{e}_z dS_0$. The second vector may also be decomposed into two components:

$$\mathbf{E}_z dS = (\mathbf{e}_z - \mathbf{E}_{q1} - \mathbf{E}_{q2}) dS_0 \quad (4.55)$$

where

$$\mathbf{E}_{q1} = \begin{Bmatrix} \frac{\partial w}{\partial x} \\ \frac{\partial w}{\partial y} \\ -\frac{\partial u}{\partial x} - \frac{\partial v}{\partial y} \end{Bmatrix} \quad (4.56)$$

and

$$\mathbf{E}_{q2} = \begin{Bmatrix} \frac{\partial v}{\partial y} \frac{\partial w}{\partial x} - \frac{\partial v}{\partial x} \frac{\partial w}{\partial y} \\ \frac{\partial u}{\partial x} \frac{\partial w}{\partial y} - \frac{\partial u}{\partial y} \frac{\partial w}{\partial x} \\ \frac{\partial v}{\partial x} \frac{\partial u}{\partial y} - \frac{\partial u}{\partial x} \frac{\partial v}{\partial y} \end{Bmatrix} \quad (4.57)$$

Thus, Equation 2.13 may be written as

$$\mathbf{F} = q \int_{S_0} \mathbf{N}^T \mathbf{e}_x dS_0 - q \int_{S_0} \mathbf{N}^T \mathbf{E}_{q1} dS_0 - q \int_{S_0} \mathbf{N}^T \mathbf{E}_{q2} dS_0 \quad (4.58)$$

or

$$\mathbf{F} = \mathbf{F}_{q0} - \mathbf{F}_{q1} - \mathbf{F}_{q2} \quad (4.59)$$

where

$$\left. \begin{aligned} \mathbf{F}_{q0} &= q \int_{S_0} \mathbf{N}^T \mathbf{e}_x dS_0 \\ \mathbf{F}_{q1} &= q \int_{S_0} \mathbf{N}^T \mathbf{E}_{q1} dS_0 \\ \mathbf{F}_{q2} &= q \int_{S_0} \mathbf{N}^T \mathbf{E}_{q2} dS_0 \end{aligned} \right\} \quad (4.60)$$

\mathbf{F}_{q0} is the load vector corresponding to the case of conservative loading.



With the help of Equation 2.8, the following expressions may be written

$$\mathbf{E}_{q1} = \mathbf{A}_{q1} \mathbf{N} \mathbf{a} \quad \mathbf{E}_{q2} = \frac{1}{2} \mathbf{A}_{q2} \boldsymbol{\theta} \quad (4.61)$$

where

$$\mathbf{A}_{q1} = \begin{bmatrix} 0 & 0 & \frac{\partial}{\partial x} \\ 0 & 0 & \frac{\partial}{\partial y} \\ -\frac{\partial}{\partial x} & -\frac{\partial}{\partial y} & 0 \end{bmatrix} \quad (4.62a)$$

$$\mathbf{A}_{q2} = \begin{bmatrix} 0 & -\frac{\partial w}{\partial y} & \frac{\partial v}{\partial y} & 0 & \frac{\partial w}{\partial x} & -\frac{\partial v}{\partial x} \\ \frac{\partial w}{\partial y} & 0 & -\frac{\partial u}{\partial y} & -\frac{\partial w}{\partial x} & 0 & \frac{\partial u}{\partial x} \\ -\frac{\partial v}{\partial y} & \frac{\partial u}{\partial y} & 0 & \frac{\partial v}{\partial x} & -\frac{\partial u}{\partial x} & 0 \end{bmatrix} \quad (4.62b)$$

and

$$\boldsymbol{\theta} = \left\{ \frac{\partial u}{\partial x}, \frac{\partial v}{\partial x}, \frac{\partial w}{\partial x}, \frac{\partial u}{\partial y}, \frac{\partial v}{\partial y}, \frac{\partial w}{\partial y} \right\}^T \quad (4.62c)$$

Differentiating Equation 4.59 gives

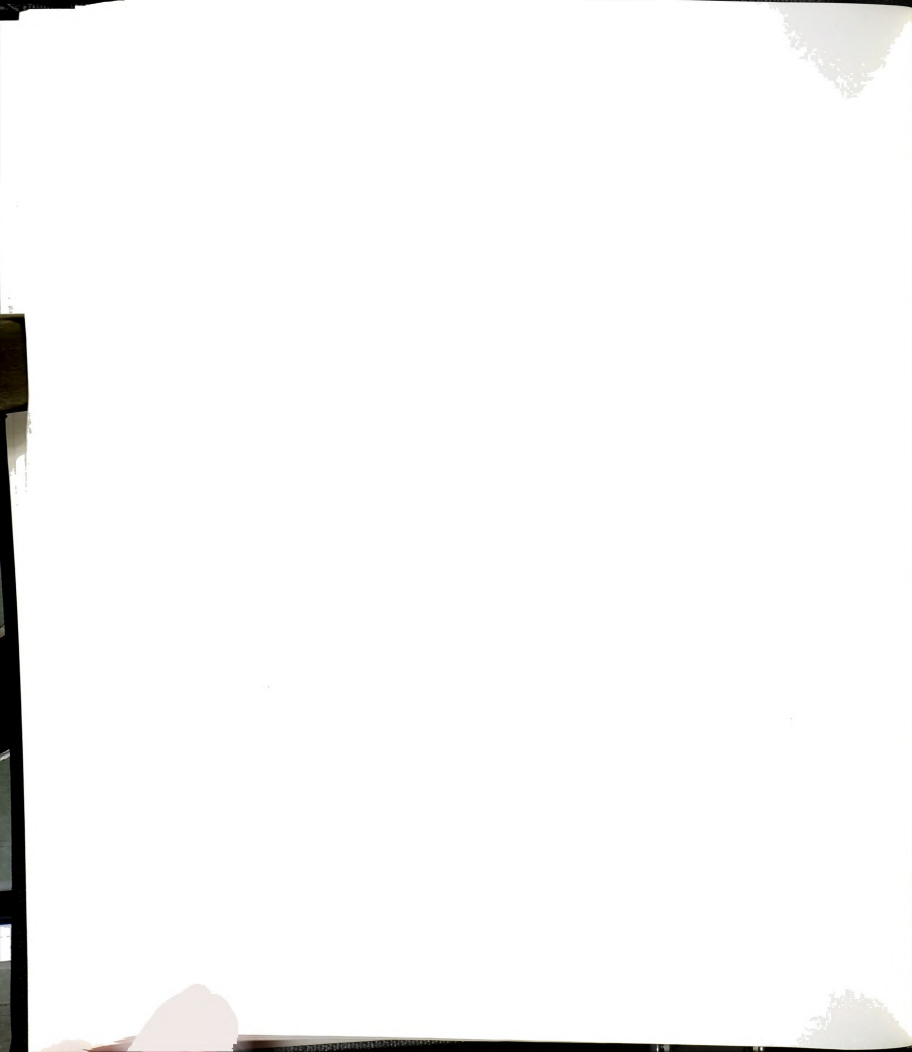
$$d\mathbf{F} = -d\mathbf{F}_{q1} - d\mathbf{F}_{q2} \quad (4.63)$$

Substitution into Equations 4.60 and 4.61, leads to

$$\mathbf{F}_{q1} = q \int_{s_0} \mathbf{N}^T \mathbf{A}_{q1} \mathbf{N} dS_0 \mathbf{a} \quad d\mathbf{F}_{q1} = \mathbf{K}_{q1} d\mathbf{a} \quad (4.64)$$

where

$$\mathbf{K}_{q1} = q \int_{s_0} \mathbf{N}^T \mathbf{A}_{q1} \mathbf{N} ds_0 \quad (4.65)$$



Also

$$d\mathbf{F}_{q2} = q \int_{s_0} \mathbf{N}^T d\mathbf{E}_{q2} dS_0 \quad (4.66)$$

$$d\mathbf{E}_{q2} = \frac{1}{2} d\mathbf{A}_{q2} \theta + \frac{1}{2} \mathbf{A}_{q2} d\theta \quad (4.67)$$

but, noting that

$$d\mathbf{A}_{q2} \theta = \mathbf{A}_{q2} d\theta \quad (4.68)$$

Equation 4.67 becomes

$$d\mathbf{E}_{q2} = \mathbf{A}_{q2} d\theta \quad (4.69)$$

Noting also that

$$\theta = \mathbf{G} \mathbf{a} \quad \mathbf{G} = [\mathbf{G}_1 | \dots | \mathbf{G}_I | \dots | \mathbf{G}_8] \quad (4.70)$$

where

$$\mathbf{G}_1 = \begin{bmatrix} \frac{\partial N_i}{\partial x} & 0 & 0 \\ 0 & \frac{\partial N_i}{\partial x} & 0 \\ 0 & 0 & \frac{\partial N_i}{\partial x} \\ \frac{\partial N_i}{\partial y} & 0 & 0 \\ 0 & \frac{\partial N_i}{\partial y} & 0 \\ 0 & 0 & \frac{\partial N_i}{\partial y} \end{bmatrix} \quad (4.71)$$



Therefore

$$d\theta = G da \quad dE_{q2} = A_{q2} G da \quad (4.72)$$

and

$$dF_{q2} = K_{q2} da \quad (4.73)$$

where

$$K_{q2} = q \int_{S_0} N^T A_{q2} G dS_0 \quad (4.74)$$

Thus Equation 4.63 may be rewritten as

$$dF = -K_q da \quad (4.75)$$

K_q may be called the "load stiffness matrix", and is given by

$$K_q = K_{q1} + K_{q2} \quad (4.76)$$

Introducing nondimensional variables,

$$A_{q1} = \frac{1}{L} \tilde{A}_{q1} \quad G = \frac{1}{L} \tilde{G} \quad (4.77)$$

letting

$$K_{q1} = \frac{Eh}{1-\nu^2} K'_{q1} \quad (4.78)$$

and using Equation 3.76, gives

$$K'_{q1} = \frac{k}{2L} K_1 \quad k_1 = \int_{S_0} N^T A_{q1} N dS_0 \quad (4.79)$$

$$K_1 = L \tilde{K}_1 \quad \tilde{K}_1 = \int_{\tilde{S}_0} N^T \tilde{A}_{q1} N d\tilde{S}_0 \quad (4.80)$$



$$\kappa'_{q1} = \frac{k}{2} \tilde{\kappa}_1 \quad (4.81)$$

Also, if

$$\kappa_{q2} = \frac{Eh}{1-\nu^2} \kappa'_{q2} \quad (4.82)$$

then

$$\kappa'_{q2} = \frac{k}{2L} \kappa_2 \quad \kappa_2 = \int_{S_0} \mathbf{N}^T \mathbf{A}_{q2} \mathbf{G} dS_0 \quad (4.83)$$

By writing

$$\mathbf{A}_{q2} = \mathbf{A}_{q2,1} + \mathbf{A}_{q2,2} \quad (4.84)$$

where

$$\mathbf{A}_{q2,1} = \begin{bmatrix} 0 & -\frac{\partial w}{\partial y} & 0 & 0 & \frac{\partial w}{\partial x} & 0 \\ \frac{\partial w}{\partial y} & 0 & 0 & -\frac{\partial w}{\partial x} & 0 & 0 \\ 0 & 0 & 0 & 0 & 0 & 0 \end{bmatrix} \quad (4.85a)$$

$$\mathbf{A}_{q2,2} = \begin{bmatrix} 0 & 0 & \frac{\partial v}{\partial y} & 0 & 0 & -\frac{\partial v}{\partial x} \\ 0 & 0 & -\frac{\partial u}{\partial y} & 0 & 0 & \frac{\partial u}{\partial x} \\ -\frac{\partial v}{\partial y} & \frac{\partial u}{\partial y} & 0 & \frac{\partial v}{\partial x} & -\frac{\partial u}{\partial x} & 0 \end{bmatrix} \quad (4.85b)$$

then

$$\kappa_2 = \kappa_{2,1} + \kappa_{2,2} \quad (4.86)$$

where

$$\kappa_{2,1} = \int_{S_0} \mathbf{N}^T \mathbf{A}_{q2,1} \mathbf{G} dS_0 \quad \kappa_{2,2} = \int_{S_0} \mathbf{N}^T \mathbf{A}_{q2,2} \mathbf{G} dS_0 \quad (4.87)$$



Noting that

$$A_{q2,1} = k^{\frac{1}{3}} \tilde{A}_{q2,1} \quad A_{q2,2} = k^{\frac{2}{3}} \tilde{A}_{q2,2} \quad (4.88)$$

$$K_{2,1} = Lk^{\frac{1}{3}} \tilde{K}_{2,1} \quad K_{2,2} = Lk^{\frac{2}{3}} \tilde{K}_{2,2} \quad (4.89)$$

then

$$K_2 = Lk^{\frac{1}{3}} \tilde{K}_2 \quad K'_{q2} = \frac{k^{\frac{4}{3}}}{2} \tilde{K}_2 \quad (4.90)$$

where

$$\tilde{K}_2 = \tilde{K}_{2,1} + k^{\frac{1}{3}} \tilde{K}_{2,2} \quad (4.91)$$

and

$$\begin{aligned} K_q &= \frac{Eh}{1-\nu^2} (K'_{q1} + K'_{q2}) \\ &= \frac{2qL}{k} \left(\frac{k}{2} \tilde{K}_1 + \frac{k^{\frac{4}{3}}}{2} \tilde{K}_2 \right) \\ K_q &= \frac{2qL}{k^{\frac{2}{3}}} \left\{ \frac{k^{\frac{2}{3}}}{2} \left[\tilde{K}_1 + k^{\frac{2}{3}} \left(\frac{1}{k^{\frac{1}{3}}} \tilde{K}_{2,1} + \tilde{K}_{2,2} \right) \right] \right\} \end{aligned} \quad (4.92)$$

Letting

$$\tilde{K}_{2,1}^* = \frac{1}{k^{\frac{1}{3}}} \tilde{K}_{2,1} M \quad \tilde{K}_{2,2}^* = \tilde{K}_{2,2} M \quad (4.93a)$$

and

$$\tilde{K}_1^* = \tilde{K}_1 M \quad \tilde{K}_2^* = \tilde{K}_{2,1}^* + \tilde{K}_{2,2}^* \quad (4.93b)$$



it may be shown that

$$\kappa_q \Delta a = \frac{2qL^2}{k^{\frac{1}{3}}} \tilde{\kappa}_q^* \tilde{a} \quad (4.94)$$

where

$$\tilde{\kappa}_q^* = \frac{k^{\frac{2}{3}}}{2} [\tilde{\kappa}_1^* + k^{\frac{2}{3}} \tilde{\kappa}_2^*] \quad (4.95)$$

The coefficients of the 3×3 submatrix corresponding to $\tilde{\kappa}_q^*$ are given by

$$\left. \begin{aligned} \tilde{\kappa}_q^{ij*}(1,1) &= 0 \\ \tilde{\kappa}_q^{ij*}(1,2) &= \frac{k^{\frac{4}{3}}}{2} N_i (B_4 - B_3) \\ \tilde{\kappa}_q^{ij*}(1,3) &= \frac{k^{\frac{2}{3}}}{2} N_i \left[\frac{\partial N_j}{\partial \tilde{x}} + k^{\frac{2}{3}} (F_3 - F_4) \right] \\ \tilde{\kappa}_q^{ij*}(2,1) &= -\tilde{\kappa}_q^{ij*}(1,2) \\ \tilde{\kappa}_q^{ij*}(2,2) &= 0 \\ \tilde{\kappa}_q^{ij*}(2,3) &= \frac{k^{\frac{2}{3}}}{2} N_i \left[\frac{\partial N_j}{\partial \tilde{y}} + k^{\frac{2}{3}} (E_4 - E_3) \right] \\ \tilde{\kappa}_q^{ij*}(3,1) &= -k^{\frac{1}{3}} \tilde{\kappa}_q^{ij*}(1,3) \\ \tilde{\kappa}_q^{ij*}(3,2) &= -k^{\frac{1}{3}} \tilde{\kappa}_q^{ij*}(2,3) \\ \tilde{\kappa}_q^{ij*}(3,3) &= 0 \end{aligned} \right\} \quad (4.96)$$



The nondimensional incremental equilibrium equations are then given by Equation 4.49, provided that

$$\tilde{\mathbf{K}}'_{r2} = \tilde{\mathbf{K}}'_{r1} + \Delta\tilde{\mathbf{K}}'_r + \tilde{\mathbf{K}}'_q \quad (4.97)$$

and that k is replaced by k_m in the expressions of element matrices.

The extension to external pressure loading is also valid for the von Kármán model.



5. Solution Technique

5.1 Assemblage of Structure Matrices

Since the nondimensional element stiffness matrices and the nondimensional load vector were derived for a typical membrane finite element, they hold for any element in the finite element mesh.

The assemblage process to obtain the nondimensional tangent stiffness matrix may be written in symbolic form as

$$\tilde{\mathbf{K}}_T = \sum_n \tilde{\mathbf{K}}_T^{(n)} \quad (5.1)$$

where the term under the summation symbol is the nondimensional tangent stiffness matrix of the typical element, and the summation goes over all elements in the finite element mesh. Similarly, the nondimensional load vector is assembled from the element nondimensional load vectors.

It should be mentioned that the nondimensional tangent stiffness matrix is not symmetric (see Equations 3.96, 4.46, and 4.96). The loss of the symmetry property is due to the form of the matrix \mathbf{M} (see Equations 3.78b and 3.78c).

5.2 Solution of Equilibrium Equations

5.2.1 The Incremental Iterative Solution Strategy

The nonlinear incremental equations to be solved are given by Equations 3.108 and 4.49 and may be written as

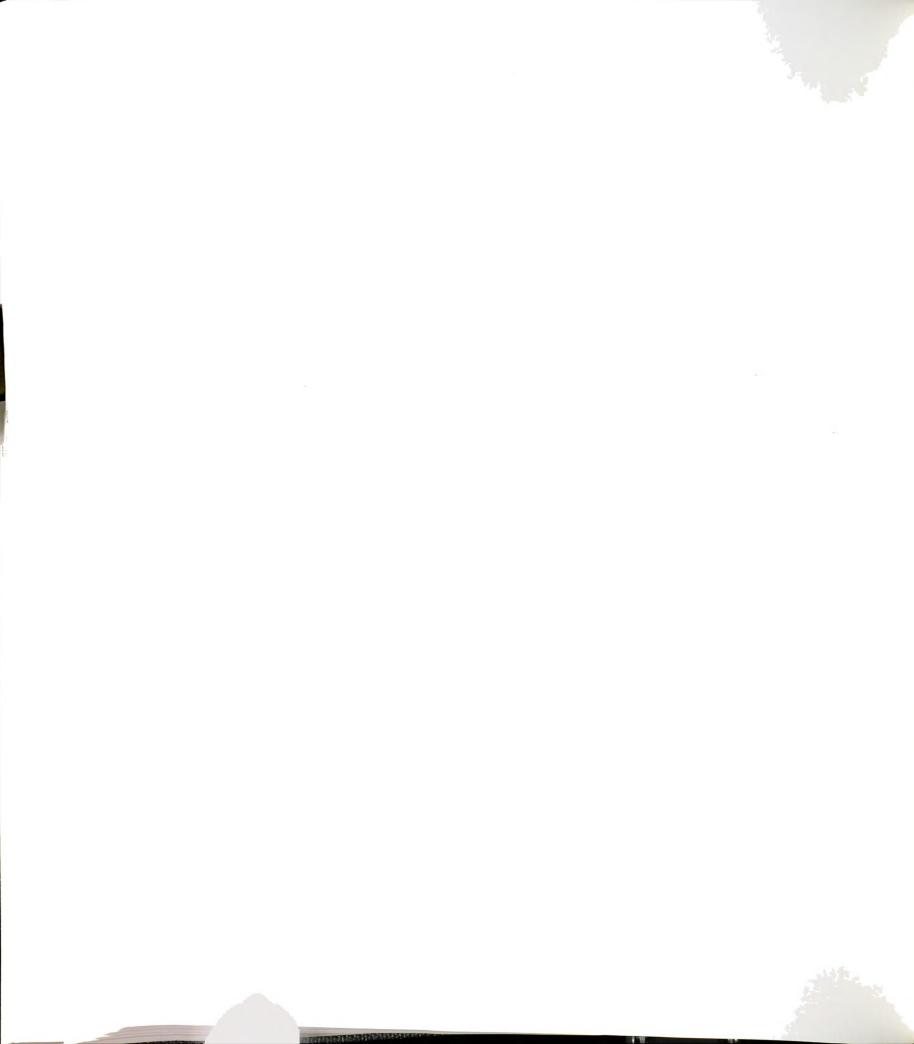


$$[\tilde{\mathbf{K}}_T^*]_m^{(i-1)} \{\Delta \tilde{\mathbf{a}}\}_m^{(i)} = \frac{\alpha_m^{\frac{1}{3}}}{2} k^{\frac{1}{3}} \tilde{\mathbf{F}}_m^{(i)} - \tilde{\mathbf{P}}_m^{(i-1)} \quad (5.2)$$

where the full Newton-Raphson iteration method in conjunction with an incremental loading procedure is implied. In this method, each load step consists of the application of an increment of external load and subsequent iterations to restore equilibrium. This implies that the tangent stiffness matrix has to be updated at each iteration. Since the major computational cost per iteration lies in the evaluation and factorization of the tangent stiffness matrix, it is in general more effective to use some modification of the full Newton-Raphson algorithm²¹. In this work, the modified Newton-Raphson iteration procedure was used. Therefore, the tangent stiffness matrix is assumed to be constant within each increment, and is updated only at the start of the next increment. This is clearly more economical at each step but convergence is slower. The modified nonlinear equations to be solved are then

$$[\tilde{\mathbf{K}}_T^*]_m^{(0)} \{\Delta \tilde{\mathbf{a}}\}_m^{(i)} = \frac{\alpha_m^{\frac{1}{3}}}{2} k^{\frac{1}{3}} \tilde{\mathbf{F}}_m^{(i)} - \tilde{\mathbf{P}}_m^{(i-1)} \quad (5.3)$$

where $[\tilde{\mathbf{K}}_T^*]_m^{(0)}$ is the value of the tangent stiffness matrix at the beginning of the m th increment based upon the nodal displacement solution vector obtained in the last iteration of the $(m-1)$ th increment.



5.2.2 Convergence Criteria

A problem associated with iterative techniques is the decision as to whether the current iterate is sufficiently close to the solution which is unknown. To overcome this problem, a convergence criterion must be set. A displacement criterion based on the maximum norm will be used to measure the size of the error ²⁴. The maximum norm is defined by

$$\|\epsilon\|_{\infty} = \max_i^N \left| \frac{\Delta a_i}{a_{i,ref}} \right| \quad (5.4)$$

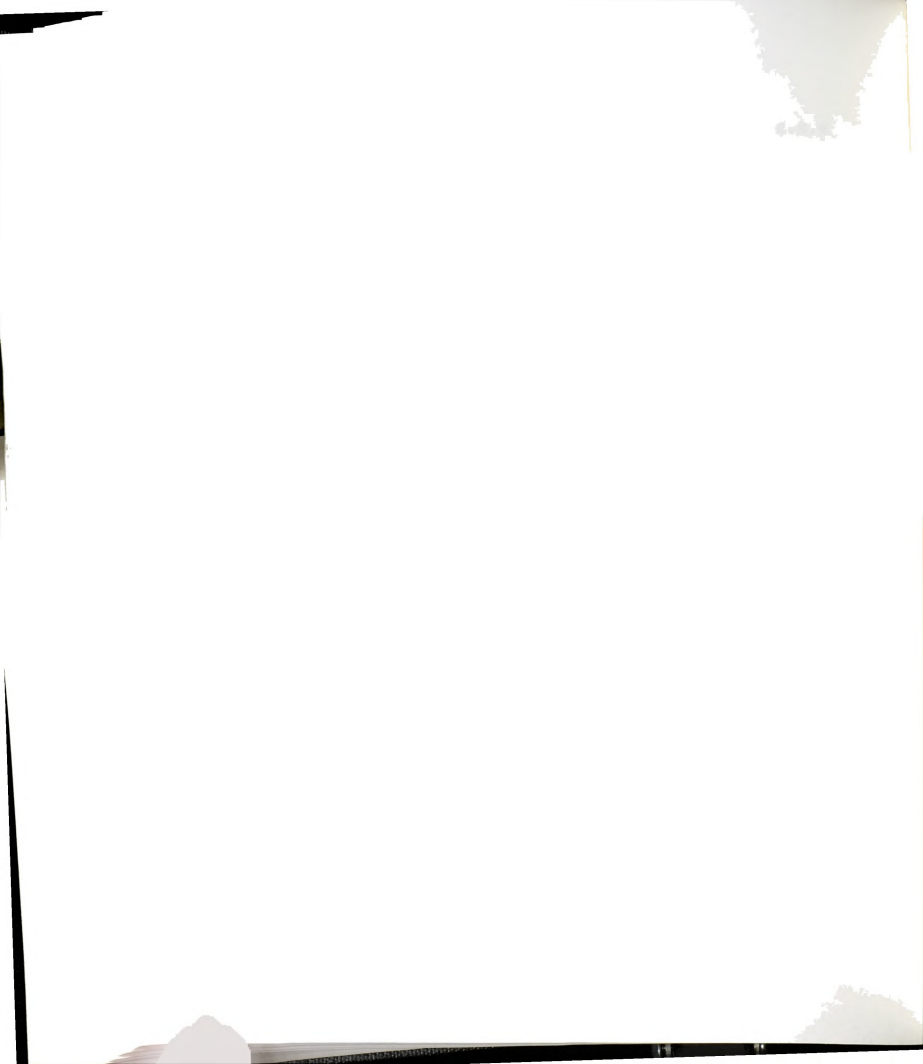
where N is the total number of unknown displacement components; Δa_i is the change in displacement component i during a given iteration; and $a_{i,ref}$ is a reference displacement quantity equal to the absolute value of the largest displacement component of the corresponding type (u , v , or w). The convergence criterion is then

$$\|\epsilon\|_{\infty} < \mu \quad (5.5)$$

The value of μ is usually between 10^{-2} and 10^{-6} , depending on the accuracy desired.

5.2.3 The Initial Virtual Prestressing Technique

In nonlinear finite element analysis, the linear solution is often used as the initial guess in the iteration procedure. For initially thin flat membranes which are subjected to transverse loading, there is no linear solution due to the lack of bending stiffness. Therefore, the analyst has to make



an initial guess to start the iteration procedure. As mentioned earlier in the literature review, the initial guess used in previous work involved all of the unknown displacement components. To avoid dealing with all of the components of the displacement vector in formulating an initial guess, a new technique referred to as the "initial virtual prestressing technique" is introduced.

Unless the membrane is very strongly prestressed prior to service loading, the tangent stiffness matrix in the first stages of the incremental iterative procedure is either singular or close to singular. Therefore, an ill-conditioned problem arise. The basic idea of the initial virtual prestressing technique is to circumvent this ill-conditioning problem by introducing an imaginary initial prestressing so that the tangent stiffness matrix is far from singularity. The membrane problem is then modified. Since the main purpose in the analysis is the evaluation of the final equilibrium configuration of the membrane and its state of stress under the true service loading, it is necessary to remove this virtual prestressing before the final configuration is reached. This can be done by removing part of the virtual prestressing at the beginning of each load increment so that by the end of the procedure the virtual prestressing is removed completely.



By letting the following vectors

$$\sigma_0^v = \begin{Bmatrix} \sigma_{0x}^v \\ \sigma_{0y}^v \\ \sigma_{0xy}^v \end{Bmatrix} \quad \sigma_0^t = \begin{Bmatrix} \sigma_{0x}^t \\ \sigma_{0y}^t \\ \sigma_{0xy}^t \end{Bmatrix} \quad (5.6)$$

be, respectively, the initial virtual prestressing vector and the initial true stress vector, the initial stress vector at the first load increment becomes

$$\sigma_0^{(1)} = \sigma_0^v + \sigma_0^t \quad (5.7)$$

To reduce the initial virtual prestressing in subsequent increments, a reduction factor λ_m is introduced so that at the m th increment

$$\sigma_0^{(m)} = \sigma_0^t + \lambda_m \sigma_0^v \quad (5.8)$$

and at the last increment

$$\sigma_0^{(M)} = \sigma_0^t \quad (5.9)$$

where M is the total number of increments, and λ_m is a function of m . The initial prestressing may be suitably expressed in terms of an equivalent initial prestraining as

$$\sigma_0^t = E \epsilon_0^t \quad \sigma_0^v = E \epsilon_0^v \quad (5.10)$$

in which

$$\epsilon_0^t = \begin{Bmatrix} \epsilon_{0x}^t \\ \epsilon_{0y}^t \\ \epsilon_{0xy}^t \end{Bmatrix} \quad \epsilon_0^v = \begin{Bmatrix} \epsilon_{0x}^v \\ \epsilon_{0y}^v \\ \epsilon_{0xy}^v \end{Bmatrix} \quad (5.11)$$



By using Equations 4.23, 4.32 and 4.37, the nondimensional stress at the m th increment may be written

$$\tilde{\sigma}_0' = (1 - \nu^2) (\tilde{\epsilon}_0^t + \lambda_m \tilde{\epsilon}_0^v) \quad (5.12)$$

The reduction factor λ_m should be a decreasing function of m , and should satisfy the following conditions

$$\left. \begin{aligned} \lambda_1 &= \lambda_m(m=1) = 1 \\ \lambda_M &= \lambda_m(m=M) = 0 \end{aligned} \right\} \quad (5.13)$$

Many possible choices for λ_m can be used. The initial choice for this work was

$$\lambda_m = \begin{cases} 1 & \text{for } m=1 \\ 1 - \frac{1}{(1+\beta)^{M-m}} & \text{for } m \geq 2 \end{cases} \quad (5.14)$$

where β is a constant between 0 and 1. From preliminary computations, it was found that a small value of β ($0 < \beta < 0.3$) ensures numerical stability when a small number of increments is considered. However, with five increments, $\beta=1$ was used successfully. To speed up convergence, the following alternative reduction factor was considered

$$\lambda_m = \begin{cases} 1 & \text{for } m=1 \\ \frac{1}{m^{\frac{2}{3}}} \left[1 - \frac{1}{(1+\beta)^{M-m}} \right] & \text{for } m \geq 2 \end{cases} \quad (5.15)$$

With the latter reduction factor, the average number of iterations per increment required for convergence was about



one third of that obtained with the reduction factor given by Equation 5.14.

By using the new method, all that is needed to start the incremental iterative procedure is an initial guess of the three components of the initial virtual stress vector. An "optimum" guess of these values may be obtained by trying different values with a coarse finite element mesh, and then use this optimum with finer finite element meshes.

5.3 Evaluation of Strains and Stresses

5.3.1 Evaluation of Strains

Once the element nodal displacements are obtained, the strains at any point can be evaluated as (see Equations 3.80, 3.82a, 4.32 and 4.33)

$$\epsilon = k^{\frac{2}{3}} \tilde{\epsilon} \quad \tilde{\epsilon} = \tilde{B}' \tilde{a} \quad (5.16)$$

5.3.2 Evaluation of Second Piola-Kirchhoff Stresses

The nondimensional second Piola-Kirchhoff stresses are obtained using the following stress-strain relationships (see Equations 3.84 and 4.37)

$$\tilde{\sigma}' = D' \tilde{\epsilon} + \tilde{\sigma}_0' \quad (5.17)$$

Using Equations 3.28, 3.83, 4.24, and 4.36, the second Piola-Kirchhoff stresses are given by

$$\sigma = \frac{E}{1-\nu^2} k^{\frac{2}{3}} \tilde{\sigma}' \quad (5.18)$$



5.3.3 Evaluation of Cauchy Stresses

The Cauchy stress tensor is defined as¹⁹

$$\boldsymbol{\tau} = \frac{\rho}{\rho_0} \mathbf{X} \boldsymbol{\sigma} \mathbf{X}^T \quad (5.19)$$

where ρ is the mass density in the final configurations, ρ_0 is the mass density in the initial configuration, $\boldsymbol{\sigma}$ is the second Piola-Kirchhoff stress tensor, and \mathbf{X} is the deformation gradient given by

$$\mathbf{X} = \begin{bmatrix} 1 + \frac{\partial u}{\partial x} & \frac{\partial u}{\partial y} \\ \frac{\partial v}{\partial x} & 1 + \frac{\partial v}{\partial y} \end{bmatrix} \quad (5.20)$$

and

$$\left. \begin{aligned} \rho_0 &= \rho \det \mathbf{X} \\ \det \mathbf{X} &= \left(1 + \frac{\partial u}{\partial x}\right) \left(1 + \frac{\partial v}{\partial y}\right) - \frac{\partial v}{\partial x} \frac{\partial u}{\partial y} \end{aligned} \right\} \quad (5.21)$$

The components of the Cauchy stress tensor in terms of the components of the second Piola-Kirchhoff stress tensor are then given by

$$\tau_x = \frac{1}{\det \mathbf{X}} \left[\sigma_x \left(1 + \frac{\partial u}{\partial x}\right)^2 + \sigma_y \left(\frac{\partial u}{\partial y}\right)^2 + 2 \sigma_{xy} \frac{\partial u}{\partial y} \left(1 + \frac{\partial u}{\partial x}\right) \right] \quad (5.22a)$$

$$\tau_y = \frac{1}{\det \mathbf{X}} \left[\sigma_y \left(1 + \frac{\partial v}{\partial y}\right)^2 + \sigma_x \left(\frac{\partial v}{\partial x}\right)^2 + 2 \sigma_{xy} \frac{\partial v}{\partial x} \left(1 + \frac{\partial v}{\partial y}\right) \right] \quad (5.22b)$$

$$\tau_{xy} = \frac{1}{\det \mathbf{X}} \left[\sigma_x \frac{\partial v}{\partial x} \left(1 + \frac{\partial u}{\partial x}\right) + \sigma_y \frac{\partial u}{\partial y} \left(1 + \frac{\partial v}{\partial y}\right) + \sigma_{xy} \left[\frac{\partial u}{\partial y} \frac{\partial v}{\partial x} + \left(1 + \frac{\partial u}{\partial x}\right) \left(1 + \frac{\partial v}{\partial y}\right) \right] \right] \quad (5.22c)$$



6. Model Validation and Parametric Studies

A computer program was developed to test and validate the theoretical models described in the previous chapters, and was used to undertake some parametric studies. The initial virtual prestressing technique was implemented in the computer program.

To allow for an adequate comparison of the results of this work with previous research, the membrane deflections and stresses are conveniently presented in the form:

$$\left. \begin{aligned} w &= \alpha L \left(\frac{qL}{Eh} \right)^{\frac{1}{3}} \\ \sigma &= \beta \left(\frac{q^2 L^2 E}{h^2} \right)^{\frac{1}{3}} \\ \tau &= \gamma \left(\frac{q^2 L^2 E}{h^2} \right)^{\frac{1}{3}} \end{aligned} \right\} \quad (6.1)$$

The coefficients α, β and γ are, respectively, the normal deflection coefficient, the second Piola-Kirchhoff stress coefficient, and the Cauchy stress coefficient.

6.1 Model Validation

6.1.1 Convergence of the von Kármán Model

To study the convergence characteristics of the von Kármán model, a square membrane and a rectangular membrane with two different aspect ratios were analyzed (see Figure 2). The aspect ratio η is defined as the length of the membrane's shorter side over the length of its longer side:

$$\eta = \frac{b}{a} \quad (6.2)$$

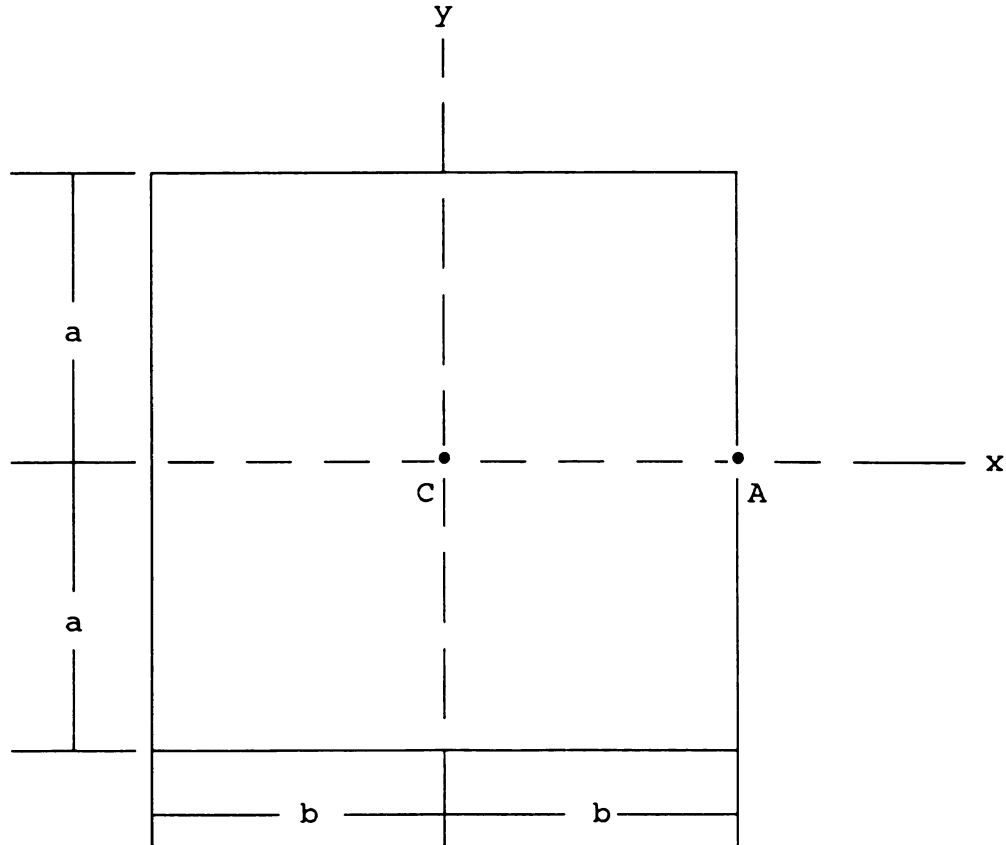


Figure 2: Region for Rectangular Membrane



Letting $L=b$, Equation 5.1 becomes

$$\left. \begin{aligned} w &= \alpha b \left(\frac{qb}{Eh} \right)^{\frac{1}{3}} \\ \sigma &= \beta \left(\frac{q^2 b^2 E}{h^2} \right)^{\frac{1}{3}} \\ \tau &= \gamma \left(\frac{q^2 b^2 E}{h^2} \right)^{\frac{1}{3}} \end{aligned} \right\} \quad (6.3)$$

In all cases, the membrane was assumed to be fixed along its four edges ($u=v=w=0$), and the transverse loading acting on the membrane was considered uniform and deformation-independent.

Due to double symmetry, only a quarter of the membrane was required in the analysis. Different mesh sizes were considered. The number of subdivisions in the x-direction N_x and in the y-direction N_y were chosen to be identical ($N_x=N_y=N$). Figures 3, 4 and 5 show the variation of the central deflection and central and maximum principal second Piola-Kirchhoff stresses with mesh refinement. It is evident from the results that the von Kármán model exhibits good convergence characteristics. The value of the nondimensional coefficient k used to plot Figures 3, 4, and 5 was taken to be equal to 1, and Poisson's ratio was taken equal to 0.3.



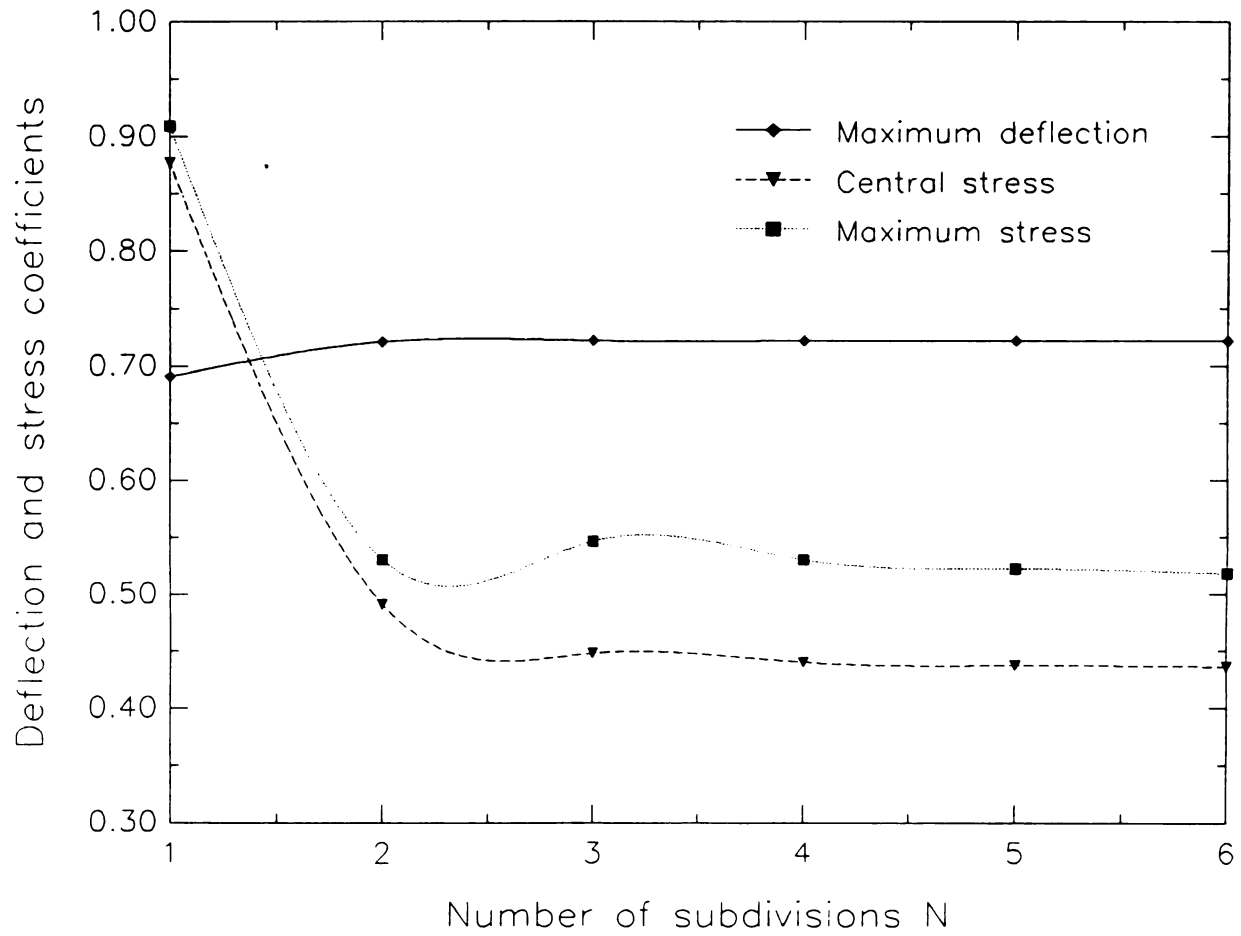
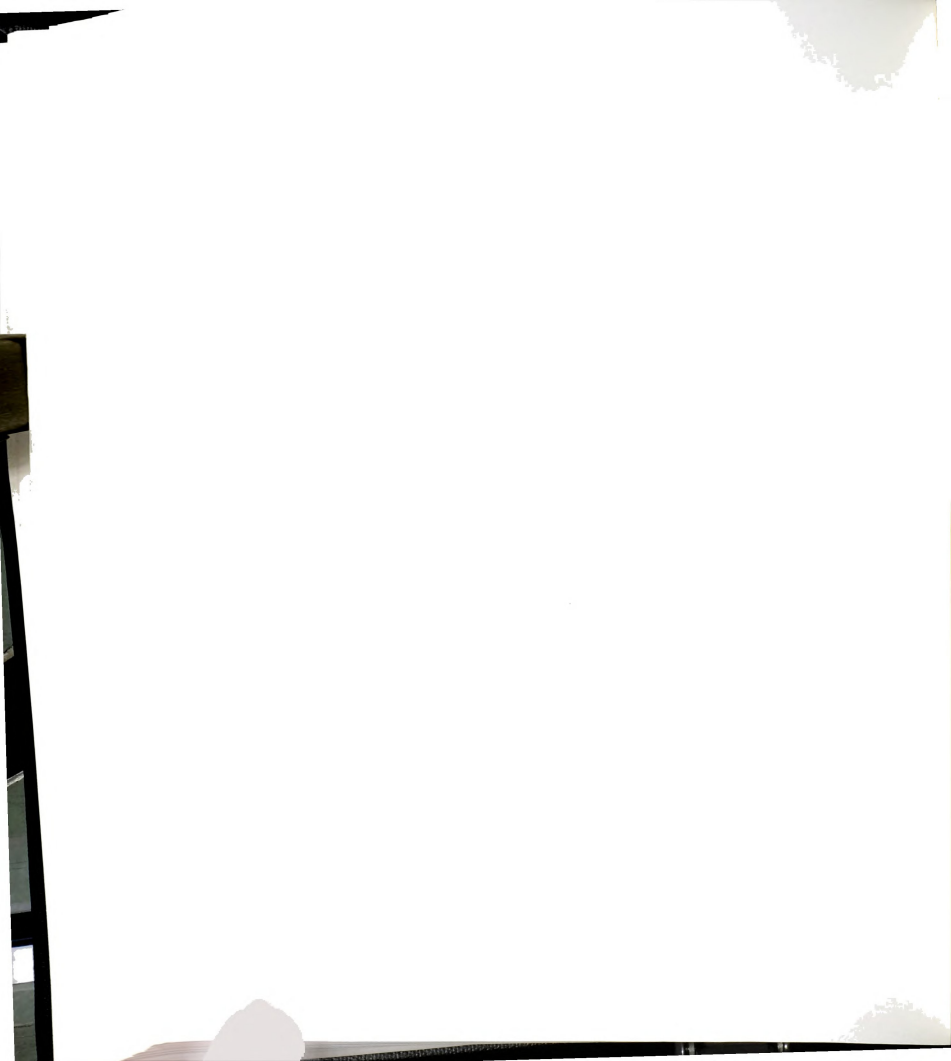


Figure 3: Convergence of Deflection and Stresses for a Square Membrane



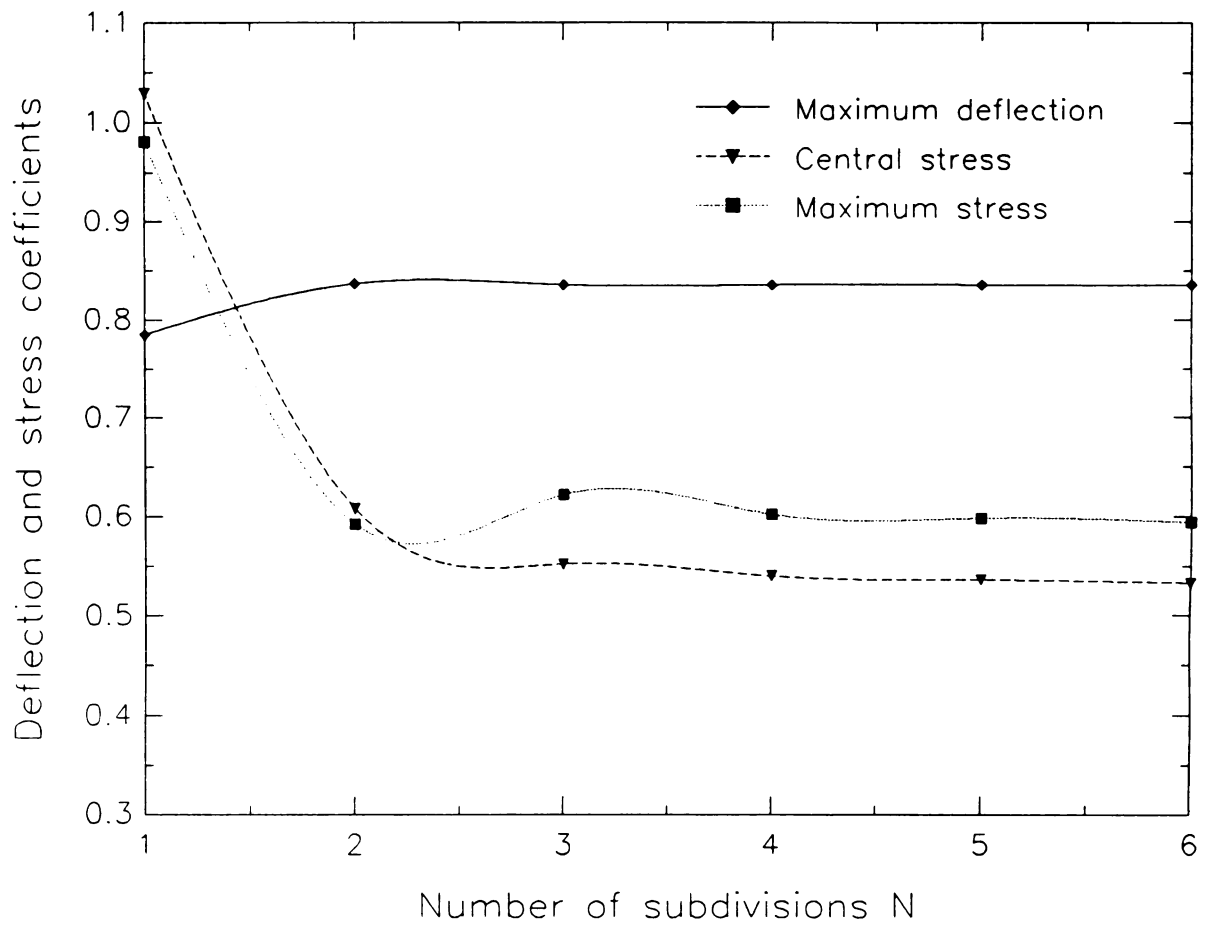
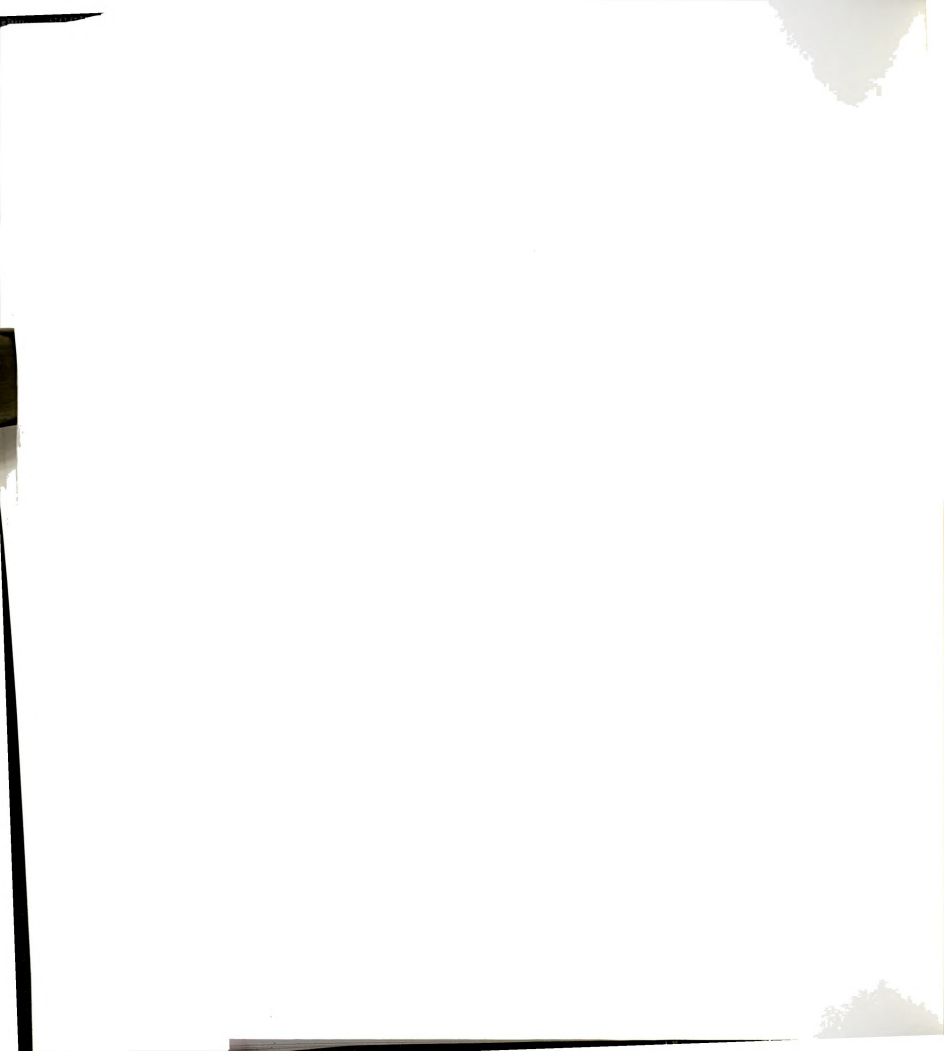


Figure 4: Convergence of Deflection and Stresses for a Rectangular Membrane ($\eta=5/7$)



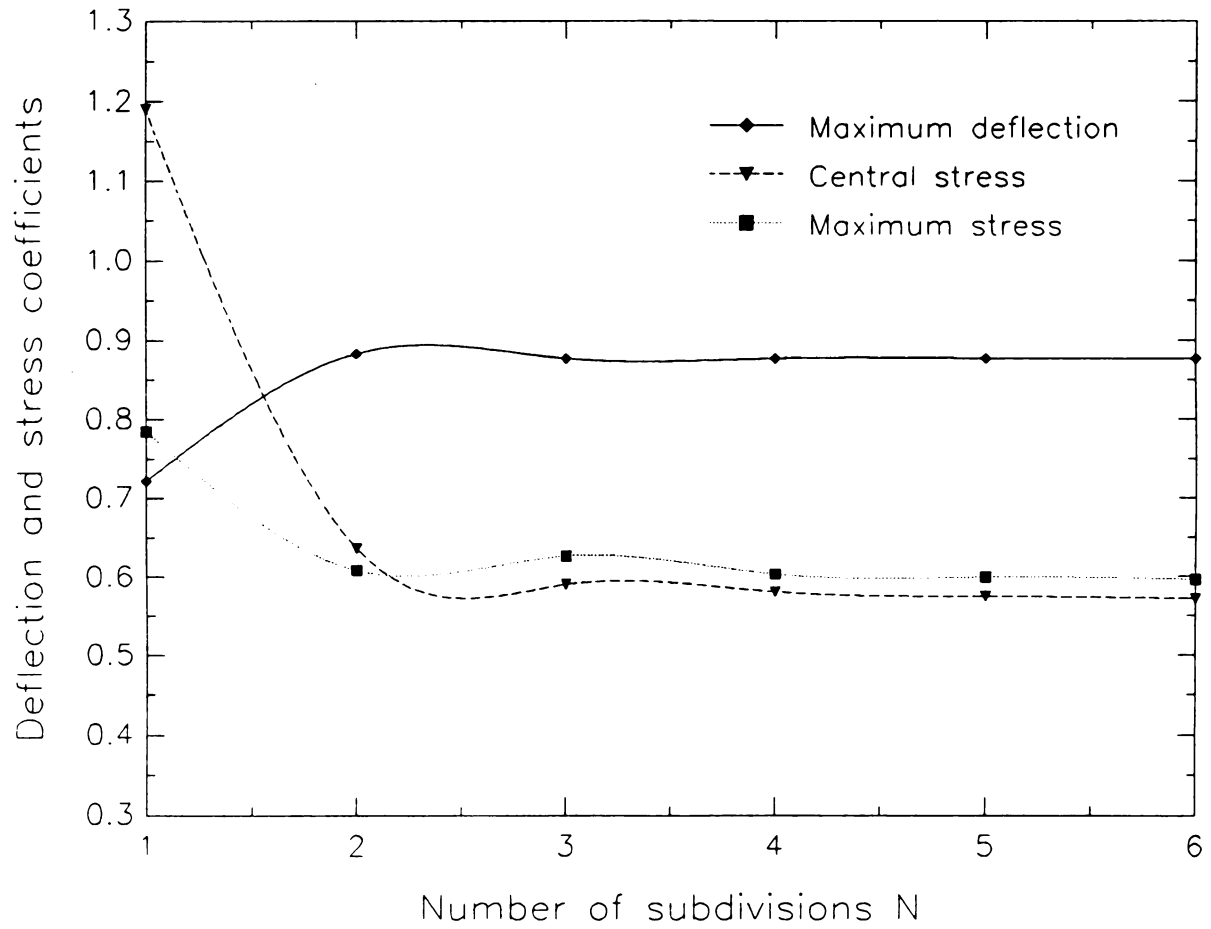


Figure 5: Convergence of Deflection and Stresses for a Rectangular Membrane ($\eta=2/5$)

6.1.2 Comparison of the von Kármán Model with Previous Models

To test the validity of the numerical implementation of the von Kármán model, a square membrane and a rectangular membrane with two different aspect ratios ($\eta=5/7$ and $\eta=2/5$) were analyzed.

Because the nondimensional coefficient k enters the fundamental incremental equilibrium equation to be solved (see Equation 3.108), the analysis was carried out with seven different values of k ranging from 0.0001 to 1, i.e. values of 0.0001, 0.001, 0.01, 0.05, 0.1, 0.5 and 1. However, it was found that the values of the central deflection and the central and maximum second Piola-Kirchhoff stresses were not affected by the variation of k . Then, a comparison was made of the results for the central deflection and central and maximum principal second Piola-Kirchhoff stresses with the results of Föppl¹¹, Hencky¹², Borg¹³, Shaw and Perrone⁸, Kao and Perrone¹⁷, and Allen and Al-Qarra¹⁸. The results given in terms of deflection and stress coefficients are shown in Tables 1, 2 and 3.

Table 1: Square Membrane Under Uniform Transverse Loading
Comparing different Models

Model	Maximum deflection	Central stress	Maximum stress
Föppl	0.8	0.409	0.56
Hencky	0.716	0.436	0.458
Kao & Perrone	0.723	0.439	0.497
Allen & Al-Qarra	0.722	0.435	0.518
Present work von Kármán model	0.722	0.436	0.518

Table 2: Rectangular Membrane Under Uniform Transverse
Loading ($\eta=5/7$) Comparing different Models

Model	Maximum deflection	Central stress	Maximum stress
Föppl	0.943	0.543	0.735
Borg	0.864	0.504	-
Shaw and Perrone	0.824	0.520	0.591
Kao & Perrone	0.841	0.522	0.574
Allen & Al-Qarra	0.836	0.536	0.598
Present work von Kármán model	0.836	0.533	0.594



Table 3: Rectangular Membrane Under Uniform Transverse Loading ($\eta=2/5$) Comparing different Models

Model	Maximum deflection	Central stress	Maximum stress
Föppl	1.069	0.642	0.889
Borg	0.875	0.553	-
Kao & Perrone	0.895	0.551	0.582
Allen & Al-Qarra	0.877	0.581	0.605
Present work von Kármán model	0.877	0.572	0.596

It is evident from the comparison, that the numerical implementation of the von Kármán model is consistent with the implementation done by other investigators. In the author's model, the second Piola-Kirchhoff stresses were evaluated at the element nodes and the center of each element. This may account for some of the discrepancy between the tabulated values and those obtained by Borg and by Kao and Perrone, since those investigators do not specify where stresses were evaluated. Also, it is important to note that the maximum second Piola-Kirchhoff stress occurs at the middle of the longest edge of the rectangular membrane (see point A in Figure 2).

6.1.3 Discussion

As was mentioned in the literature review, second Piola-Kirchhoff stresses do not represent "real" membrane stresses when large displacements are considered, and in practice



Cauchy stresses should be computed. A comparison between second Piola-Kirchhoff stress coefficients and Cauchy stress coefficients, using the von Kármán model, is presented in Tables 4, 5, and 6.

Table 4: Stress Coefficients for a Square Membrane

k	2nd Piola-Kirchhoff Stresses		Cauchy Stresses	
	Central Stress	Maximum Stress	Central Stress	Maximum Stress
0.0001	0.436	0.518	0.436	0.522
0.001	0.436	0.518	0.436	0.520
0.01	0.436	0.518	0.436	0.509
0.05	0.436	0.518	0.436	0.484
0.1	0.436	0.518	0.436	0.461
0.5	0.436	0.518	0.436	0.342
1.0	0.436	0.518	0.436	0.346

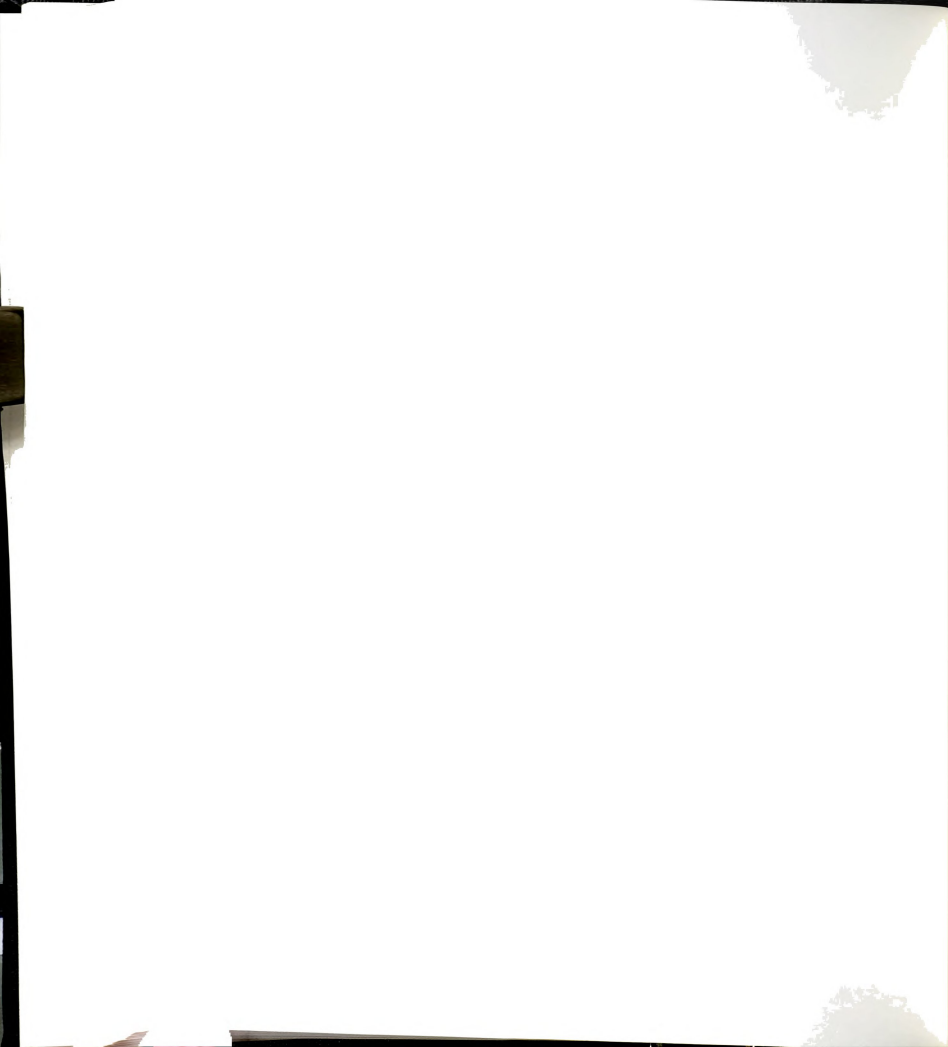


Table 5: Stress Coefficients for a Rectangular Membrane $(\eta=5/7)$

k	2nd Piola-Kirchhoff Stresses		Cauchy Stresses	
	Central Stress	Maximum Stress	Central Stress	Maximum Stress
0.0001	0.533	0.594	0.536	0.597
0.001	0.533	0.594	0.536	0.594
0.01	0.533	0.594	0.539	0.581
0.05	0.533	0.594	0.546	0.550
0.1	0.533	0.594	0.552	0.522
0.5	0.533	0.594	0.582	0.376
1.0	0.533	0.594	0.606	0.436

Table 6: Stress Coefficients for a Rectangular Membrane $(\eta=2/5)$

k	2nd Piola-Kirchhoff Stresses		Cauchy Stresses	
	Central Stress	Maximum Stress	Central Stress	Maximum Stress
0.0001	0.572	0.596	0.575	0.599
0.001	0.572	0.596	0.577	0.595
0.01	0.572	0.596	0.583	0.581
0.05	0.572	0.596	0.598	0.547
0.1	0.572	0.596	0.612	0.515
0.5	0.572	0.596	0.681	0.354
1.0	0.572	0.596	0.741	0.513



Table 7 shows the relative error when second Piola-Kirchhoff stresses are used instead of Cauchy stresses. The relative error in the stress coefficients is defined as:

$$\Delta\tau = \frac{\sigma - \tau}{\tau} \quad (6.4)$$

where σ and τ are, respectively, the second Piola-Kirchhoff stress and the Cauchy stress.

Table 7: Relative Error in Stress Coefficients

k	Relative Error %					
	Central Stress			Maximum Stress		
	$\eta=1$	$\eta=5/7$	$\eta=2/5$	$\eta=1$	$\eta=5/7$	$\eta=2/5$
0.0001	0	-0.56	-0.52	-0.77	-0.50	-0.50
0.001	0	-0.56	-0.87	-0.38	0	0.17
0.01	0	-1.11	-1.89	1.77	2.24	2.58
0.05	0	-2.38	-4.35	7.02	8.00	8.96
0.1	0	-3.44	-6.54	12.4	13.8	15.7
0.5	0	-8.42	-16.0	51.5	58.0	68.4
1.0	0	-12.0	-22.8	49.7	36.2	16.2

It is evident from the above results that, in general, the use of second Piola-Kirchhoff stresses instead of Cauchy stresses underestimates the central stresses but overestimates the maximum stresses. For values of k smaller than 0.01, the use of second Piola-Kirchhoff stresses leads to results that are sufficiently accurate for most purposes, but Cauchy stresses need to be used for values of k greater than 0.05.



However, for high values of strains, the membrane may exhibit an inelastic behavior. When this is the case, the assumption of elastic behavior may no longer valid, and new constitutive relationships modelling the material behavior should be considered.

To check the state of strain in the membrane, the central and maximum actual strains were computed, and are listed in Tables 8, 9, and 10.

Table 8: Strains in a Square Membrane

k	Central Strain %	Maximum Strain %
0.0001	0.04	0.07
0.001	0.21	0.32
0.01	0.95	1.48
0.05	2.79	4.33
0.1	4.42	6.87
0.5	12.9	20.1
1.0	20.5	31.9

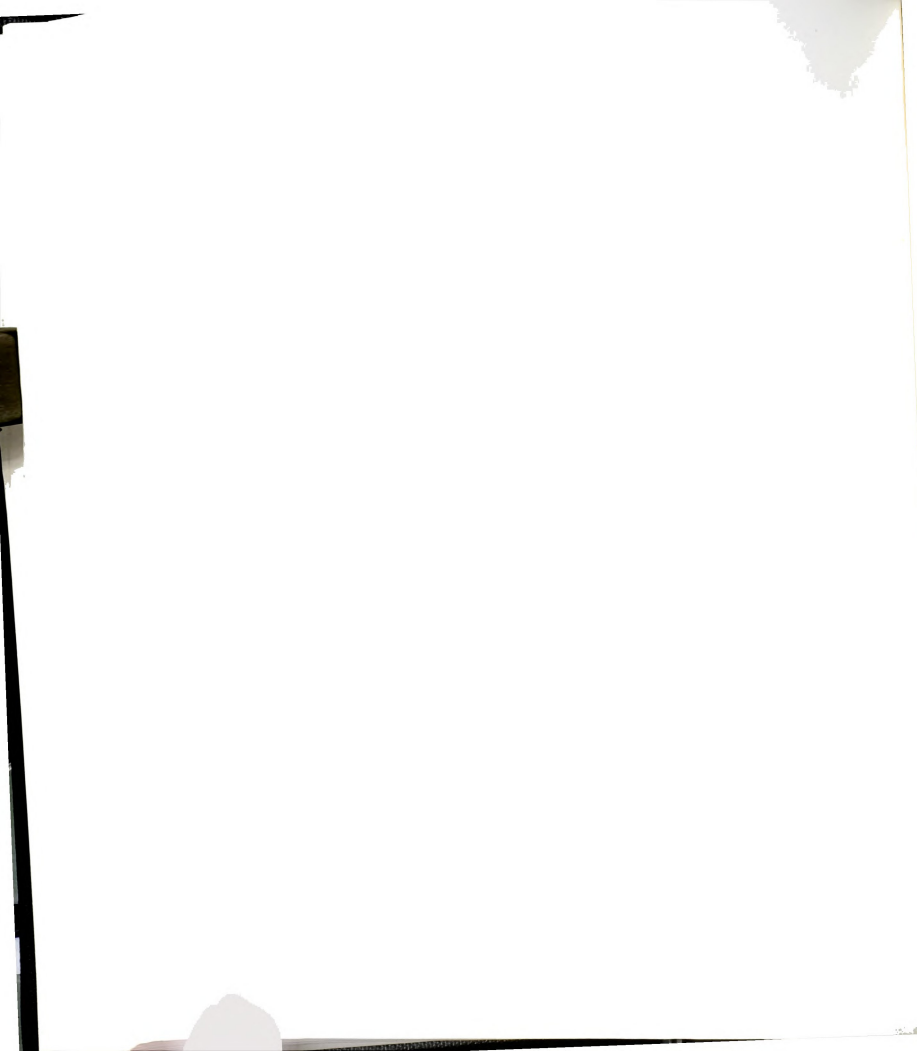


Table 9: Strains in a Rectangular Membrane ($\eta=5/7$)

k	Central Strain %	Maximum Strain %
0.0001	0.06	0.08
0.001	0.29	0.36
0.01	1.33	1.69
0.05	3.88	4.95
0.1	6.16	7.86
0.5	18.0	23.0
1.0	28.6	36.5

Table 10: Strains in a Rectangular Membrane ($\eta=2/5$)

k	Central Strain %	Maximum Strain %
0.0001	0.07	0.08
0.001	0.34	0.37
0.01	1.57	1.70
0.05	4.60	4.97
0.1	7.31	7.88
0.5	21.4	23.1
1.0	33.9	36.6

6.1.4 Comparison of the von Kármán Model with the General Model

To determine the limitations of the von Kármán model and therefore its range of applicability, the three membrane cases studied above were analyzed using the general model. Figures 6, 7 and 8, which are plotted for $k=1$, demonstrate that



convergence for the general model is comparable to that of the von Kármán model (Figures 3, 4 and 5).



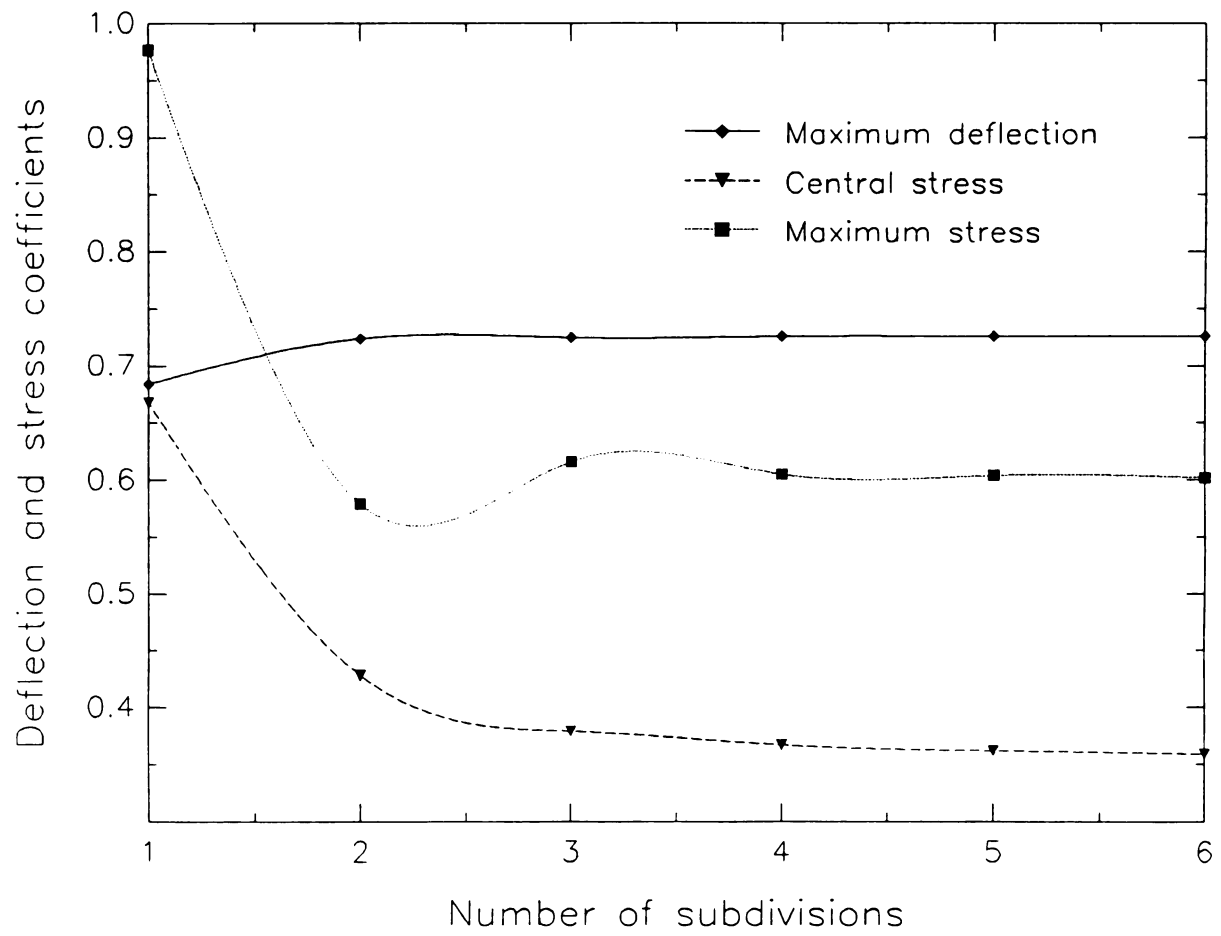
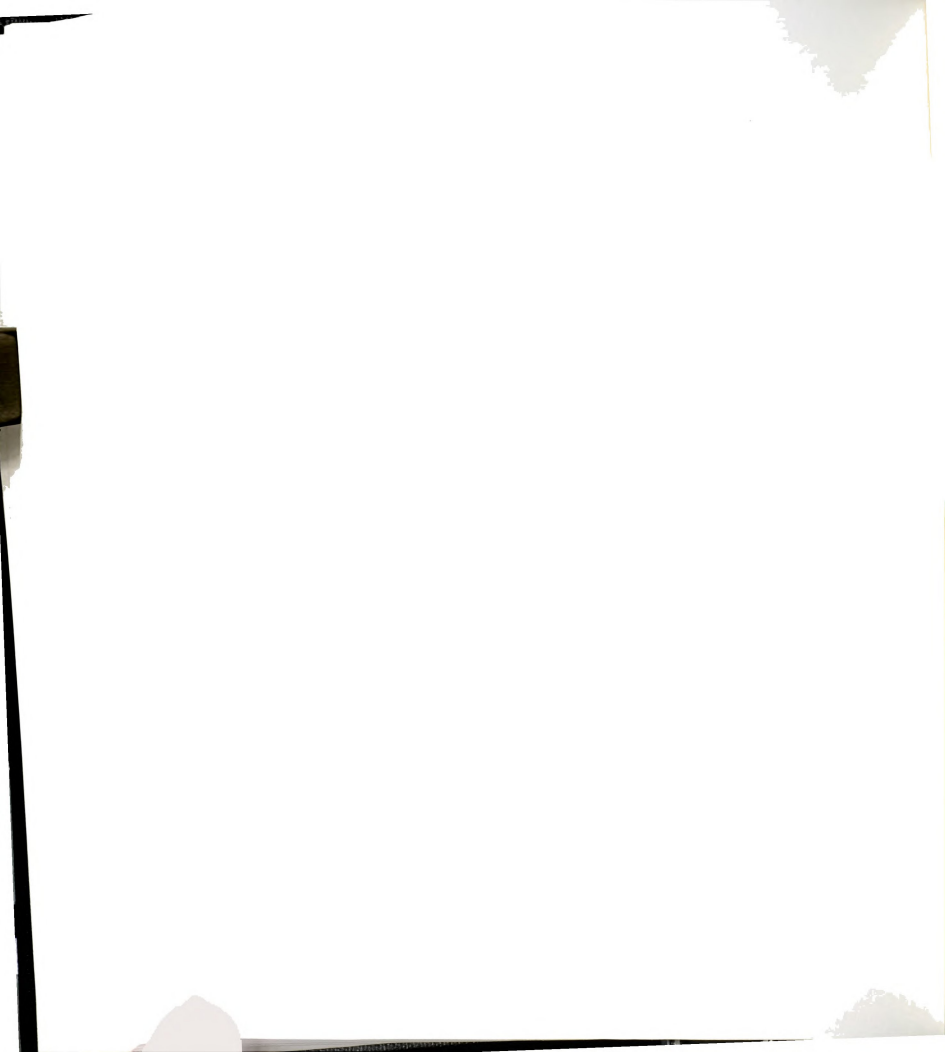


Figure 6: General Model Convergence of Deflection and Stresses for a Square Membrane



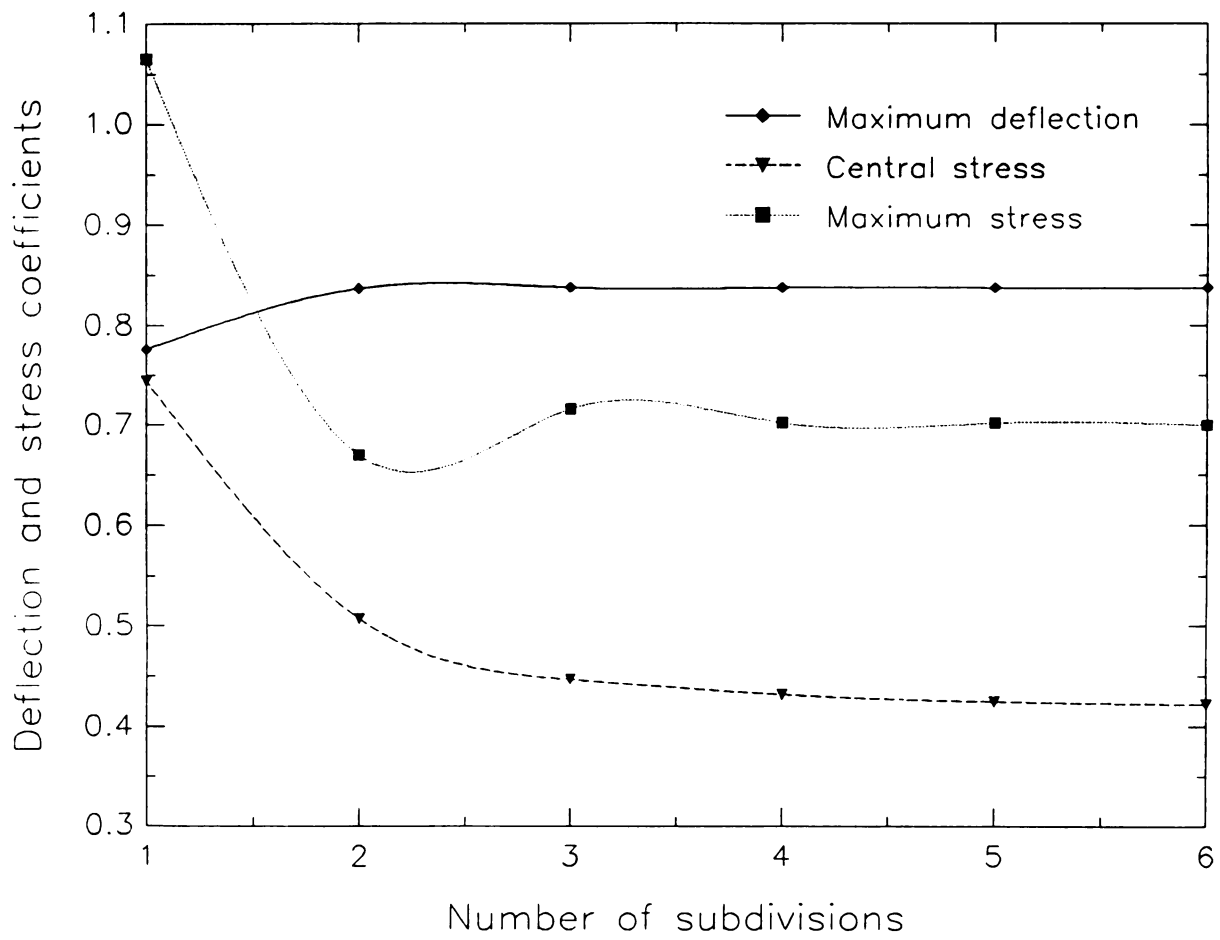
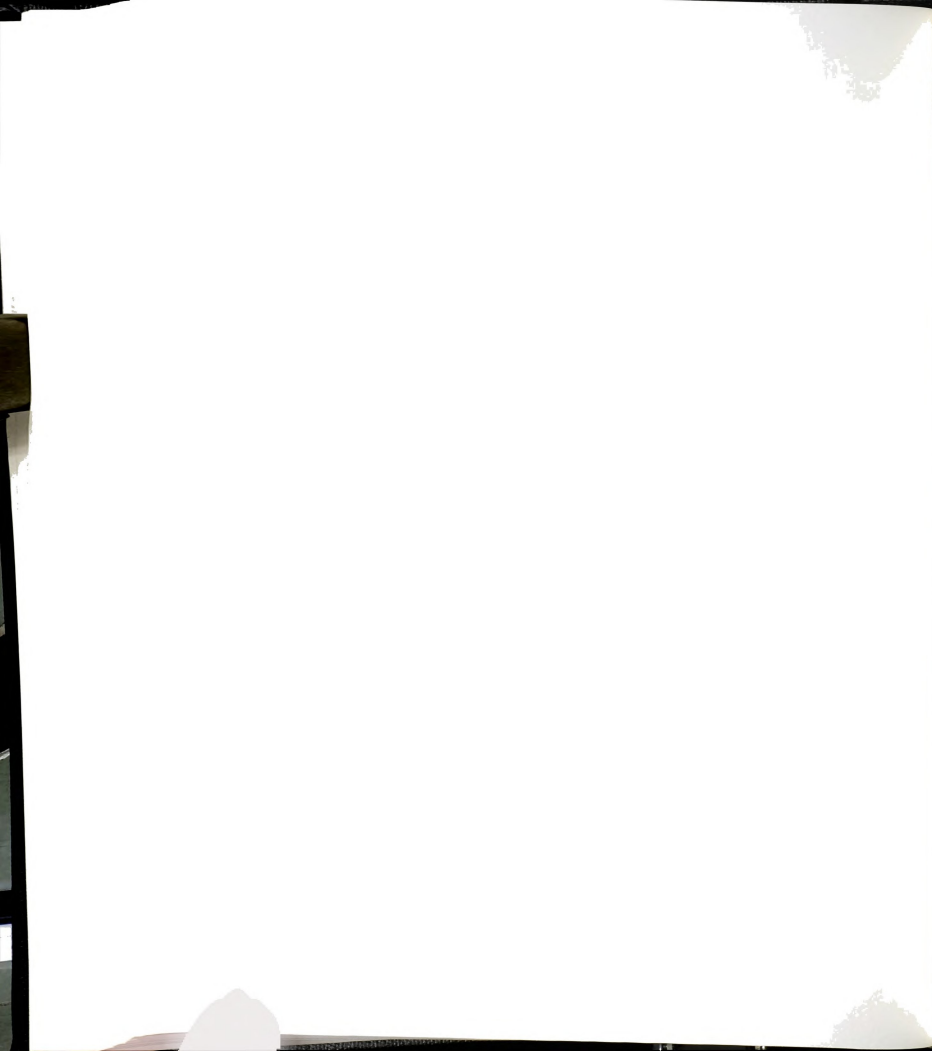


Figure 7: General Model Convergence of Deflection and Stresses for a Rectangular Membrane ($\eta=5/7$)



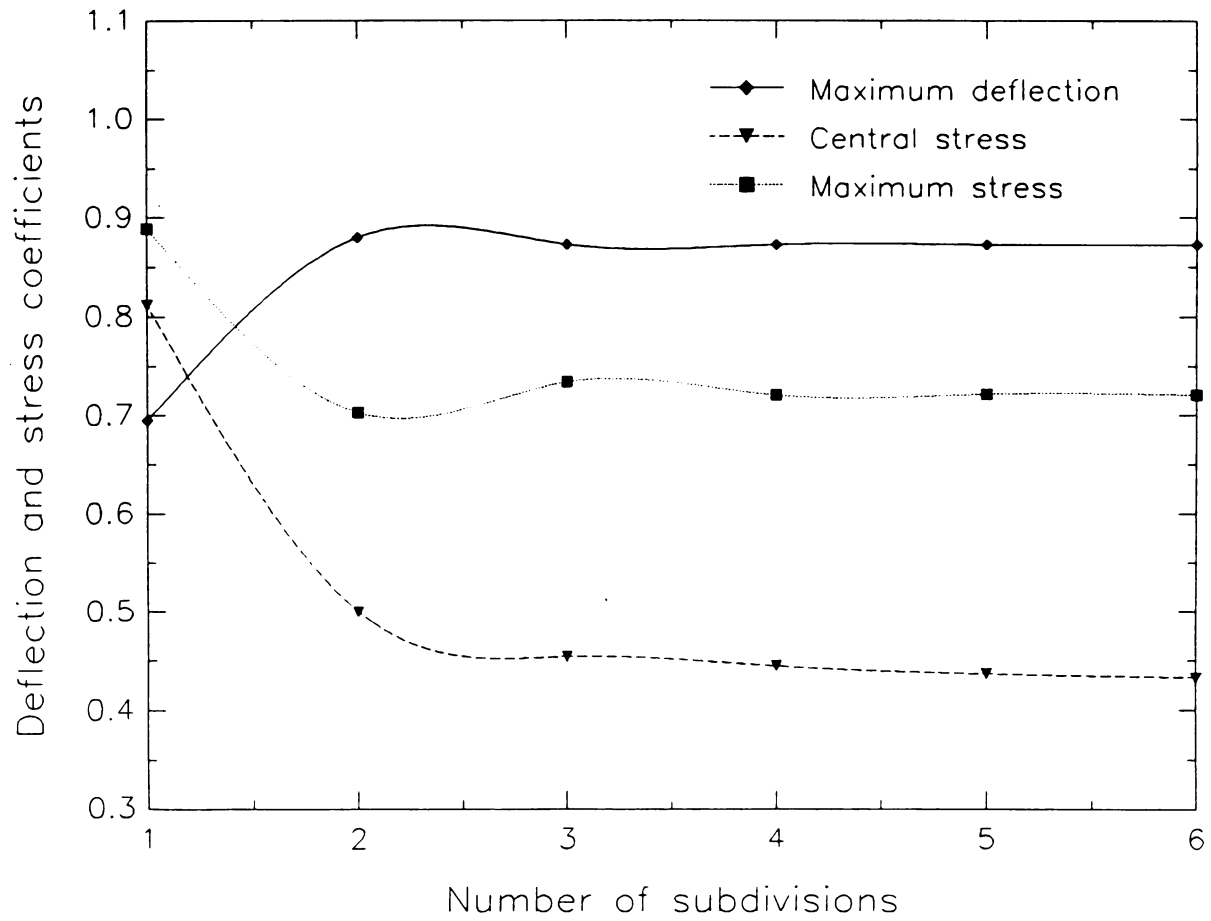


Figure 8: General Model Convergence of Deflection and Stresses for a Rectangular Membrane ($\eta=2/5$)



A comparison was made of the general model with the von Kármán model for the central deflection, and the central and maximum Cauchy stresses. The results, given in terms of deflection and stress coefficients, are shown in Tables 11, 12, 13 and 14.

Table 11: Central Deflection Coefficients

	Von Kármán Model			General model		
	Aspect ratio			Aspect ratio		
k	1	5/7	2/5	1	5/7	2/5
0.0001	0.722	0.836	0.877	0.722	0.836	0.877
0.001	0.722	0.836	0.877	0.722	0.836	0.876
0.01	0.722	0.836	0.877	0.722	0.836	0.876
0.05	0.722	0.836	0.877	0.722	0.835	0.874
0.1	0.722	0.836	0.877	0.722	0.835	0.873
0.5	0.722	0.836	0.877	0.724	0.836	0.872
1.0	0.722	0.836	0.877	0.726	0.838	0.873

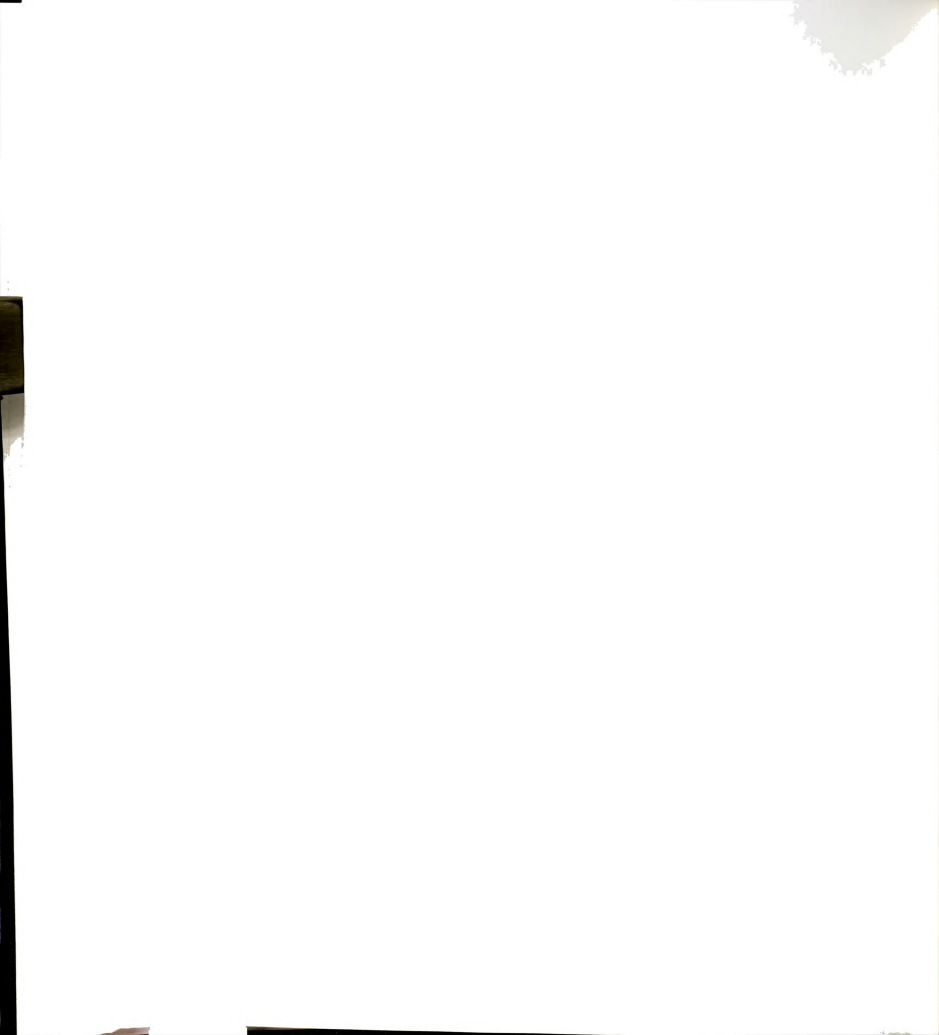


Table 12: Cauchy Stress Coefficients in a Square Membrane

	Von Kármán Model		General Model	
k	Central Stress	Maximum Stress	Central Stress	Maximum Stress
0.0001	0.436	0.522	0.437	0.522
0.001	0.436	0.520	0.436	0.521
0.01	0.436	0.509	0.432	0.517
0.05	0.436	0.484	0.422	0.507
0.1	0.436	0.461	0.415	0.499
0.5	0.436	0.342	0.383	0.466
1.0	0.436	0.346	0.362	0.445

Table 13: Cauchy Stress Coefficients in a Rectangular Membrane $(\eta=5/7)$

	Von Kármán Model		General Model	
k	Central Stress	Maximum Stress	Central Stress	Maximum Stress
0.0001	0.536	0.597	0.535	0.597
0.001	0.536	0.594	0.534	0.596
0.01	0.539	0.581	0.531	0.592
0.05	0.546	0.550	0.522	0.582
0.1	0.552	0.522	0.514	0.574
0.5	0.582	0.376	0.484	0.543
1.0	0.606	0.436	0.465	0.523

Table 14: Cauchy Stress Coefficients in a Rectangular Membrane
($\eta=2/5$)

	Von Kármán Model		General Model	
k	Central Stress	Maximum Stress	Central Stress	Maximum Stress
0.0001	0.575	0.599	0.575	0.599
0.001	0.577	0.595	0.574	0.598
0.01	0.583	0.581	0.571	0.594
0.05	0.598	0.547	0.565	0.585
0.1	0.612	0.515	0.559	0.577
0.5	0.681	0.354	0.539	0.549
1.0	0.741	0.513	0.527	0.531

Tables 15, 16 and 17 show the relative error in deflection and stress coefficients when the von Kármán model is used instead of the general model. The relative error in a variable Q (deflection coefficient or stress coefficient) is defined as:

$$\Delta Q = \frac{Q_v - Q_g}{Q_g} \quad (6.5)$$

where Q_v is the corresponding variable in the von Kármán model, and Q_g is the corresponding quantity in the general model.

Table 15: Relative Error for a Square Membrane

k	Relative Error %		
	Central Deflection	Central Stress	Maximum Stress
0.0001	0	-0.23	0
0.001	0	0	-0.19
0.01	0	0.93	-1.55
0.05	0	3.32	-4.54
0.1	0	5.06	-9.62
0.5	-0.28	13.8	-26.6
1	-0.55	20.4	-22.2

Table 16: Relative Error for a Rectangular Membrane ($\eta=5/7$)

k	Relative Error %		
	Central Deflection	Central Stress	Maximum Stress
0.0001	0	0.19	0
0.001	0	0.37	-0.34
0.01	0	1.50	-1.86
0.05	0.12	4.60	-5.50
0.1	0.12	7.39	-9.06
0.5	0	20.2	-30.8
1	-0.23	30.3	-16.6



Table 17: Relative Error for a Rectangular Membrane ($\eta=2/5$)

k	Relative Error %		
	Central Deflection	Central Stress	Maximum Stress
0.0001	0	0	0
0.001	0.11	0.52	-0.50
0.01	0.11	2.10	-2.19
0.05	0.34	5.84	-6.50
0.1	0.46	9.48	-10.7
0.5	0.57	26.3	-35.5
1	0.46	40.6	-3.39

It appears from the above results that the von Kármán model overestimates the central stress but underestimates the maximum stress. The accuracy of the von Kármán model declines sharply as k increases beyond 0.01.

In addition, a comparison between the two models for the central and maximum actual strains is made. The corresponding results are shown in Tables 18, 19 and 20.



Table 18: Comparison of Strains for a Square Membrane

k	Von Kármán Model		General Model	
	Central Strain %	Maximum Strain %	Central Strain %	Maximum Strain %
0.0001	0.04	0.07	0.04	0.07
0.001	0.21	0.32	0.20	0.32
0.01	0.95	1.48	0.94	1.50
0.05	2.79	4.33	2.69	4.49
0.1	4.42	6.87	4.20	7.25
0.5	12.9	20.1	11.3	22.5
1.0	20.5	31.9	17.0	36.8

Table 19: Comparison of Strains for a Rectangular Membrane $(\eta=5/7)$

k	Von Kármán Model		General Model	
	Central Strain %	Maximum Strain %	Central Strain %	Maximum Strain %
0.0001	0.06	0.08	0.06	0.08
0.001	0.29	0.36	0.28	0.37
0.01	1.33	1.69	1.31	1.72
0.05	3.88	4.95	3.71	5.17
0.1	6.16	7.86	5.74	8.38
0.5	18.0	23.0	15.2	26.2
1.0	28.6	36.5	22.7	42.8



Table 20: Comparison of Strains for a Rectangular Membrane
($\eta=2/5$)

k	Von Kármán Model		General Model	
	Central Strain %	Maximum Strain %	Central Strain %	Maximum Strain %
0.0001	0.07	0.08	0.07	0.08
0.001	0.34	0.37	0.34	0.37
0.01	1.57	1.70	1.54	1.73
0.05	4.60	4.97	4.36	5.23
0.1	7.31	7.88	6.73	8.49
0.5	21.4	23.1	17.6	26.8
1.0	33.9	36.6	26.0	44.0

The von Kármán model overestimates the central strain but underestimates the maximum strain. Again, it should be mentioned that for higher values of strains the membrane may exhibit an anelastic behavior. When this is the case, the assumption of elastic behavior is no longer valid, and new constitutive relationships modelling the material behavior should be considered.

To illustrate the distribution of deflections and stresses within the membrane, the deflection and stress coefficients for the three membrane cases studied were plotted along the center lines a-a and d-d, quarter lines b-b and e-e, and edge lines c-c and f-f as shown in Figure 9. Figures 10 to 19 illustrate the results. The nondimensional coefficient k was taken equal to 0.01.



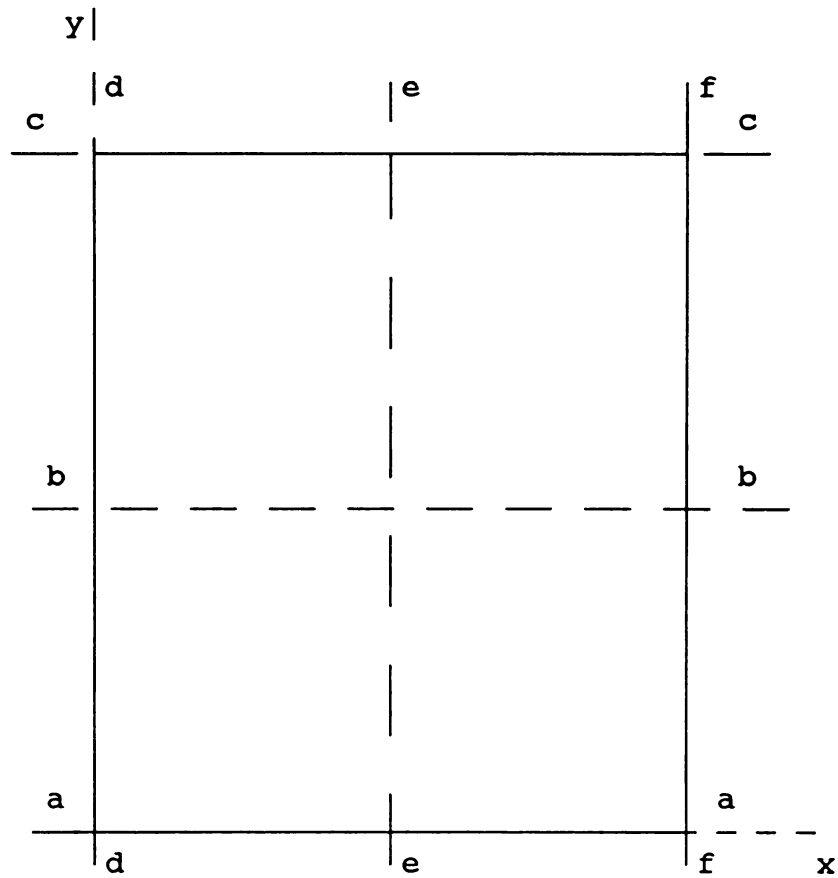
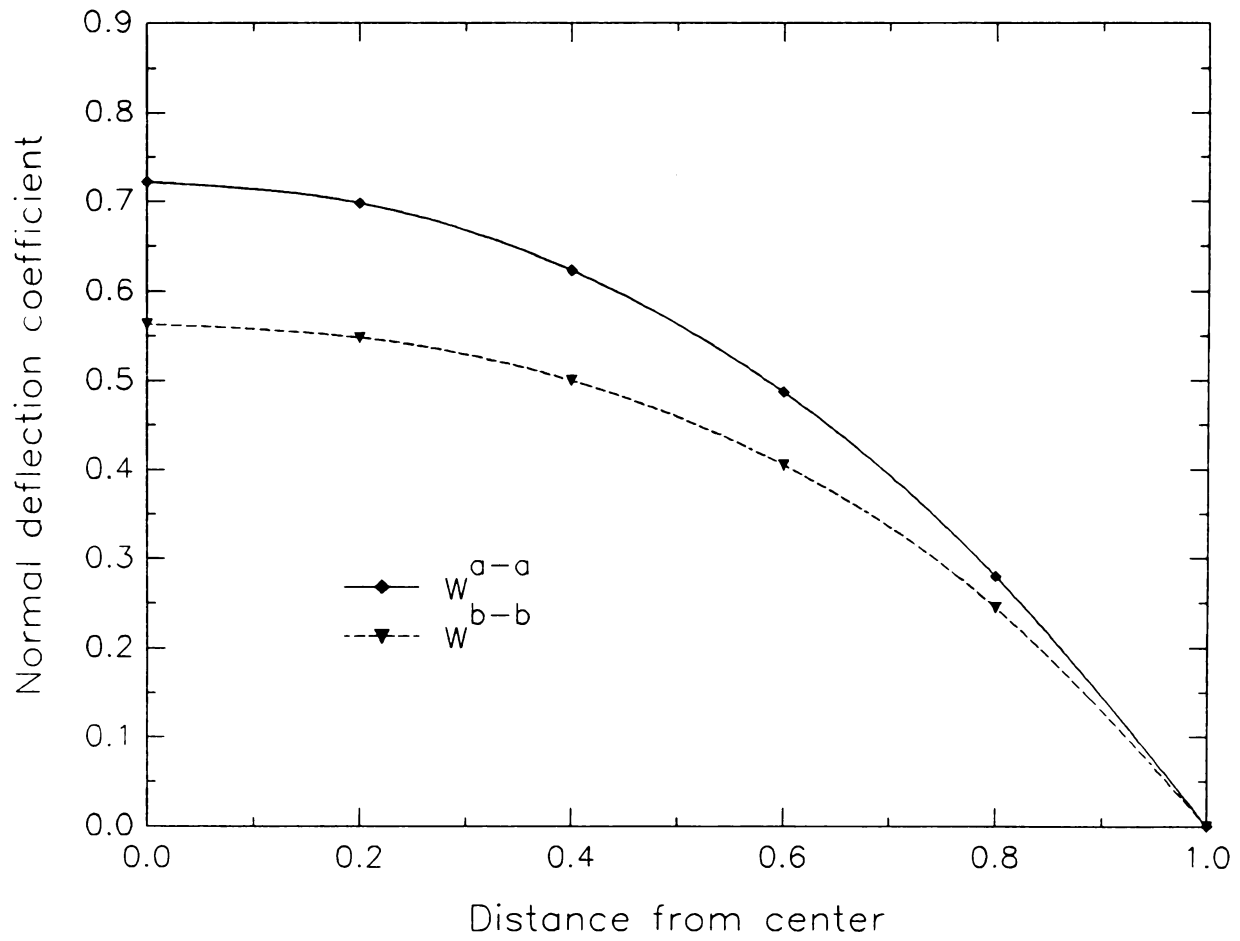


Figure 9: Typical Quarter of a Membrane





**Figure 10: Deflection Coefficient Distribution
for a Square Membrane**



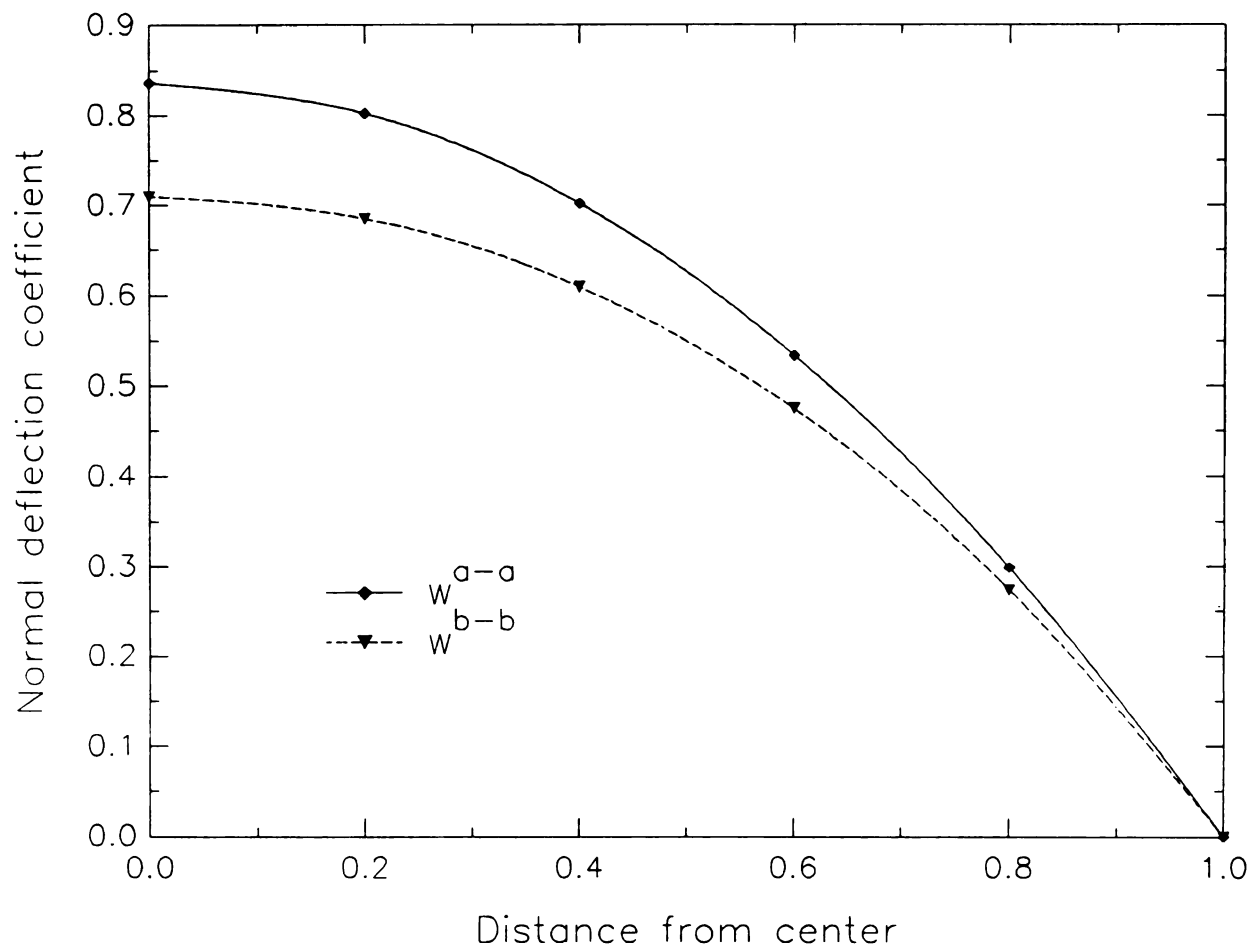


Figure 11: Deflection Coefficient Distribution Along the Shorter Side of a Rectangular Membrane ($\eta=5/7$)

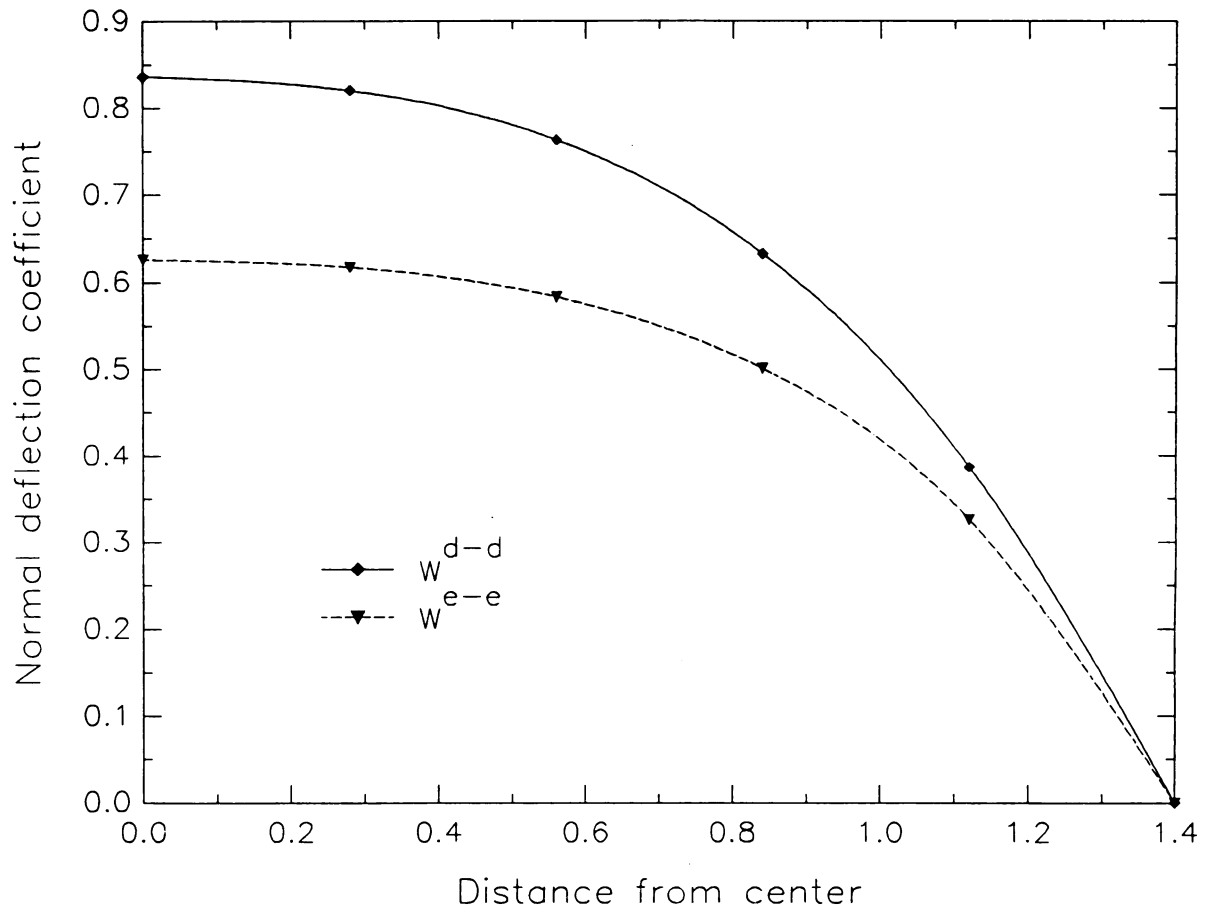


Figure 12: Deflection Coefficient Distribution Along the
the Longer Side in a Rectangular Membrane ($\eta=5/7$)



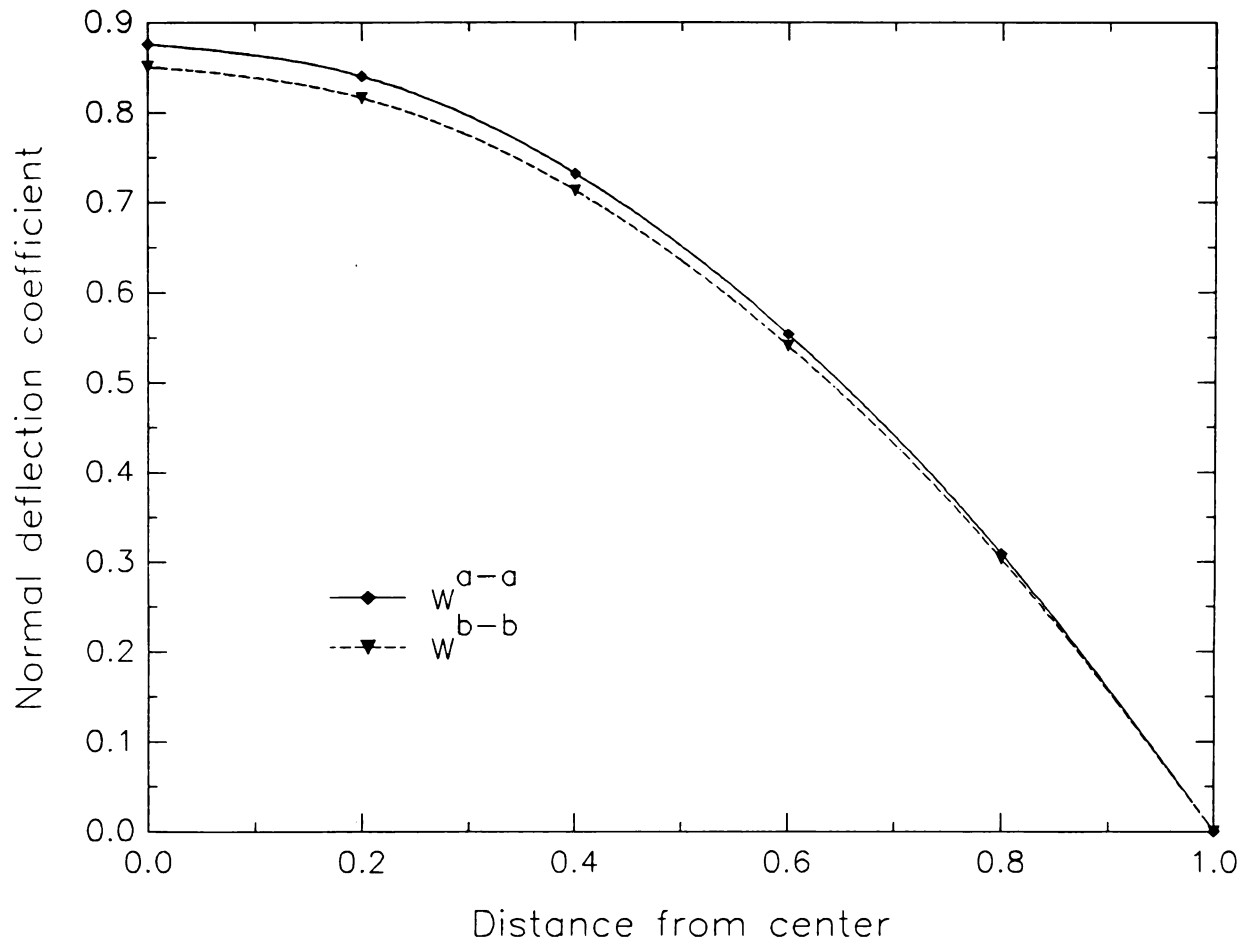


Figure 13: Deflection Coefficient Distribution Along the Shorter Side of a Rectangular Membrane ($\eta=2/5$)



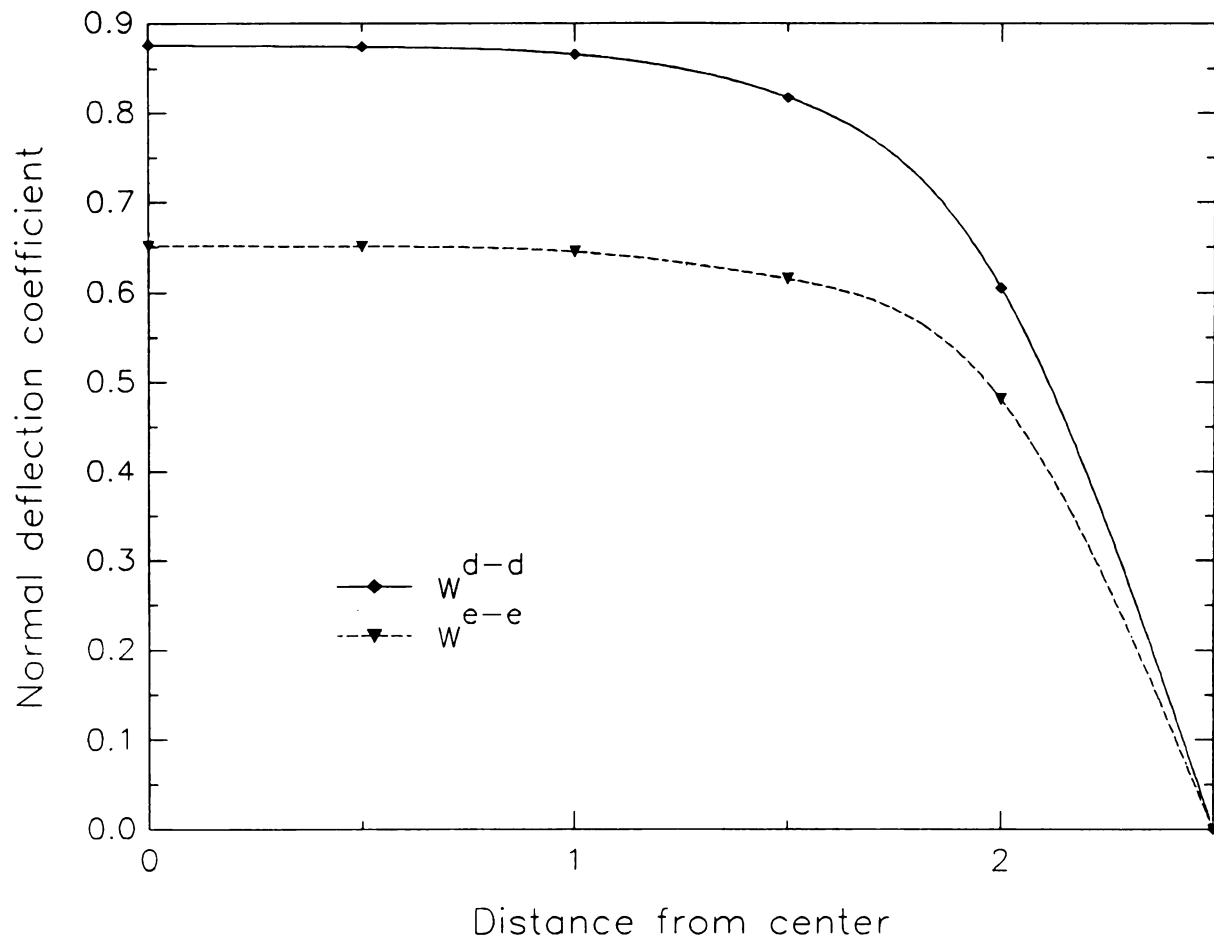
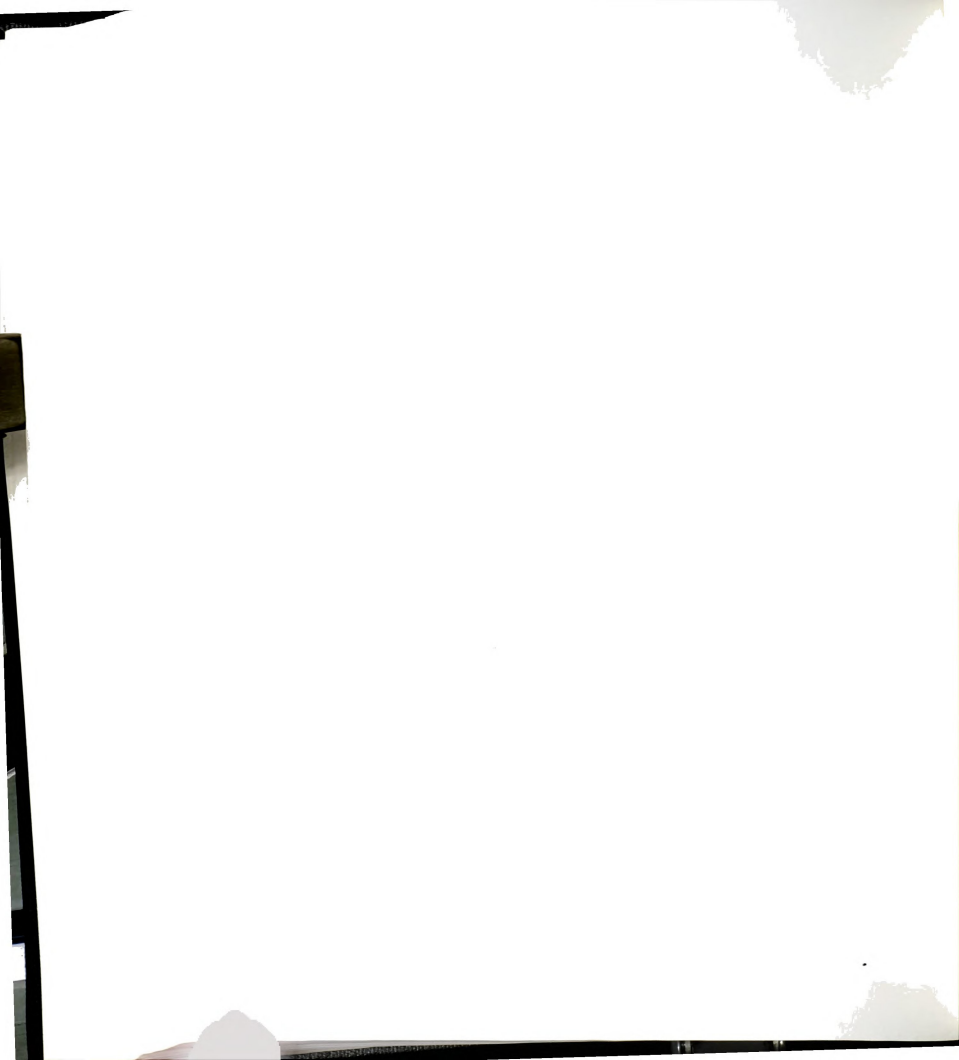


Figure 14: Deflection Coefficient Distribution Along the the Longer Side in a Rectangular Membrane ($\eta=2/5$)



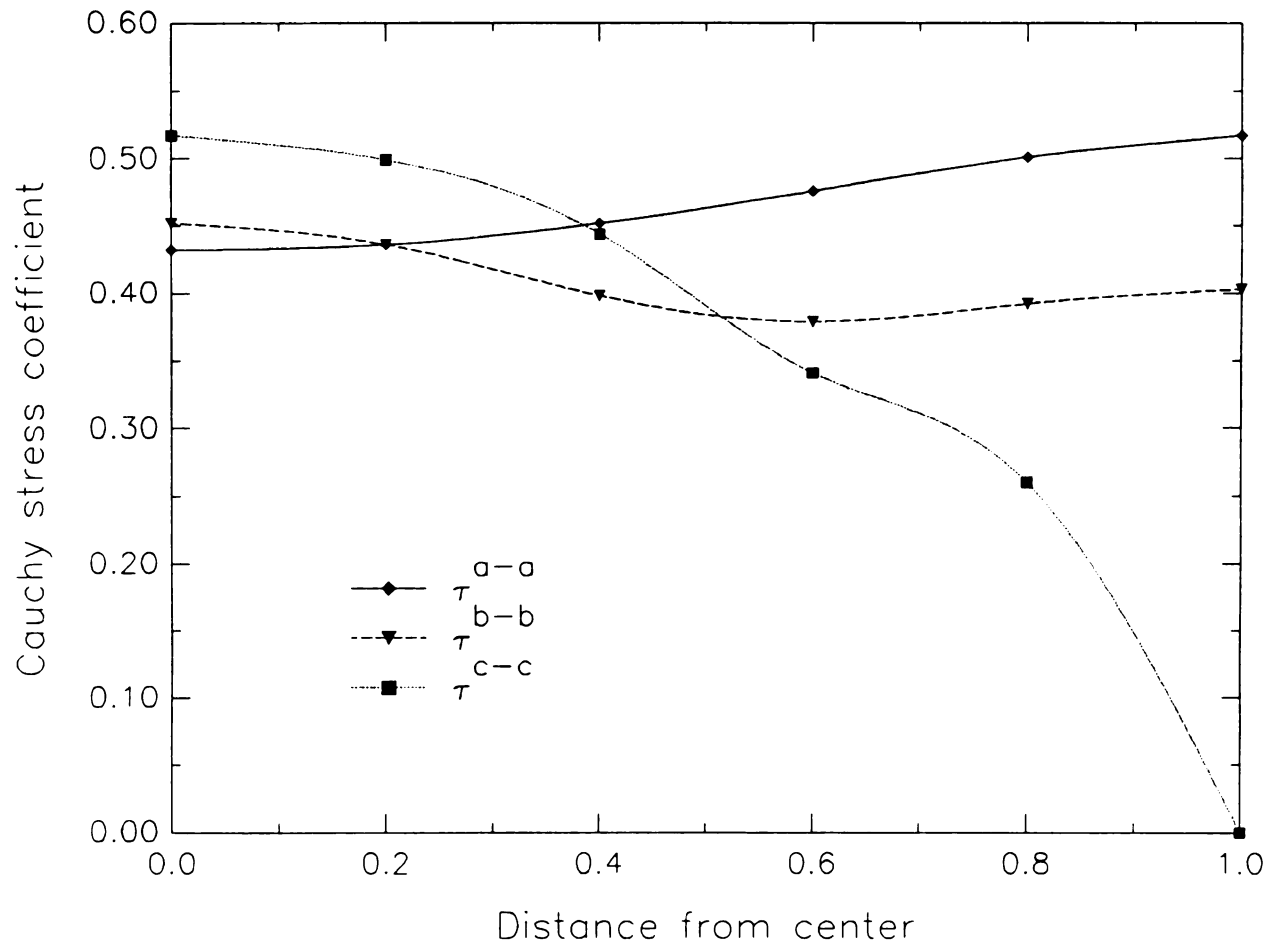


Figure 15: Stress Coefficient Distribution for a Square Membrane



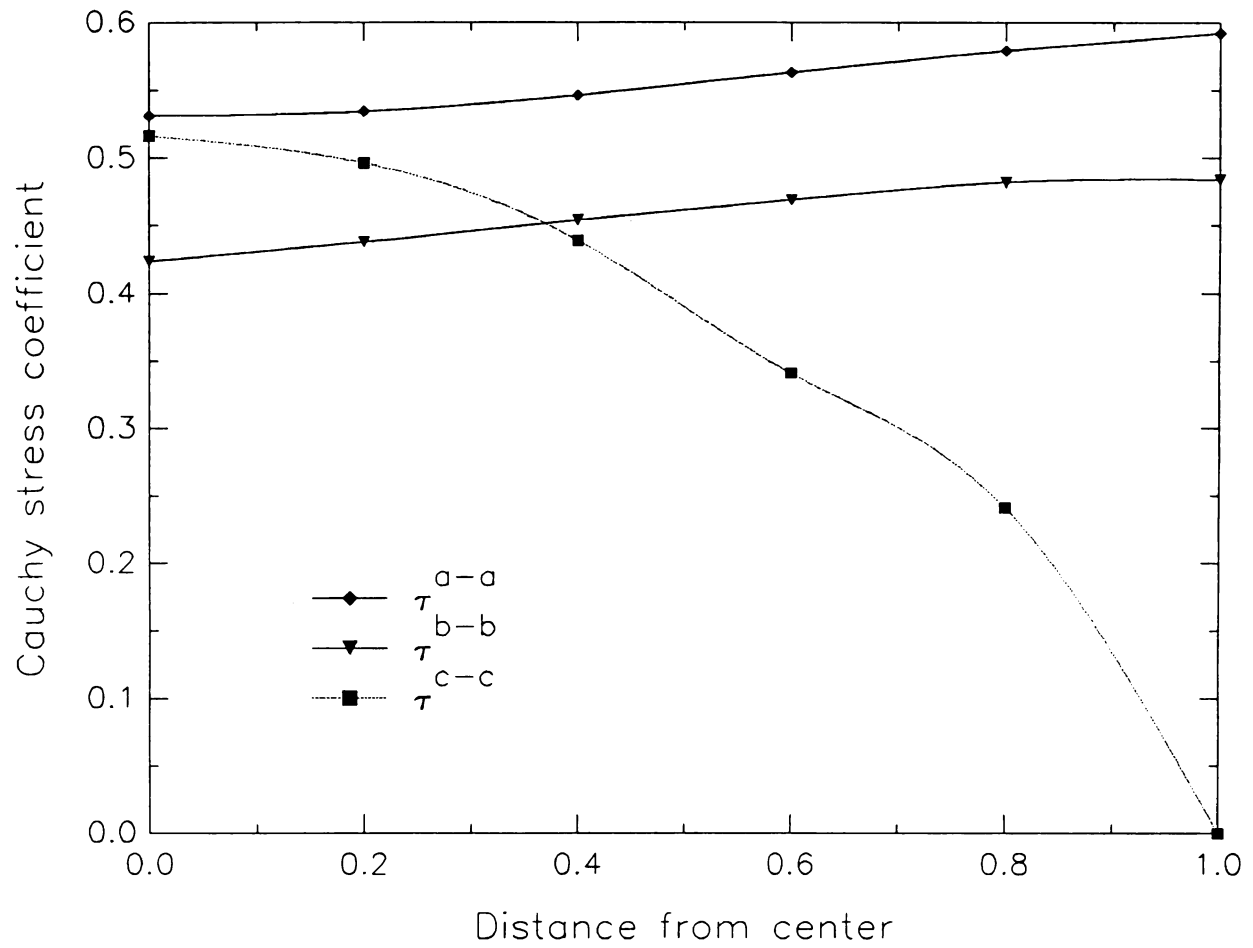


Figure 16: Stress Coefficient Distribution Along the Shorter Side of a Rectangular Membrane ($\eta=5/7$)



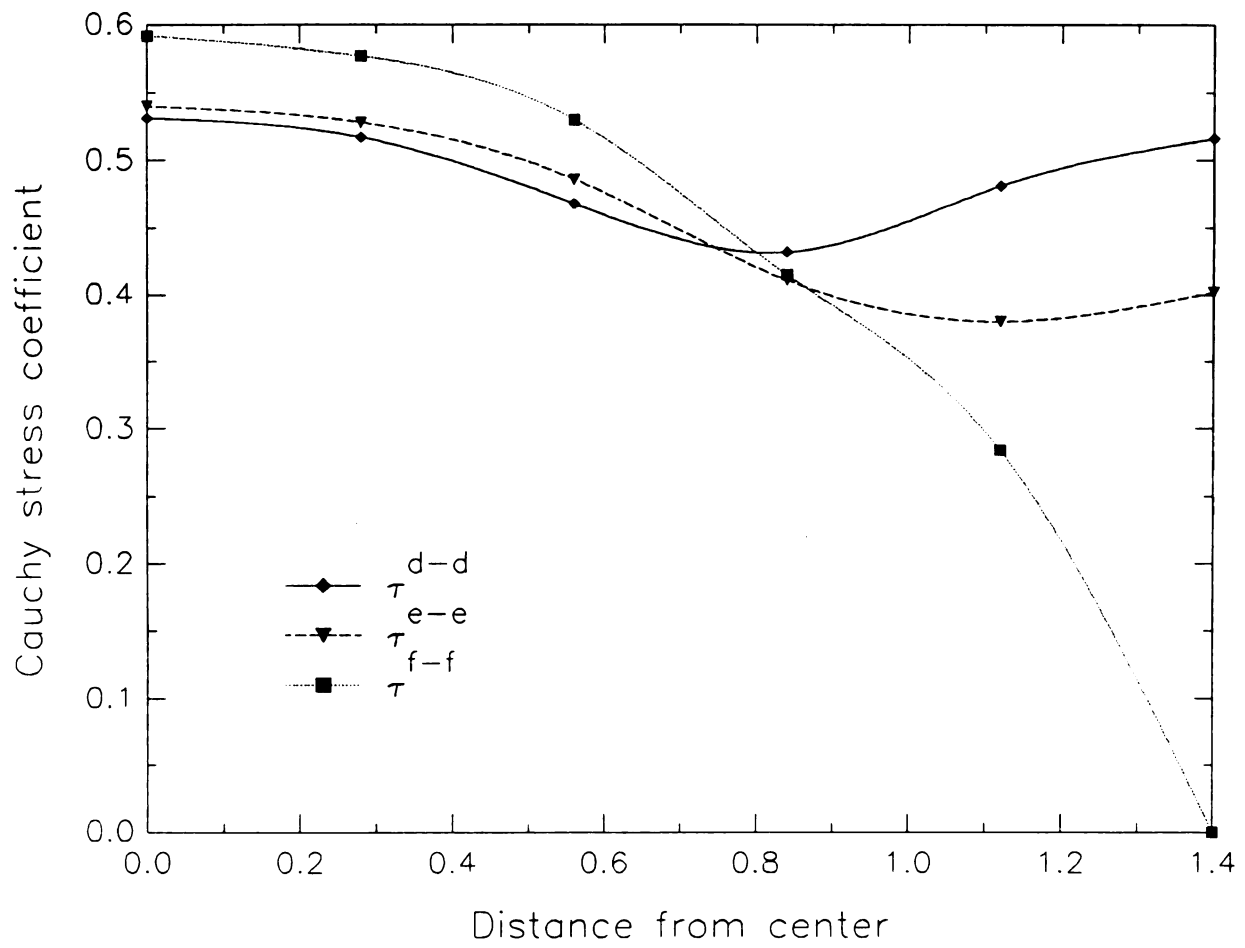
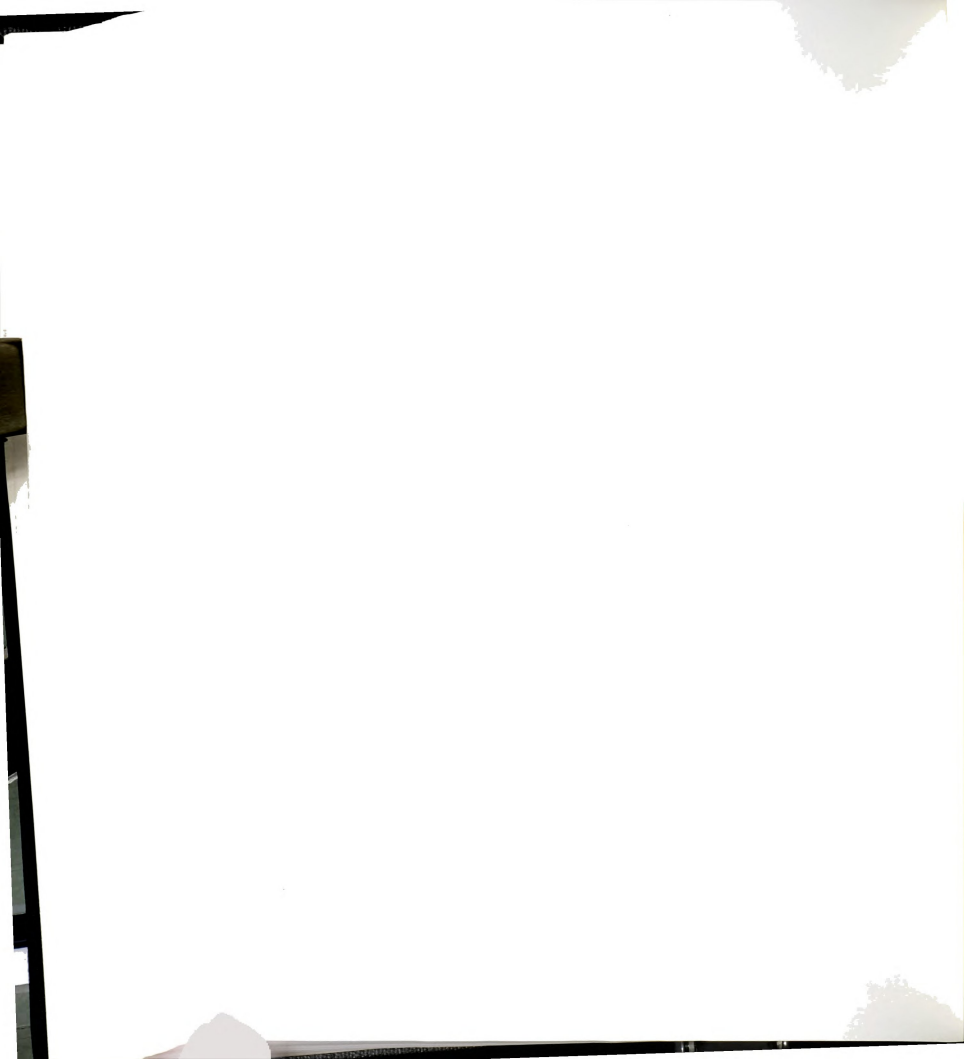


Figure 17: Stress Coefficient Distribution Along the
the Longer Side in a Rectangular Membrane ($\eta=5/7$)



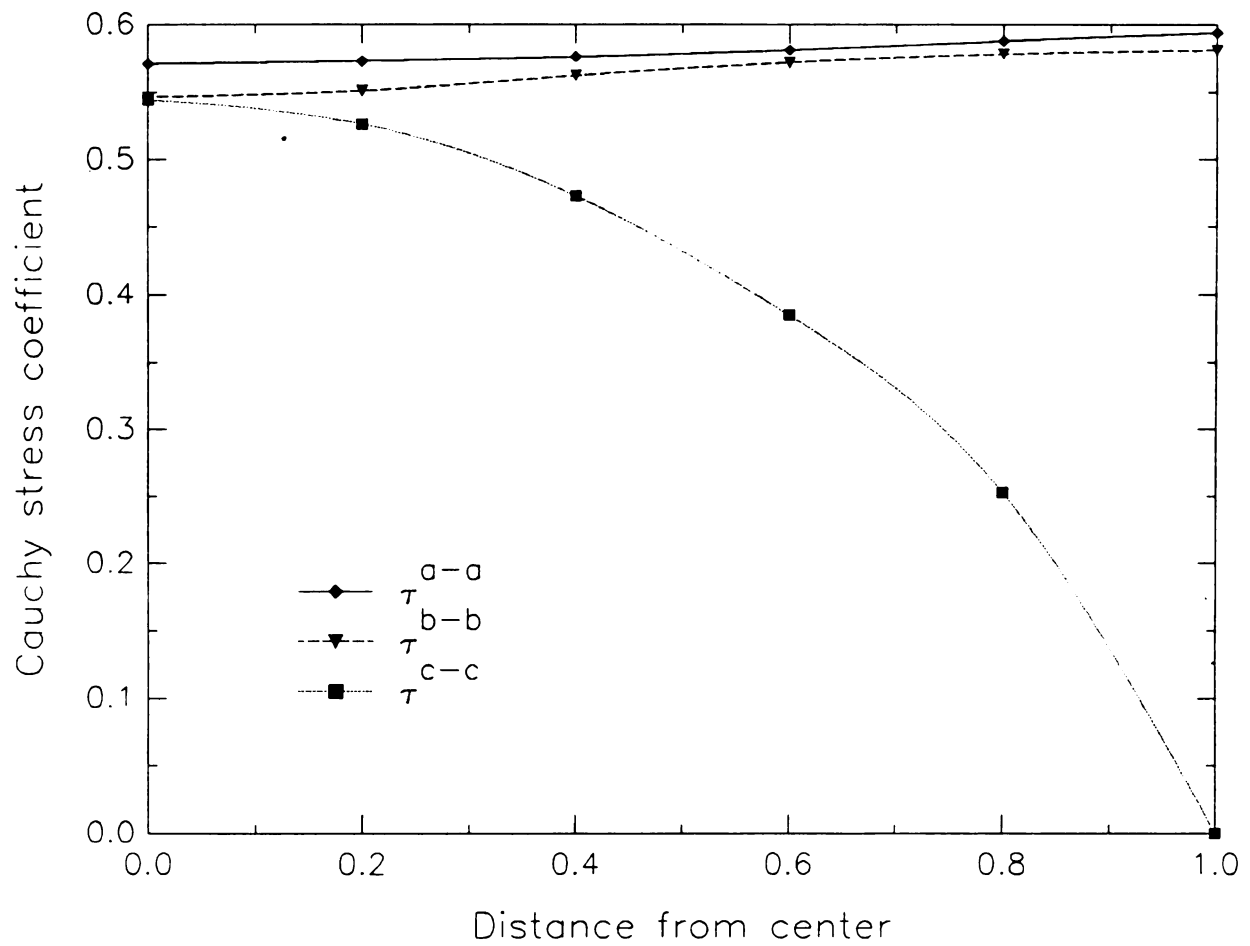


Figure 18: Stress Coefficient Distribution Along the Shorter Side of a Rectangular Membrane ($\eta=2/5$)



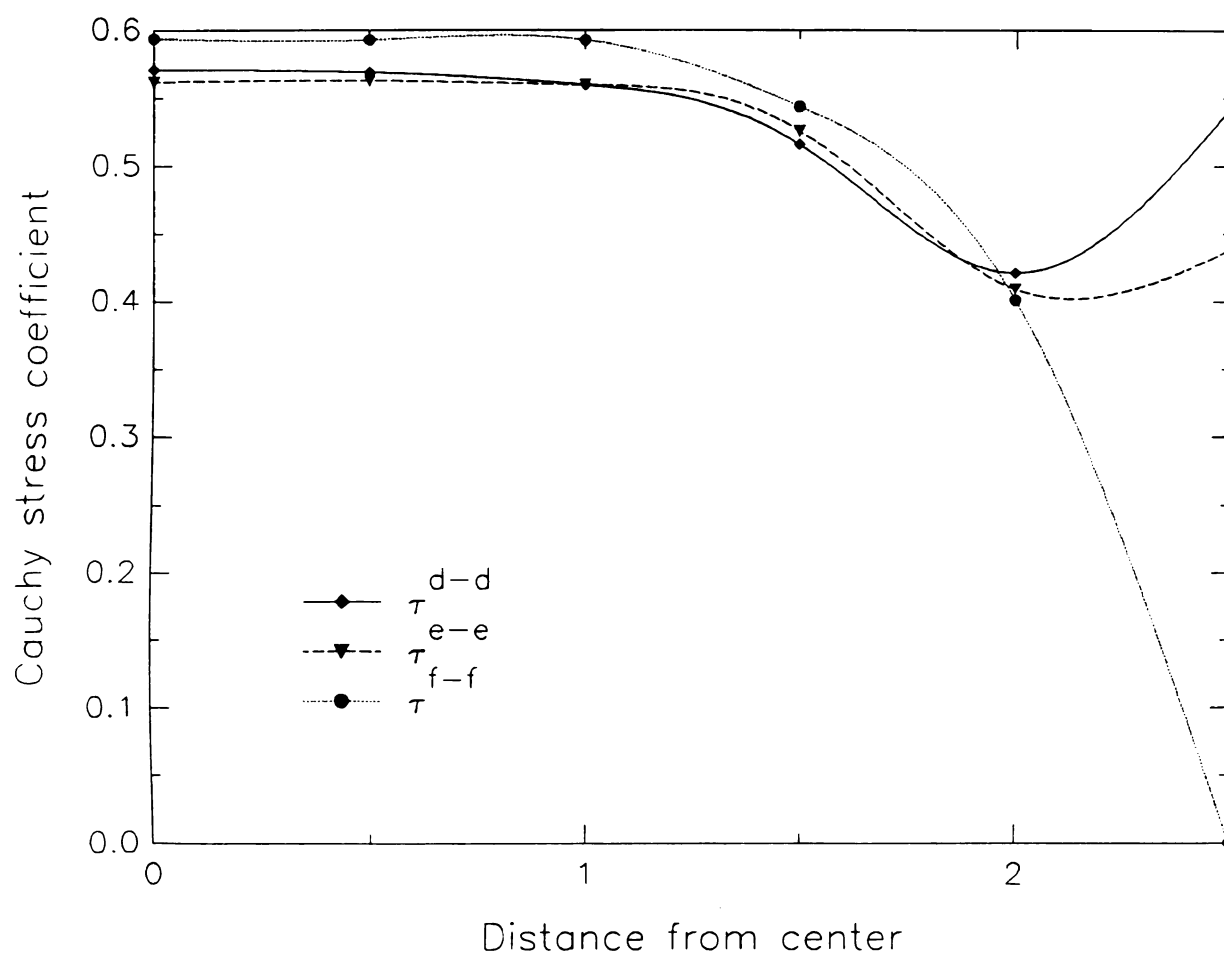


Figure 19: Stress Coefficient Distribution Along the
the Longer Side in a Rectangular Membrane ($\eta=2/5$)



6.2 Parametric Studies

6.2.1 Effect of Poisson's Ratio

To investigate the effect of Poisson's ratio on deflections and stresses, a square membrane was analyzed. Nine different values of Poisson's ratio ranging from 0.2 to 0.48 were considered. These values are: 0.2, 0.25, 0.3, 0.33, 0.37, 0.4, 0.43, 0.45, and 0.48. Figure 20 shows the variation of the central deflection, the central stress, and the maximum stress with Poisson's ratio.

It is evident from the results that as Poisson's ratio increases, the deflections decrease and the stresses increase. From $\nu=0.2$ to $\lambda=0.48$, the variation in the central deflection coefficient, the central stress coefficient, and the maximum stress coefficient are, respectively, 10.7%, 10.5%, and 3.9%.



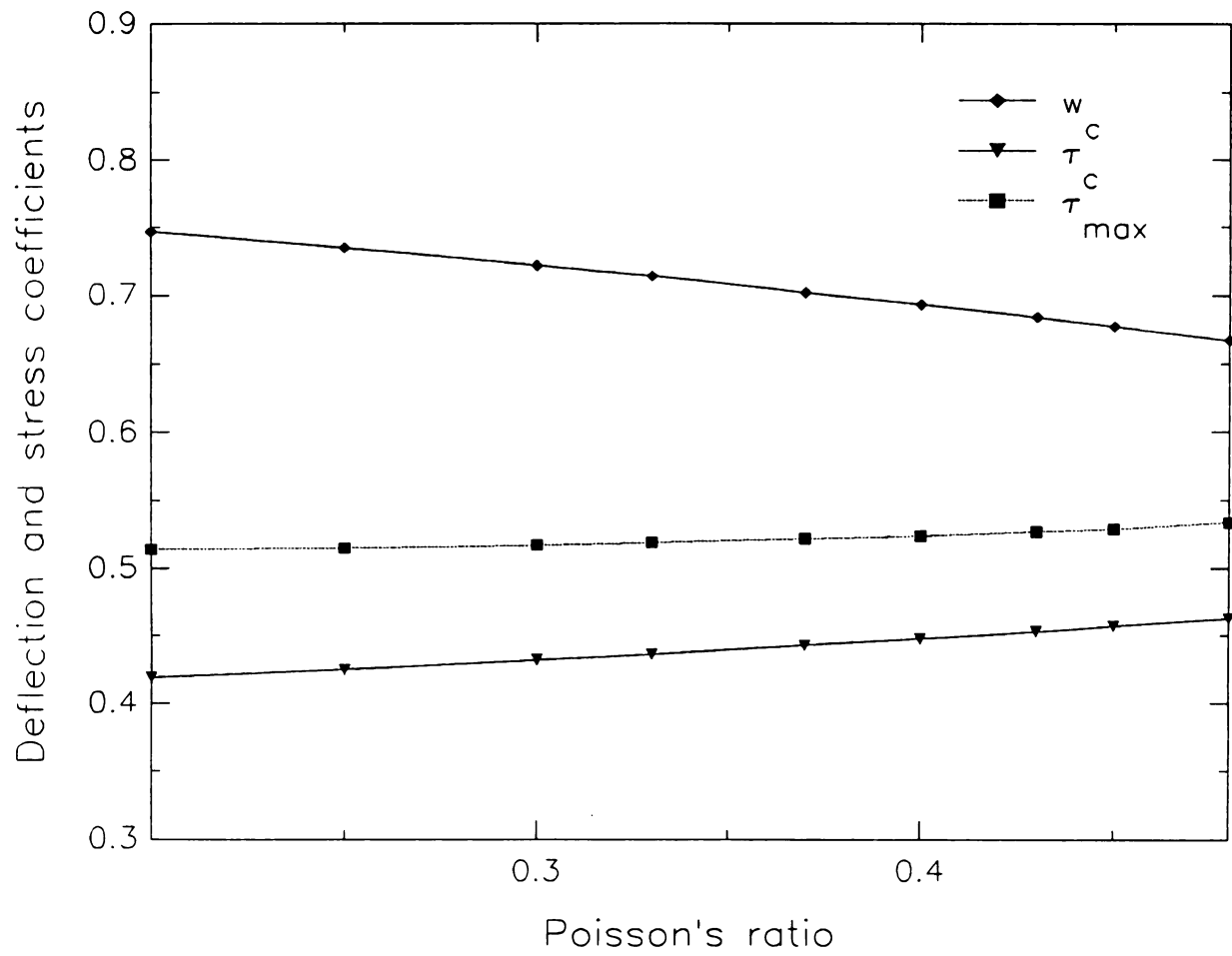
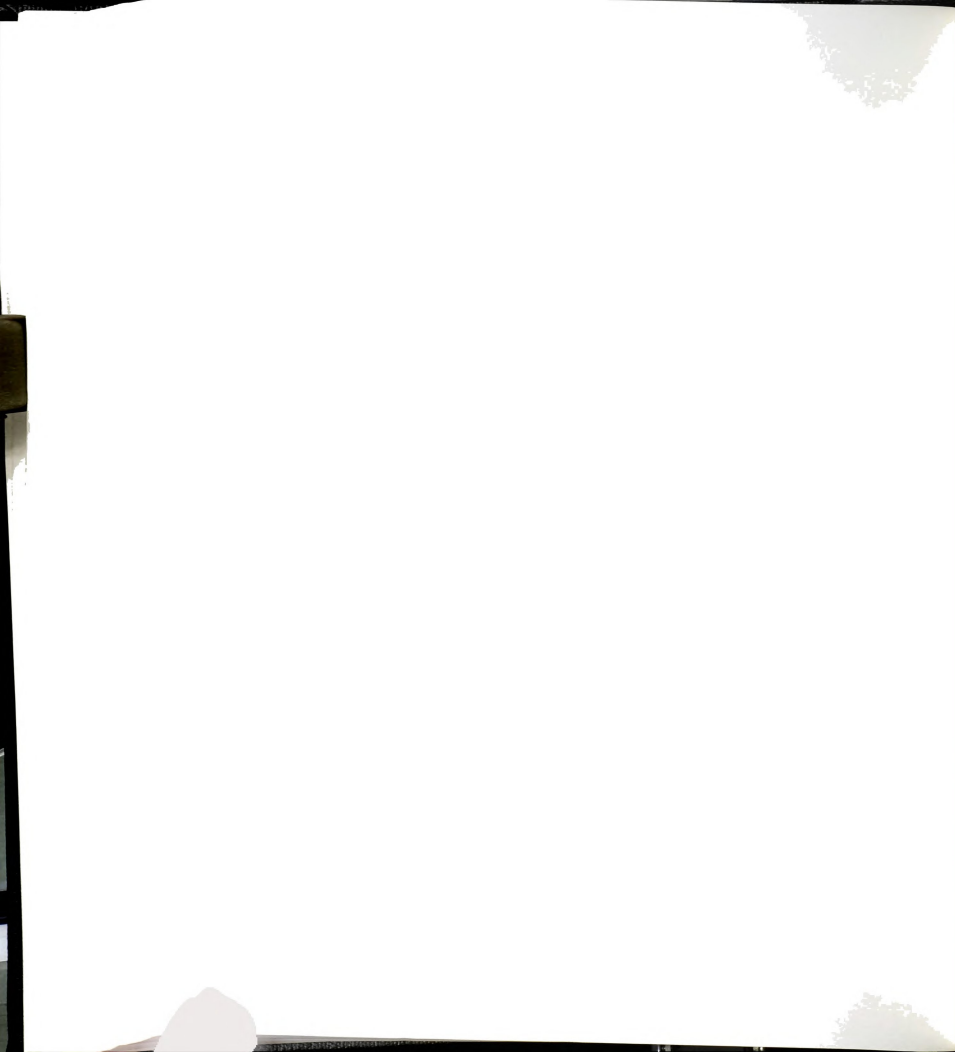


Figure 20: Effect of Poisson's Ratio



6.2.2 Effect of Initial Prestressing

The membrane cases studied above were assumed to be stress-free before the application of normal loading. In actual use, it is common to prestress membranes in order to compensate for the lack of bending stiffness. To investigate the effect of initial prestressing on membrane deflections and stresses, a square membrane initially prestressed along the x-direction was analyzed. For the purpose of generality, initial prestressing is expressed in terms of initial prestraining. Different values of initial prestraining up to 1.4% were considered. Poisson's ratio was taken equal to 0.4. Figure 21 shows the variation of the central deflection coefficient, and the central and maximum stress coefficients with these values.

As expected, the central deflection decreases as the initial prestressing increases. The membrane behaves as if it has an initial bending stiffness. Nevertheless, the stresses increase with the increase of the initial prestressing. Therefore the latter may contribute to premature tearing of the membrane. The variation of the central deflection coefficient, and the central and maximum stress coefficients are, respectively, 10.8%, 36.6%, and 29% when the value of the initial prestraining varies from 0 to 1.4%.



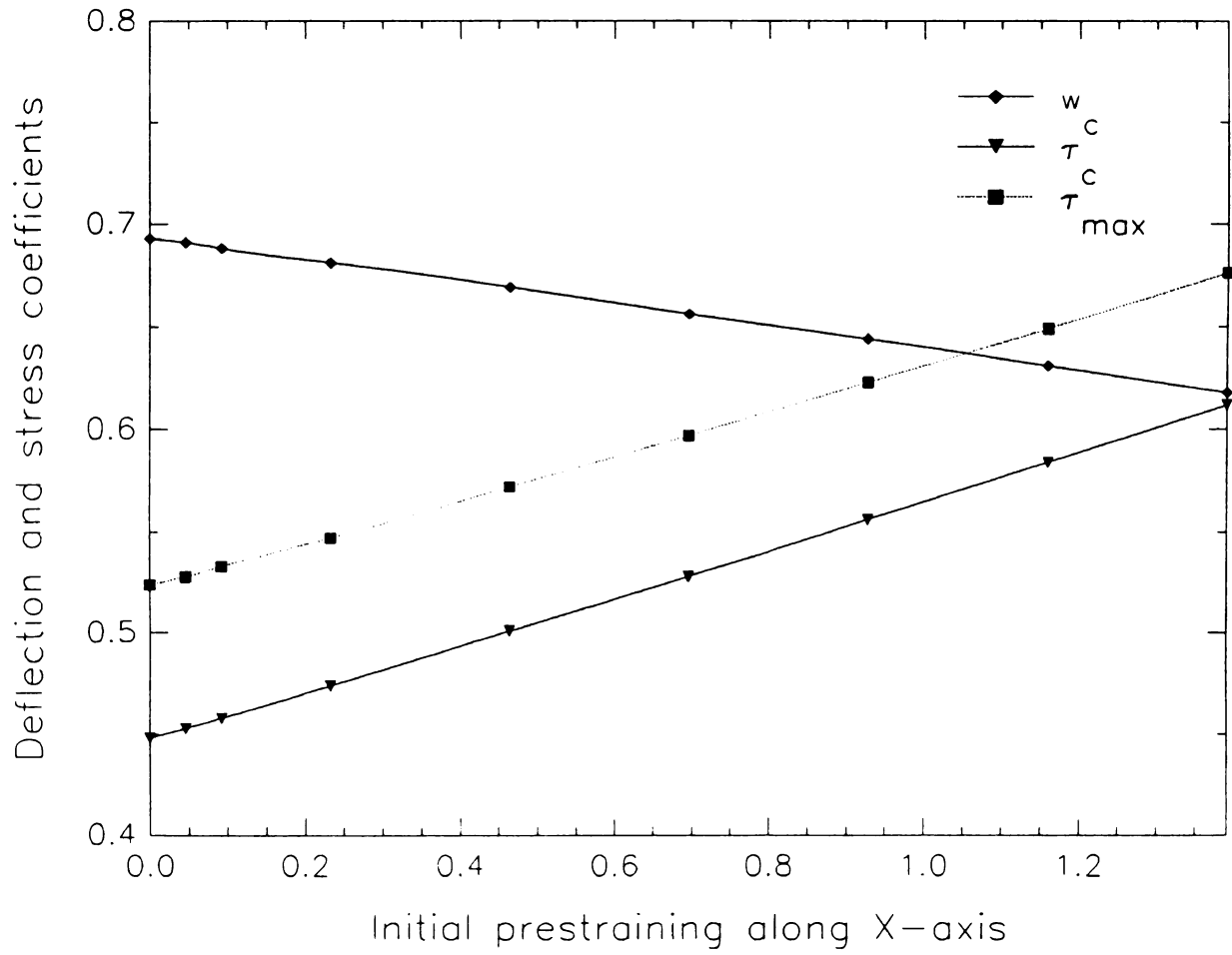
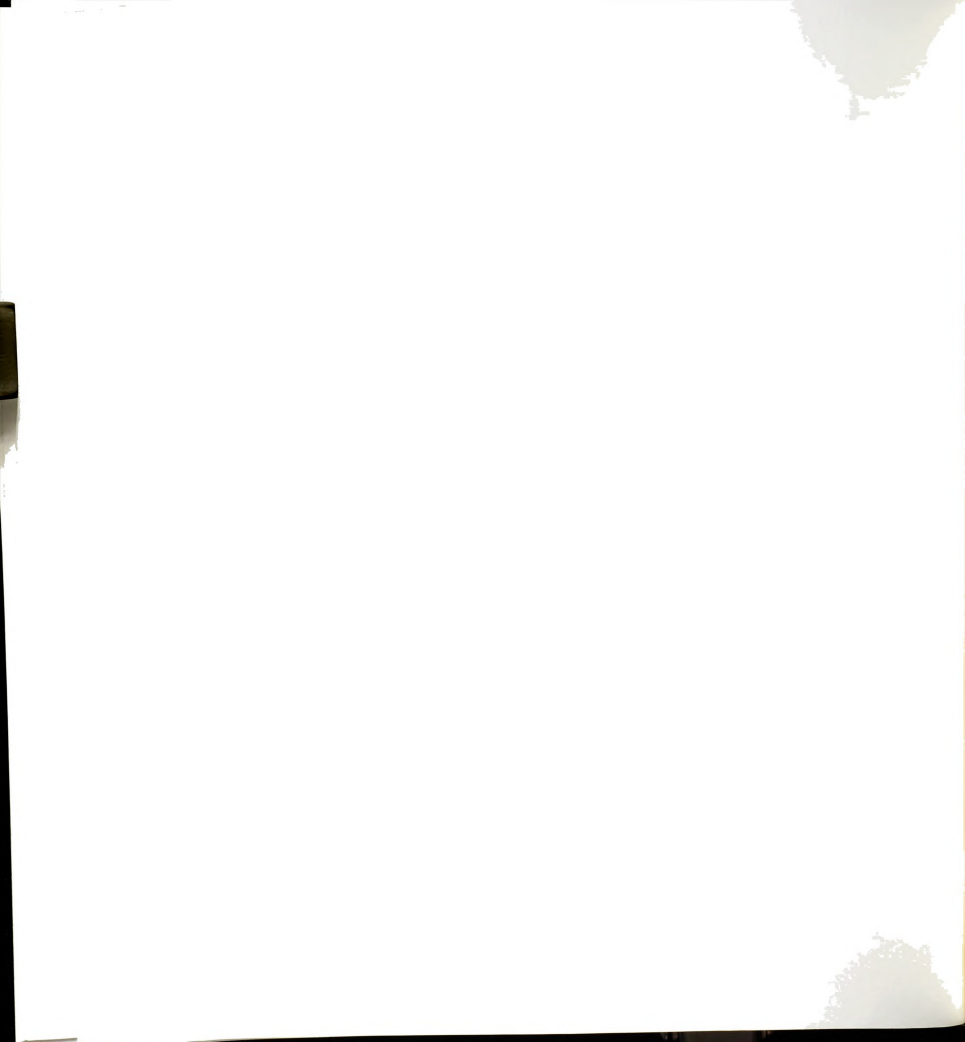


Figure 21: Effect of Initial Prestraining



6.2.3 Effect of the Boundary Conditions

In the examples studied in the previous sections the membrane was assumed to be fixed along its four edges. In this section, the membrane is assumed to have the two edges parallel to the x-axis free, while the other two edges remain fixed. This type of membrane boundary conditions is common in plastic greenhouses.

Deflections and stresses of a square membrane, for this type of boundary conditions and the one considered previously, are compared in Figures 22, 23, 24 and 25. The superscripts bc1 and bc2 refer, respectively, to the previous case and the present case. The values of the nondimensional coefficient k and Poisson's ratio ν considered were, respectively, 0.01 and 0.3.

Deflections and stress coefficients corresponding to the present case are higher than in the previous case (23.1% for the central deflection, and 12.4% for the maximum stress).



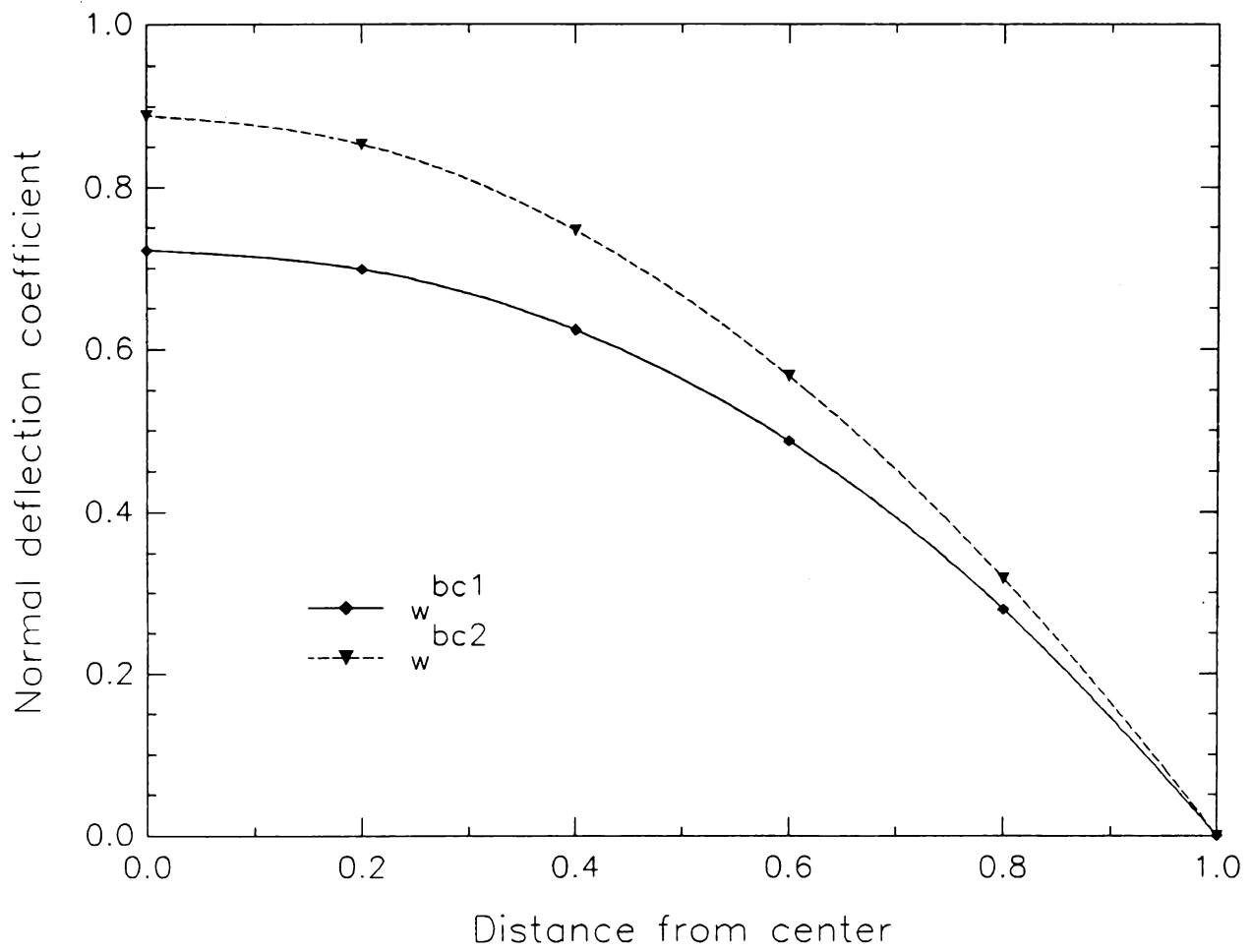


Figure 22: Comparison of Normal Deflections Along the Center Line a-a



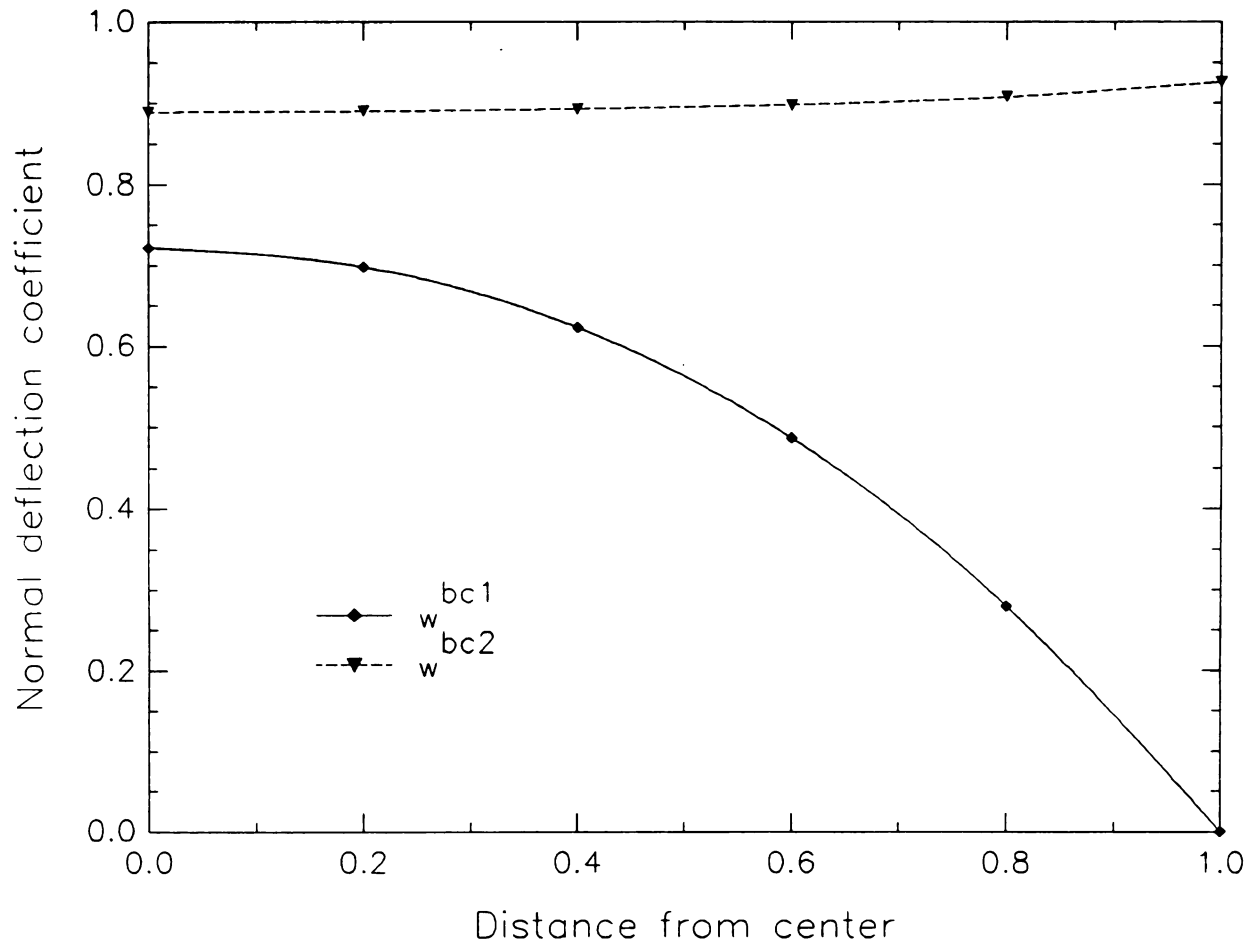


Figure 23: Comparison of Normal Deflections Along the Center Line d-d



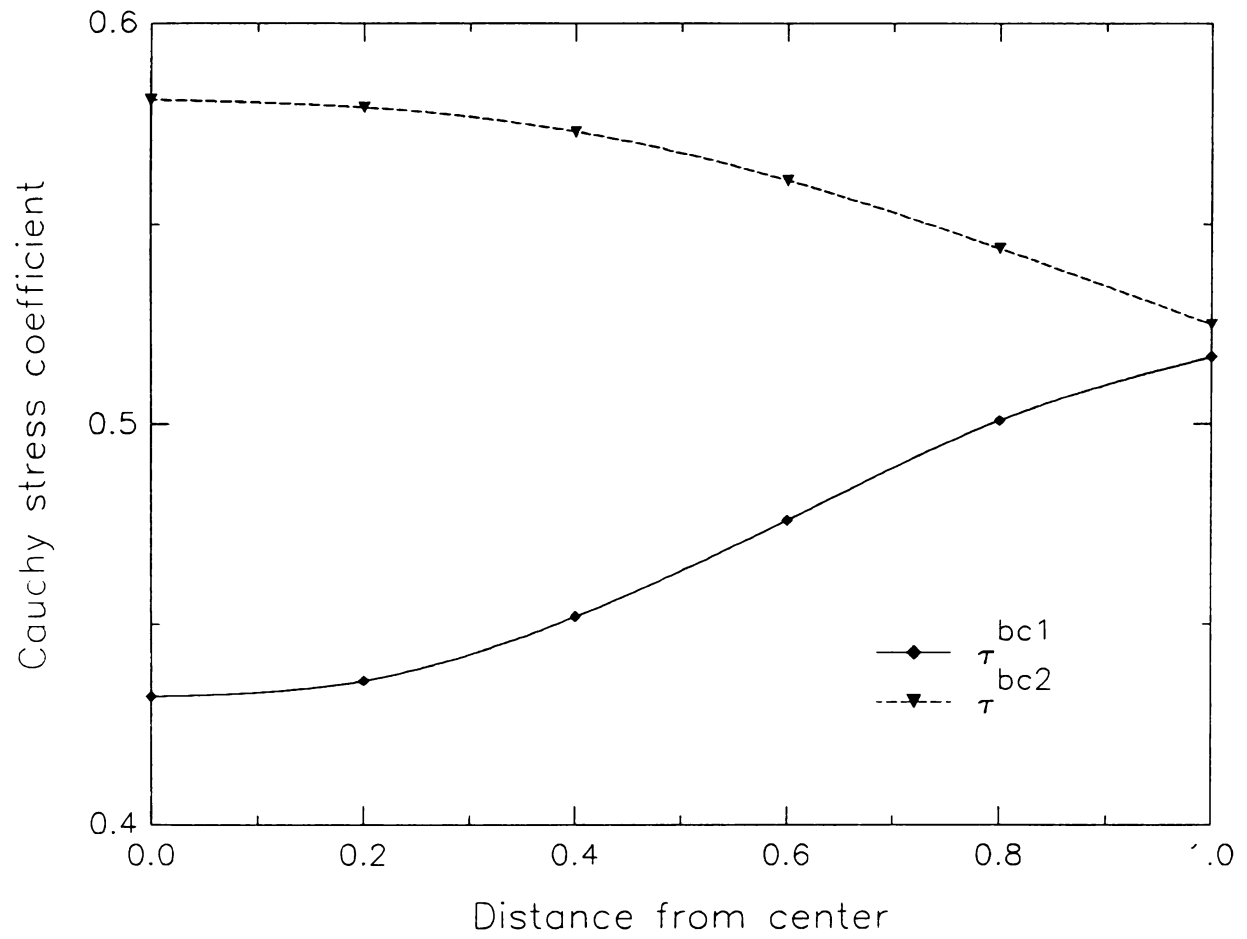


Figure 24: Comparison of Cauchy Stresses Along the Center Line a-a



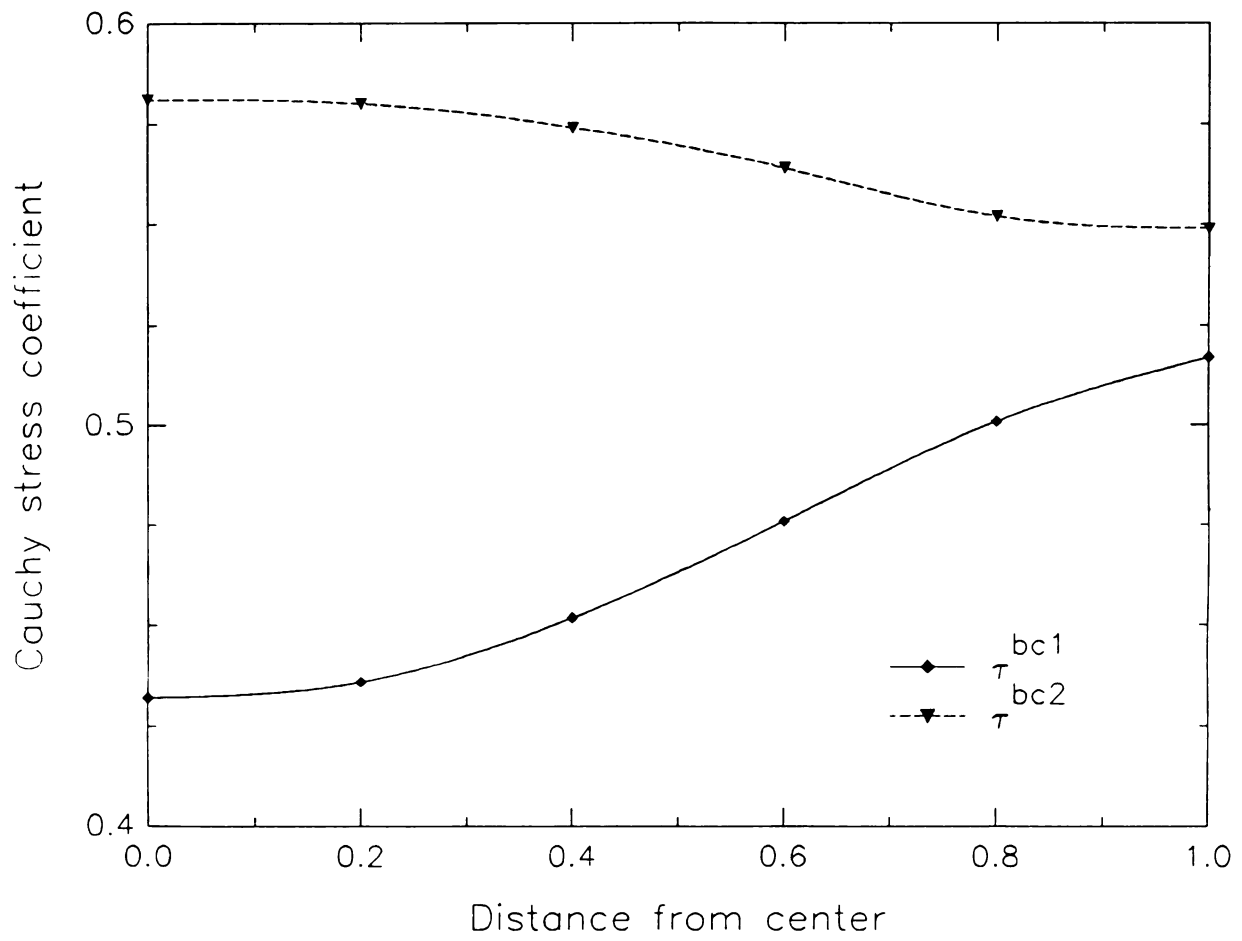


Figure 25: Comparison of Cauchy Stresses Along the Center Line d-d



6.2.4 Effect of Nonconservative Loading: Case of External Pressure

So far, the normal loading acting on the membrane was assumed to be deformation-independent. In this section, a deformation-dependent loading is considered. A square membrane subjected to this type of loading was analyzed.

For values of the nondimensional coefficient k ranging from 0.0001 to 0.05, the maximum deflection coefficients for the two types of loading were identical to three significant digits, as were the maximum stress coefficients. Apparently, the assumption that the loading is deformation-independent is quite accurate in the range of straining considered.

6.2.5 Comments About the Initial Virtual Prestressing Technique

In all the numerical cases studied, the "optimum" initial guess of the initial virtual prestressing vector was obtained with a 3×3 finite element mesh, using the reduction factor defined by Equation 5.15. Then, this optimum guess was used with a 5×5 finite element mesh.

For the case of membranes fixed along their four edges, the minimum number of increments needed was five, and the average number of iterations per increment required for convergence was 5.6. However, in the free-fixed square membrane studied in section 6.2.3, 15 increments were required while the average number of iterations per increment was only 2.4.



7. Summary and Conclusions

7.1 Summary

This research investigated the static nonlinear behavior of structural thin flat membranes which are subjected to transverse loading. The membrane material was assumed to have a linear elastic constitutive behavior. Only geometric nonlinearities were considered. An incremental nonlinear finite element method using nondimensional variables was employed.

First, a geometric nonlinear model referred to as the von Kármán model was developed. This model was based on simplified strain-displacement relationships in which the squares and products of derivatives of the in-plane displacement components were neglected. An incremental-iterative procedure was used to solve the equilibrium equations for the nodal displacements. To overcome the difficulty associated with the ill-conditioning arising at the start of this procedure, a new technique referred to as "initial virtual prestressing" was developed.

To validate this model, a square membrane and rectangular membranes with two different aspect ratios were analyzed. Then, results for the central deflection and central and maximum second Piola-Kirchhoff stresses were compared with the results of previous investigators who also had used the von



Kármán simplification of the strain-displacement relationships. Cauchy stresses were also computed and compared to second Piola-Kirchhoff stresses to determine whether the use of the latter was appropriate. To the best of the investigator's knowledge the comparison of the two types of stresses has never been published.

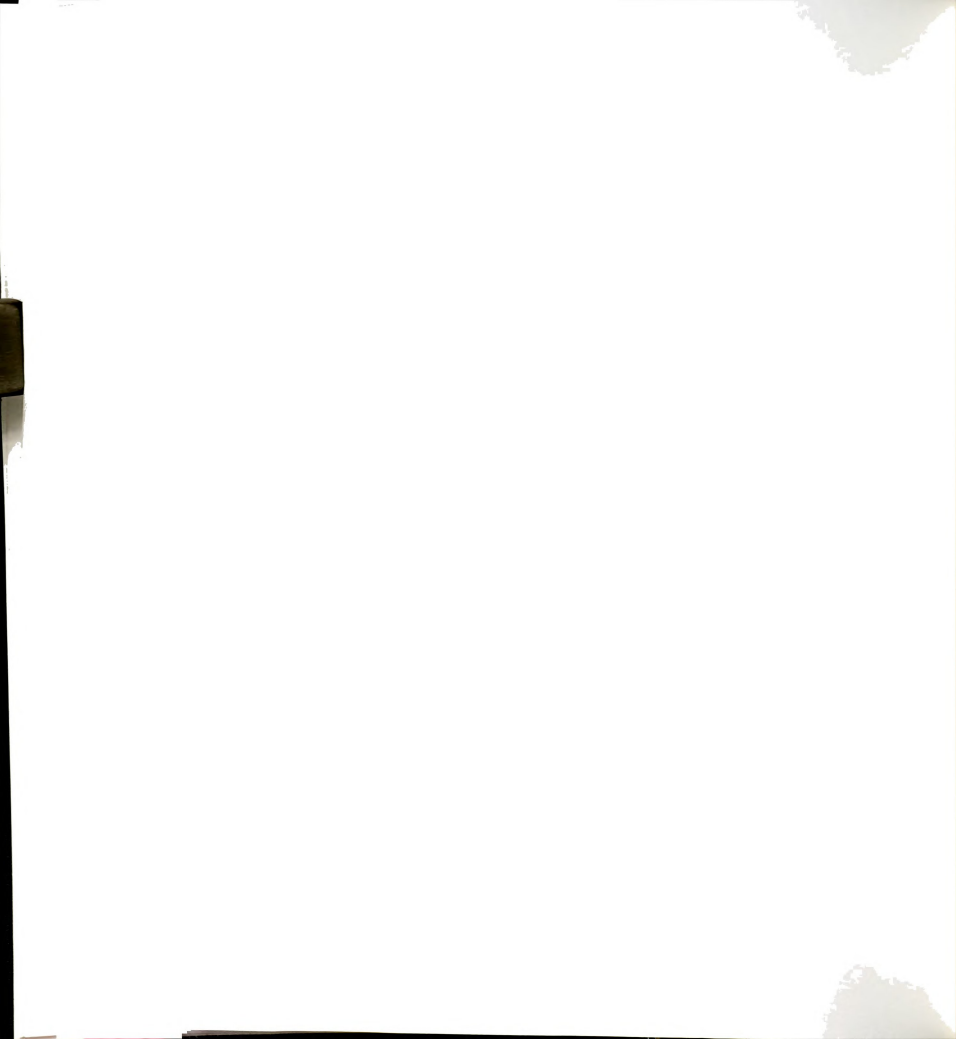
Next, a general geometric nonlinear model using the exact strain-displacement relationships was developed. This model is referred to as the general model. It was used to analyze the three membrane cases mentioned above. A comparison of its results with those of the von Kármán model was made to assess the limitations of the latter model. To the best of the investigator's knowledge the comparison of the comparison between the two models has never been published.

Finally, some parametric studies were conducted to investigate the effect of varying Poisson's ratio, introducing initial real prestressing and changing the boundary conditions. The effect of nonconservative loading also was investigated.

7.2 Conclusions

7.2.1 Comparison of the von Kármán Model to previously developed models

Comparison of the results of the von Kármán model with those obtained by previous investigators shows overall agreement, particularly for deflections. Because the



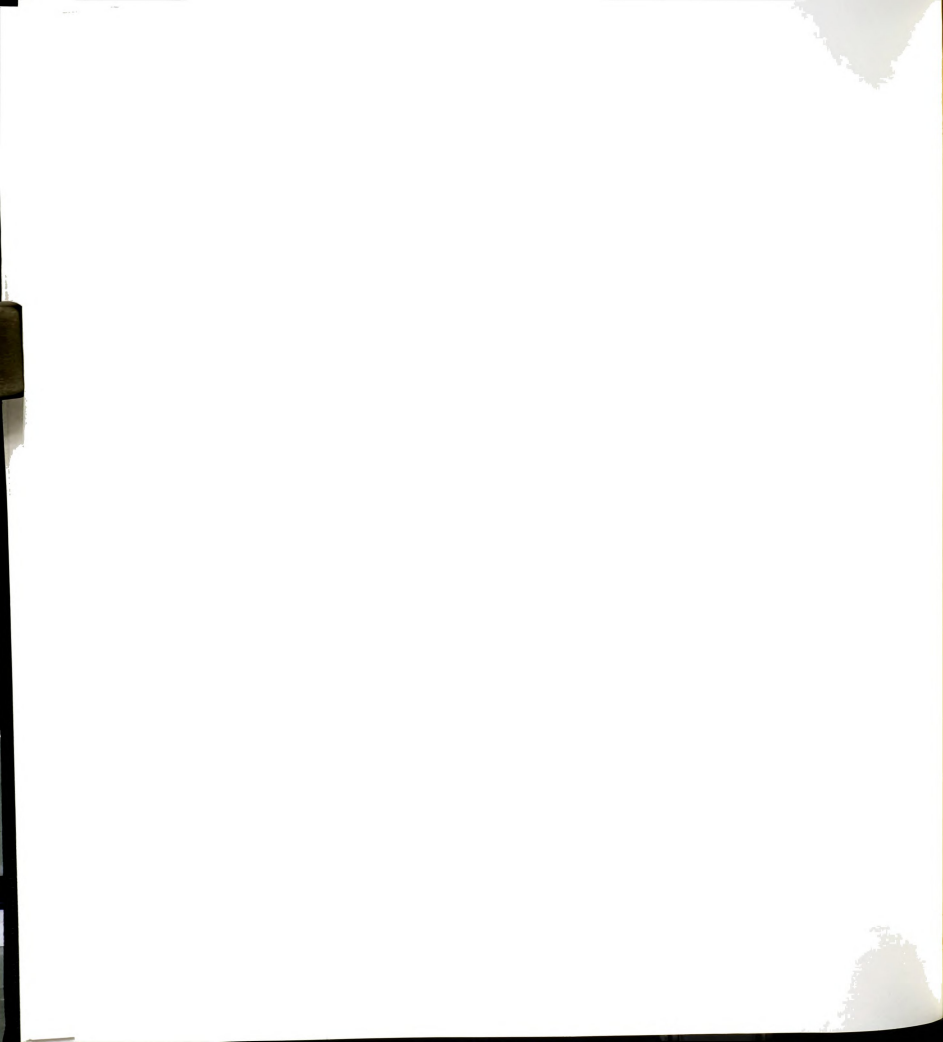
nondimensional coefficient k enters the fundamental incremental equilibrium equations, the analysis was carried out for different values of k ranging from 0.0001 to 1. It was shown that the central deflection coefficient and the central and the maximum second Piola-Kirchhoff stresses were not affected by the variation of k .

7.2.2 Second Piola-Kirchhoff Stresses and Cauchy Stresses

Unlike the second Piola-Kirchhoff stresses, Cauchy stresses vary with k . From the theoretical point of view, the Cauchy stress represents the real membrane stress. A comparison of these stresses with second Piola-Kirchhoff stresses for different values of the nondimensional coefficient k shows that the use of second Piola-Kirchhoff stress leads to an underestimation of the central stress, and an overestimation of the maximum stress. Nevertheless, for values of k smaller than 0.01, the differences are negligible for design purposes.

7.2.3 Limitation of the von Kármán Model

A comparison of the results for the central deflection coefficient and the central and maximum Cauchy stress coefficients with those obtained using the general model shows that the von Kármán model overestimates the central stress, but underestimates the maximum stress. However, for values of k smaller than 0.01, the von Kármán model gives results that are sufficiently accurate for design.



The nondimensional coefficient k (a function of load intensity, characteristic length of the membrane, Young's modulus, Poisson's ratio and membrane thickness) determines the state of straining in a membrane. For values of k smaller than 0.01, the maximum strain is less than 1.75%. For values of k greater than 0.05, the maximum strain exceeds 4.5%. For high values of strains, the membrane may exhibit inelastic behavior, in which case, new constitutive relationships should be considered.

7.2.4 Effect of Poisson's Ratio

To investigate the effect of Poisson's ratio on deflections and stresses, a square membrane was analyzed with different values of Poisson's ratio. The results show that the variations in the values of the central deflection coefficient, and the central and the maximum stress coefficients are, respectively, 10.7%, 10.5%, and 3.9% when the value of Poisson's ratio is varied from 0.2 to 0.48.

7.2.5 Effect of Initial Prestressing

Initial prestressing was expressed in terms of initial prestraining to allow for a general interpretation of the results. The results of the analysis of a square membrane initially prestressed along one direction show that when the initial prestraining increases from 0 to 1.4%, the central deflection coefficient decreases by 10.8%, while the central and maximum stress coefficients increase, respectively, by 36.6%, and 29%. Consequently, in practical situations, initial



prestressing might be introduced when small deflections are required, but the magnitude should be limited to avoid premature tearing of the membrane.

7.2.6 Effect of Boundary Conditions

A square membrane with the two edges parallel to the x-axis free, and the two other edges fixed, was analyzed. Comparison of results with those obtained in a membrane with four fixed edges shows that the deflections and stress coefficients corresponding to the former case are higher than in the latter case. Variations of 23.1% and 12.4% were obtained, respectively, for the central deflection and maximum stress.

7.2.7 Effect of Nonconservative Loading

External pressure on a flexible membrane is a deformation-dependent loading. To investigate the effect of this type of loading on membrane deflections and stresses, a square membrane was analyzed. The results obtained for the maximum deflection and stress coefficients, for the range of values of k between 0.0001 and 0.05, were nearly the same as those obtained when considering a conservative type of loading.

7.2.8 Use of The Initial Virtual Prestressing Technique

Newly developed for this study, the initial virtual prestressing technique was used in the incremental-iterative procedure to avoid ill-conditioning and assure convergence. The advantage of this technique is that only the three components of the initial virtual prestressing vector need to



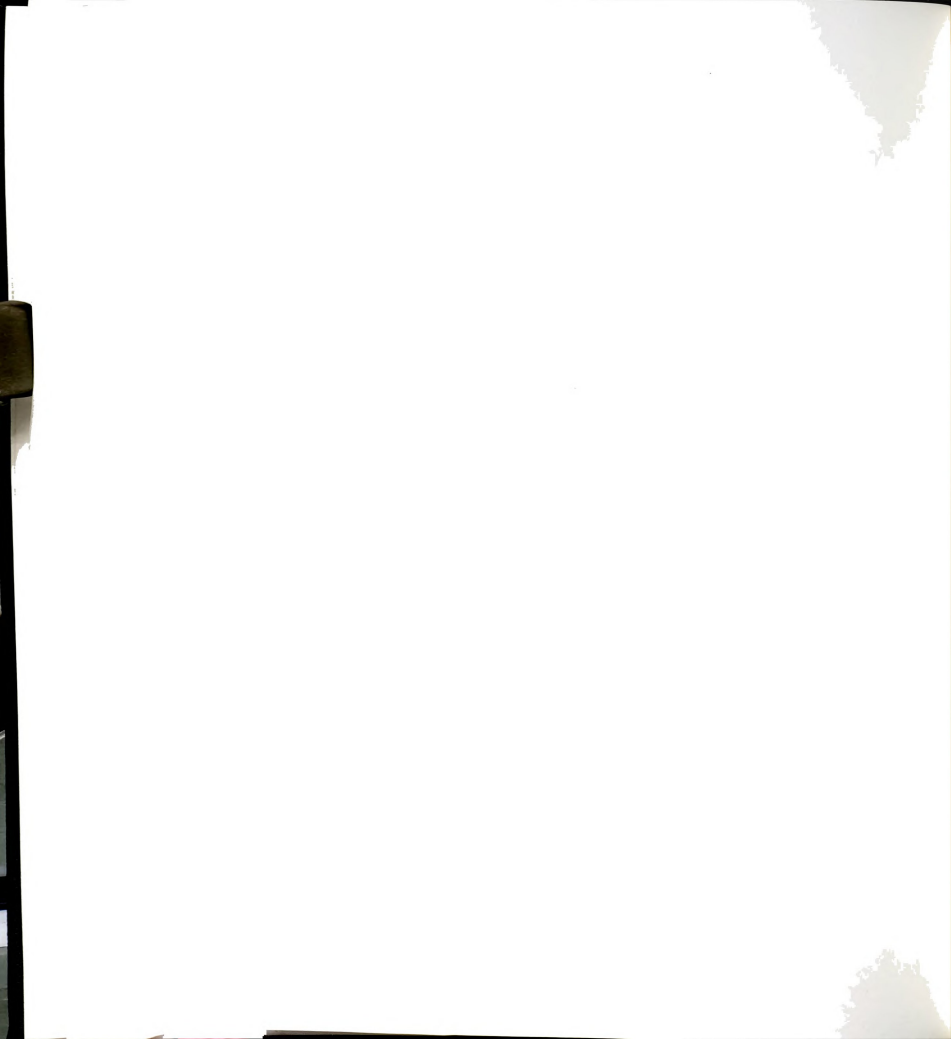
be guessed, while in previous work, an initial guess of the deflected shape of the membrane was required. The "optimum" values corresponding to the initial guess may be obtained by trial and error on a coarse finite element mesh.

7.3 Further Study

For plastic greenhouses, the practical value of the nondimensional coefficient k ranges between 0.005 and 0.05. Therefore, the models and the results for nondimensional parameters developed in this study are potentially useful in design. In particular, the assumption of linear elastic behavior might be very critical. To get a better insight of the structural behavior of membranes, a further study is needed to include more accurate constitutive relationships, particularly for low density polyethylene which exhibits a nonlinear viscoelastic behavior.



BIBLIOGRAPHY



Bibliography

1. Hoxey, R.P., and Richardson, G.M. (1984). "Measurements of wind loads on full-scale film plastic clad greenhouses.", *Journal of Wind Engineering and Industrial Aerodynamics*, vol.16, pp.57-83.
2. Janick, Jules, and Ait-Oubahou, Ahmad, (1989). "Greenhouse production of banana in Morocco." *Hortscience*, 24(1), 22-27.
3. Otto, Frei, (1967). "Tensile Structures", Vol.1: Pneumatic Structures, MIT Press, Cambridge.
4. Otto, Frei, (1969). "Tensile Structures", Vol.2: Cable Structures, MIT Press, Cambridge.
5. Krishna, P., (1978). "Cable-Suspended Roofs", McGraw-Hill, New York.
6. Irvine, H.M., (1981). "Cable structures", MIT Press, Cambridge.
7. Leonard, J.W., (1988). "Tension Structures, Behavior and Analysis, McGraw-Hill.
8. Shaw, F., and Perrone, N., (1954). "A Numerical Solution for the Nonlinear Deflection of Membranes", *J. Appl. Mech.*, 21, 117-128.
9. Föppl, A., and Teubner, B.G., (1907). "Vorlesungen über technische mechanik". Leipzig, Germany, vol.5, p.132.
10. Timoshenko, S.P., and Woinowsky-Krieger, S., (1970). "Theory of Plates and Shells", International Student Edition, Second Edition, McGraw-Hill Book Company, 416-419.
11. Föppl, A., and Föppl, L., (1920). "Drang und Zwang", R. Oldenbourg, Munich, Germany, Vol.1, p.216.
12. Hencky, H., (1921). "Die Berechnung dünner rechteckiger Platten mit verschwindender Biegungsteifigkeit", *ZAMM* 1, 81-89.
13. Borg, S.F. (1953). "A Note on the Solution for the Rectangular Membrane", *Journal of the Aeronautical Sciences*, 20, 220-221.
14. Neubert, M., and Sommer, A., (1940). "Rectangular Shell Plating Under Uniformly Distributed Hydrostatic Pressure", N.A.C.A. Technical Memorandum, No.965.

15. Head, R.M., and Sechler, E.E., (1944). "Normal Pressure Tests on Unstiffened Flat Plates", N.A.C.A., Technical Memorandum, No.943.
16. Timoshenko, S.P., (1940). "Theory of Plates and Shells, McGraw-Hill Book Company, Inc., New York and London, p.4.
17. Kao, R., and Perrone, N., (1972). "Large Deflections of Flat Arbitrary Membranes", Computers and Structures, 2, 535-546.
18. Allen, H.G., and Al-Qarra, H.H., (1987). "Geometrically Nonlinear Analysis of Structural Membranes", Computers and structures, 25(6), 876-876.
19. Bathe, Klaus-Jürgen, (1982). "Finite Element Procedures in Engineering Analysis", Prentice-Hall, pp.318-334, 380-381, 278-284.
20. Crisfield, M.A., (1991). "Nonlinear Finite Element Analysis of Solids and Structures", Vol.1 "Essentials", John Wiley & Sons, pp.121-132.
21. Oden, J.T., and Sato, T., (1967). "Finite Strains and Displacements of Elastic Membranes by the Finite Element Method", Int. J. Solids Structures, 3, 471-488.
22. Zienkiewicz, O.C., (1977). "The Finite Element Method", Third Edition, McGraw-Hill Book Company, pp.169-188, 454.
23. Kline, J. Stephen, (1965) "Similitude and Approximation Theory", McGraw-Hill Book Company, pp.16-23.
24. Bergan, G. Pål, and Clough, W. Ray, (1972). "Convergence Criteria for Iterative Processes", AIAA Journal, 10(1), 1107-1108.



MICHIGAN STATE UNIV. LIBRARIES



31293008826343